Bedrijfstakonderzoek
BTO 2022.045| August 2022

De invloed van de drinkwater-samenstelling op de uitloging van cementhoudende leidingmaterialen: modelvalidatie en gevoeligheidsanalyse

Bedrijfstakonderzoek

KWR

Bridging Science to Practice

Rapport

De invloed van de drinkwatersamenstelling op uitloging van cementhoudende materialen: modelvalidatie en gevoeligheidsstudie

BTO 2022.045 | August 2022

Dit onderzoek is onderdeel van het collectieve Bedrijfstakonderzoek van KWR, de waterbedrijven en Vewin.

Opdrachtnummer
402045-273

Projectmanager
Petra Holzhaus

Opdrachtgever
BTO - Bedrijfsonderzoek

Auteur(s)
A. (Alex) Hockin Msc., dr. ir. M. W.(Martin) Korevaar, dr. ir. K.A. (Karel) van Laarhoven

Kwaliteitsborger(s)
Dr. Ir. E. J. M (Mirjam) Blokker

Verzonden naar
Dit rapport is verspreid onder BTO-participanten.

Een jaar na publicatie is het openbaar.

Keywords

asbestos cement, leaching, PHREEQC, drinking water composition, saturation index

Jaar van publicatie
2022

Meer informatie
Alex Hockin
T 06-15608101
E alex.hockin@kwrwater.nl

PO Box 1072
3430 BB Nieuwegein
The Netherlands

T +31 (0)30 60 69 511
E info@kwrwater.nl
I www.kwrwater.nl

Managementsamenvatting

LSI beneden -0,2 is niet afdoende om uitloging van cementleidingen uit te sluiten

Auteur(s) A. (Alex) Hockin Msc., dr. ir. M. W.(Martin) Korevaar, dr. ir. K.A. (Karel) van Laarhoven

Om de uitloging van cementhoudende leidingen te beperken, eist de Drinkwaterrichtlijn een Langelier verzadigingsindex van calciet (LSI) in drinkwater boven -0,2. De effectiviteit van de LSI als maatstaf voor uitloging is echter onduidelijk: uitloging en de obstructie via calciet is een complex proces dat afhankelijk is van de gehele drinkwatersamenstelling. Een eerder ontwikkeld chemisch en transport cementmodel is verder geverifieerd en gevalideerd. Uit een gevoeligheidsanalyse om te bepalen welke fysische en chemische (waterkwaliteit)parameters het meeste effect hebben op de uitloging, op de obstructie hiervan en op de indexparameters om dit te monitoren bleek dat de *initiële eigenschappen* van het cement (capillaire porositeit) en de concentratie silicium in het instromende water de meeste invloed hebben op het uitlooggedrag van cement. De inzichten voor silicium zijn nieuw en moeten met experimenten worden gevalideerd voordat nieuwe conditioneringsstrategieën tegen uitloging met zekerheid kunnen worden aanbevolen..

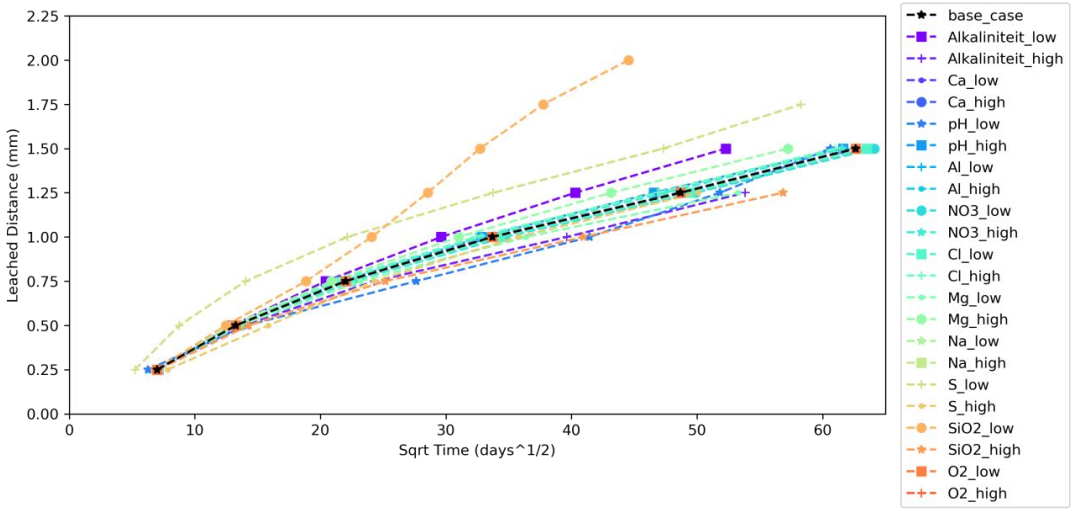

De verschillen in de uitlogingssnelheden voor verschillende waterkwaliteitsparameters worden hier weergegeven als de uitgeloogde diepte als functie van de wortel van de tijd in dagen. Uit de resultaten blijkt dat veranderingen in de SiO_2- en S--concentraties het grootste effect hebben op de uitlogingssnelheid in vergelijking met de andere parameters.

Belang: effectiviteit LSI-voorschriften voor cementbescherming onduidelijk

Om uitloging (en dus verzwakking) van asbestcement en cementhoudende leidingen te beperken, moet volgens de Drinkwaterrichtlijn de Langelier verzadigingsindex van calciet (LSI) in drinkwater boven -0,2 zijn (binnen het bereik van de norm – een SI tussen de -0,5 tot +0.5 – is de LSI vergelijkbaar een goede benadering voor de SI).

De (L)SI is een maat voor de verzadiging van calciet (calciumcarbonaat) in het water. Bij voldoende verzadigd water kan dan een laag calciumcarbonaat op de binnenwand van de buizen ontstaan, die uitloging voorkomt. Sommige waterbedrijven moeten chemicaliën doseren om de LSI op dit wettelijke niveau te krijgen, wat de kosten verhoogt en de duurzaamheid verlaagt. Bovendien is de effectiviteit van de LSI als maat voor uitspoeling onduidelijk: de vorming van de beschermlaag is een complex proces, dat afhangt van de hele

drinkwatersamenstelling. Daarom is meer inzicht nodig in de invloed van de drinkwatersamenstelling op de uitloging over de tijd.

Aanpak: verificatie, validatie en gevoeligheidsanalyse van cementmodel
In een eerder project (BTO 2021.052) is een rekenmodel voor cement ontwikkeld waarmee de uitloging als functie van de watersamenstelling kan worden bepaald. De aannames van het model zijn in dit project verder geverifieerd. Bovendien werd het model gevalideerd aan de hand van twee experimentele studies uit de literatuur en een case-study met metingen uit het veld. Met een gevoeligheidsanalyse is bepaald hoe gevoelig uitloging is voor veranderingen in de fysische en chemische (waterkwaliteit)parameters.

Resultaten: complex verband uitlooggedrag sluit onvoldoende aan bij huidige indexparameters
Het model toont aan dat kalkafzetting niet alleen het gevolg is van de neerslag van calciet uit het instromende water op de cementwanden, maar van een complex geheel van reacties tussen instromende water en afbraak van het cement. Dit geheel van reacties bepaalt de snelheid en omvang van de calcietneerslag. Daarnaast bleken gangbare index-parameters voor conditionering van drinkwater (de LSI, maar ook de internationaal veel gebruikte CCPP) het uitloog- en kalkafzettingsgedrag niet te voor-spellen. De concentratie silicium in het instromende water bleek de grootste invloed te hebben op de uitloging en de kalkafzetting, meer zelfs dan calcium. Lage siliciumconcentraties leidden tot een grotere uitloging dan hoge concentraties. Dit leidt tot een voorgesteld mechanisme waarbij lage silicaconcentraties het oplossen bevorderen van de gel van calcium-silica-hydraat (CSH-gel, een belangrijk bestanddeel van cement). Andere elementen (Ca, S, Mg) bleken hierop ook van invloed te zijn. Wij vermoeden dat de toestand van de CSH-gel (een belangrijke component van cement) van doorslaggevend belang is voor de totale uitloogsnelheid van cement.

Toepassing: nieuwe inzichten vereisen experimentele validatie
Omdat de productieomstandigheden niet konden worden geverifieerd bij deskundigen met ervaring uit de eerste hand, kunnen directe metingen van de poreuze eigenschappen van het cement een manier zijn om rechtstreeks de oorspronkelijke eigen-schappen van de cementbuizen te bepalen.

De invloed van silica, maar ook zwavel en magnesium, op de uitloging van cement is nieuw en niet eerder gerapporteerd in de internationale wetenschappelijke literatuur. Het is daarom noodzakelijk deze resultaten eerst te verifiëren in het laboratorium. Daarna kan het model gebruikt worden om optimale conditioneringsstrategieën voor het drinkwater te bepalen. Het model zou ook kunnen worden gebruikt om het uitloogpotentieel per drinkwaterproductielocatie te bepalen en op termijn mogelijk zelfs voor het inschatten van de restlevensduur van leidingen.

Rapport
Deze onderzoekslijn wordt tot op heden beschreven in beschreven in:

- *De invloed van de drinkwatersamenstelling op uitloging van cementhoudende leidingen: modelvalidatie en gevoeligheidsstudie* (BTO-2022.045). [voorliggend onderzoek]
- *De invloed van de drinkwater- samenstelling op uitloging van cementhoudende leidingmaterialen: een model* (BTO 2021.052).

Meer informatie
Alex Hockin
T 06-15608101
E alex.hockin@kwrwater.nl

PO Box 1072
3430 BB Nieuwegein
The Netherlands

Inhoud

1 Introductie

1.1 Aanleiding en doel

Er zijn veel verschillende eisen voor de chemische en fysische samenstelling van het drinkwater (Update (2013) Mededeling 100, Drinkwaterbesluit, Slaats et al., 2013). Eén van de eisen is dat de Langelier Saturatie Index (LSI), boven de waarde van -0,2 ligt[1]. (Drinkwaterbesluit, Bijlage A in Tabel IIIa, Indicatoren –Bedrijfstechnische parameters, *Drinkwaterbesluit*, 2011). Sommige waterbedrijven moeten op dit moment chemicaliën doseren om de LSI op het wettelijk niveau te krijgen. Zowel vanuit financieel als duurzaamheidsoogpunt wordt deze dosering het liefst tot het minimum beperkt.

De LSI is een maat voor de verzadiging van calciumcarbonaat. Deze parameter is opgenomen om de uitloging van asbestcement en cementhoudende leidingen te beperken: in voldoende verzadigd water kan een deklaagje van calciumcarbonaat bestaan op de binnenwand van leidingen (LeRoy et al., 1996; Schock et al., 1981). Een dergelijk deklaagje kan vervolgens als bescherming dienen tegen de degradatie van cementhoudende leidingen via uitloging van calciumhydroxide. Het is belangrijk om uitloging te voorkomen, omdat het vrijkomen van leidingmateriaal kan leiden tot een verandering van de waterkwaliteit en tot het verzwakken van de leiding.

Uit een recente beschouwing van de wetenschappelijke literatuur over dit onderwerp voor de projectgroep Praktijkcode 'Optimale samenstelling drinkwater en conditionering' (Slaats et al., 2013) – binnen het Platform Bedrijfsvoering – kwam naar voren dat de effectiviteit van de Langelier SI als maatgevende indicator voor uitloging omstreden is (bijv. Kuai et al., 2015; Le et al., 2016; Rossum et al., 1983; Torres et al., 2015; WHO, 2011). Ten eerste is het vormen van de deklaagjes een complex proces dat afhangt van de complete drinkwatersamenstelling, niet alleen van de aanwezige calcium- en waterstofcarbonaatconcentratie. Ten tweede is uit experimenten gebleken dat deklaagjes niet in alle gevallen evenveel bescherming bieden tegen de uitloging van calciumhydroxide (Schock et al., 1981).

In 2021 is in het bedrijfsonderzoek het project 'Een model voor de invloed van de drinkwatersamenstelling op uitloging' (Hockin et al., 2021) afgerond om meer inzicht te verkrijgen in de invloed van de drinkwatersamenstelling en conditionering op uitloging als proces in de tijd. Daarin is een rekenmodel ontwikkeld waarmee de invloed van de drinkwatersamenstelling op uitloging als proces over de tijd kan worden bepaald, op basis van bestaande inzichten uit de wetenschappelijke literatuur (bijv. Jacques et al., 2013). Initiële berekeningen met het model voor enkele voorbeelddrinkwatersamenstellingen lieten daarbij al een substantiële invloed van de drinkwatersamenstelling op uitloging en deklaagvorming zien (Hockin et al., 2021).

Het voorliggende rapport beschrijft onderzoek waarin voor het bovengenoemde model een gevoeligheidsstudie is uitgevoerd. Op die manier werd de invloed van de drinkwatersamenstelling op uitloging systematisch in kaart gebracht. Het doel is om met de gevoeligheidsstudie steeds de drinkwatersamenstelling te relateren aan afgeleide parameters die zich in de praktijk lenen voor monitoring, zoals: pH, (L)SI, CCPP (Calcium Carbonate Precipitation Potential, ook bekend als Totaal Afzetbaar Calcium Carbonaat en als Agressief CO_2). Op die manier wordt duidelijker welke van deze afgeleide parameters het meest geschikt zijn met het oog op bescherming tegen uitloging.

[1] De LSI is het verschil tussen de gemeten pH van het water en de pH wanneer calciet verzadigd is. De SI wordt berekend door de chemische activiteiten van de opgeloste ionen van het mineraal te vergelijken met hun oplosbaarheidsproduct. De LSI is in wezen een vereenvoudiging van het SI en in veel gevallen is de LSI een goede indicator van het SI. In het Drinkwaterbesluit wordt verwezen naar het 'SI', maar worden de eenheden van pH vermeld; daarom wordt aangenomen dat de LSI wordt bedoeld in plaats van het SI.

Op basis van inzicht in deze aspecten kunnen drinkwaterbedrijven de drinkwatersamenstelling beïnvloeden zodanig dat de uitloging van hun cementhoudende leidingen beter is te beheersen. Dit zal leiden tot een toekomstbestendiger leidingnet, waar we beter inzicht hebben welke leidingen moeten worden vervangen. De uitkomsten van de gevoeligheidsstudie leggen een essentiële basis voor een beoordeling van de (van de drinkwatersamenstelling afgeleide) indexparameters die nu worden gebruikt als maat voor het risico op uitloging.

1.2 Algemene aanpak en leeswijzer

Hoofdstuk 2 beschrijft de verificatie van de modelaannames die in het vorige project zijn vastgesteld, waaronder de implementatie van de meest recente chemische cementthermodynamische database (Cemdata18), het effect van het opnemen van elektrostatische effecten, het effect van calciet op de porositeit en diffusiviteit van cement, de productieomstandigheden van asbestcement in Nederland en de aanpak voor het modelleren van de transporteigenschappen van afbrekend cement.

Hoofdstuk 3 beschrijft de validatie van het geverifieerde model aan de hand van twee studies uit de literatuur en een case-study uit de praktijk (Texel, PWN).

Hoofdstuk 4 beschrijft de gevoeligheidsanalyse inclusief het effect van variërende fysische parameters (bijv. temperatuur, initiële capillaire porositeit) en chemische watersamenstellingsparameters gebaseerd op verwachte concentraties in drinkwater. De gevoeligheid van het model voor veranderingen in de uitlogingssnelheid, de omvang van calcietneerslagen en het effect van de verschillende parameters op de berekening van de parameters voor de conditioneringsindex van drinkwater, de Langelier Saturation Index (LSI) en het Calcium Carbonate Precipitation Potential (CCPP).

Hoofdstuk 5 bespreekt de resultaten in de context van de Nederlandse drinkwaterwaterbedrijven, de conclusies van dit project en de aanbevelingen voor verdere modelverbetering en implementatie.

De hoofdstukken 1 en 5 zijn geschreven in het Nederlands en de hoofdstukken 2, 3 en 4 in het Engels.

het model en de validatie zijn ook gepresenteerd op een wetenschappelijke conferentie wen in de publicatie: *Karel van Laarhoven, Alex Hockin, Martin Korevaar (2022) Modelling a comprehensive relation between water quality and cement degradation in the drinking water distribution network. doi: https://doi.org/10.4995/WDSA-CCWI2022.2022.14169.*

2 Verification

The model used in this research was developed in the research reported in (BTO 2021.052, Hockin et al., 2021). During that research recommendations were made to further verify (i.e. to critically examine and to test against the state of academic and practical knowledge) several model assumptions, prior to using the model for predictions. In this chapter, the recommended verifications pertinent to modelling the leaching of asbestos cement (AC) pipes are carried out. Specifically, the following points in the model were verified and refined if so needed:

- The cement database that describes the chemical properties of the modelled system;
- The assumptions regarding the role of electrostatic interactions in diffusion;
- The interactions between calcite precipitation, porosity and leaching rates that occur in the model;
- The assumptions regarding the porous properties of AC, as determined by its production process;
- The procedures for dynamically calculating the cement microstructure throughout the leaching process.

These points are sequentially addressed in the sections of this chapter.

2.1 Updated cement database

In the previous project (Hockin et al., 2021) the cement thermodynamic database (CEMDATA07) was used to model the changes in cement minerals over time (Lothenbach et al., (2008, 2006); Matschei et al., (2007). Since then, there has been a substantial update to the database in the form of CEMDATA18. The refined database was incorporated into the model as part of the verification step. This update is very important as the quality of the model depends on the accuracy and completeness of the thermodynamic database (Lothenbach et al., 2019). The most important updates in CEMDATA18 that are relevant for this project are:

- additional mineral phases and associated changes in the distribution of iron and aluminum in minerals phases and updates to the alkali phases;
- the addition of several alternative CSH[2] models.

The changes in the database are expected to lead to differences in modelling results between the two databases. In addition, practical changes in the model include adding flexibility in the code to accommodate the changes in the names of cement minerals between the databases and the ability to choose which database to use when modelling (e.g. CEMDATA07, CEMDATA18 or a custom database).

Compared to CEMDATA07, CEMDATA18 contains substantially more cement minerals (144 vs 42 mineral phases). In part this is due to the addition of the effects of relative humidity during the curing of the cement. Cement hydrates have varying water content depending on the temperature and relative humidity and depending on the conditions under which the cement is formed, minerals can have varying molar water content. This variation in the molar water content can impact the molar volume, porosity and density of the cement (Lothenbach et al., 2019). In particular, the effects of relative hydration can be important for the Afm and Aft phases (Table 12, Appendix II). In our case the affected minerals are: ettringite, hemicarbonate, monocarbonate, straetlingite and monosulphate.

[2]Cement chemistry has its own set of abbreviations for the main oxides found in cement: C for CaO, S for SiO_2, A for Al_2O_3, F for Fe_2O_3, M for MgO, K for K_2O, $\overline{S}$ for SO_3, N for Na_2O, H for H_2O and $\overline{C}$ for CO_2. Also see Table 12 in the appendix.

In relation to the updated database, the following modelling assumptions and choices are made in the current modelling approach:

- To utilize the information on the effects of relative hydration, specific production conditions should be known. Alternatively, the relative hydration of the various components can be determined in a more detailed laboratory assessment of the cement mineral phases. At the moment of writing, neither of these information sources are available. Therefore, the effects of relative hydration are ignored in the current research and the general water content for each mineral is used.
- The iron-containing hydrates were updated in CEMDATA18. However, only Fe-siliceous hydrogarnet is expected to occur in hydrated cements. In hydrated Portland Cement (PC), Fe(III) precipitates as iron hydroxide during the first hours and as siliceous hydrogarnet ($C_3(A,F)S_{0.84}H_{4.32}$) after 1 day and longer (Lothenbach et al., 2019). As in the first project (Hockin et al., 2021), iron hydrogarnet forms are not included in the model, because Jacques et al., (2009) found it led to unnecessarily complicated calculations and its inclusion had no effect on the evolution of pH, element concentrations and solid phase composition.
- Mg-Al layered double hydroxide (LDH) are similar structurally to hydrotalcite and typically occur as secondary reaction products in hydrated PC (Lothenbach et al., 2019). These hydrotalcite-like phases were updated in CEMDATA18, however the authors recommend the use of a single phase, M_4AH_{10}, for well hydrated PC.
- Two other groups, Magnesium silicate hydrates and zeolite minerals, were not included in the model though were included in the Cemdata18 update. Magnesium silicate hydrates form at the interface of clay and cement paste. As we are interested in the degradation on the inside of the pipe we do not include these in the model. Zeolite minerals were also updated in Cemdata18. These minerals are relevant for the interface between cement pastes and adjacent rocks, for example in the context of nuclear waste storage and as such they are not included in this model.
- Finally it is important to note when using CEMDATA18 for equilibrium calculations, some phases may be more stable than others but are not likely to form during the timescales modelled (De Windt et al., 2020). For example, while gibbsite can form at temperatures above 60 °C, its precipitation should be suppressed for simulations at ambient temperatures. Instead, microcystaline $Al(OH)_3$ will form (Lothenbach et al., 2019). Similarly, according to the Lothenbach et al (2019), other stable phases such as goethite (FeOOH), hematite (Fe_2O_3) and quartz (SiO_2) should be suppressed in calculations of hydrated cements in favour of microcrystalline FeOOH (or microcrystalline or amorphous $Fe(OH)_3$, depending on the timeframe considered), and amorphous SiO_2 (De Windt et al., 2020; Lothenbach et al., 2019). In our case, the iron phases are neglected and amorphous SiO_2 is included.

The calcium silicate hydrate gel (CSH) phase is a major phase in hydrated PC. Depending on the ratio of Ca/Si, the CSH phase can have variable composition and properties. In the previous model, the CSH phase was described by an ideal solid solution[3] of jennite ($Ca_9Si_6O_{18}(OH)_6{\cdot}8H_2O$) and tobermorite-II ($Ca_5Si_6O_{16}(OH)_2{\cdot}4H_2O$) and a pure phase of amorpheous silciumdioxide (SiO_2). In the CEMDATA18 update, five alternative CSH models are included. Two models, *CSH-II* and *CSHQ*, are recommended for use in PC. We use the CSH-II variant in our model because it is explicitly recommended to be compatible with both the CEMDATA07 and the CEMDATA18 databases. That way, the results of the current research are the most suitable to be compared with the results in the previous research (Hockin et al., 2021).

[3] In an ideal solid solution, the activity coefficient of the mixture is equal to 1 while in non-ideal solid solutions, the activity coefficients are great or less than 1.

Box 1. CSH Models in CEMDATA18

CSH-II solid solution model, covers the range of Ca/Si ratios from 0.83 to 1.67, for backward compatibility with the CEMDATA07 database and as an alternative to the newer models. We use this CSH solid solution in our model to be consistent with the validation in the previous project.

CSHQ models - was developed in order to address some known shortcomings of the earlier CSH-I and CSH-II models, namely the insufficient connection to the C-S-H structure and the unrealistic assumption of ideal mixing between tobermorite-like and amorphous silica end members.

ECSH-1, ESCH-2 (extended CSH) provisional models aimed to extend the CSH-I and CSH-II models, but expected to be replaced by more accurate models in the future

CSH3T for CSH phases with Ca.Si < 1.5 -> ultimately the authors recommend other models for portland cement though

CNASH_ss - (calcium (alkali) aluminosilicate hydrate (C-(N-)A-S-H) gel-like phase) recommended for alkali activated systems, not for PC.

2.2 Role of electrostatic interactions in diffusion

Currently, the multi-component diffusion is used in PHREEQC. While using this functionality, overall charge balance is maintained (Parkhurst et al., 2013) and non-uniform porosity throughout the modelled system can be evaluated. The latter is needed so that changes in the mineral concentrations and associated changes in porosity can be modelled as a function of depth. Electro-diffusive phenomena have been neglected up till now. That means that each aqueous species had the same diffusion coefficient (Jacques et al., 2011). In reality, the diffusion coefficient depends on, among other things: ion size, temperature and interaction with other diffusing species due to species charge. Oppositely charged species can accelerate diffusion while similarly charged species can retard diffusion (Appelo et al., 2005). Detailed data on the diffusion coefficients for elements is not always available, so that multi-component diffusion with an average diffusion coefficient ($1.3*10^{-9}$ m^2/s at 25 °) is commonly used (Appelo et al., 2005).

Simulations were ran to test the validity of the neglection of electro-diffusive phenomena. A 10 year period of leaching of AC in contact with four different water compositions was simulated. The water compositions are given in Appendix IV. The simulations were repeated with and without electro-diffusive phenomena modelled. For a more detailed description of the leaching simulations, see BTO 2021.052 (Hockin et al., 2021).

To include the electro-diffusive effects, available diffusion coefficients, and their dependence on temperature were added to the model. The available diffusion coefficients were taken from the phreeqc.dat database file. Note, only the diffusion coefficients for a limited number of species was available see Appendix III, Table 14. All other solution species parameters were unaltered from the original Cemdata18 database. The effect of temperature on the diffusion coefficient is calculated by PHREEQC as follows:

$$D_w^T = D_w^{298} \cdot e^{\frac{damp}{T} - \frac{damp}{T_{298}}} \cdot \frac{T}{T_{298}} \cdot \frac{\mu_{298}}{\mu_T} \qquad \textit{Eq. 1}$$

Where *damp* is the damping parameter for the temperature effect on viscosity on the diffusion coefficient [-], D_w^{298} is the diffusion coefficient at the standard temperature (25 °C, 298.15 Kelvin), D_w^T diffusion coefficient at the

solution temperature *T* (in kelvin); μ is the viscosity of the solution at temperature *T* and at the standard temperature (25 °C, 298.15 Kelvin).

The Cemdata18 database resulted in little difference in the overall leaching rate for the Vitens and PWN compositions, and larger differences for Oasen and WMD compositions compared to the Cemdata07 database (Figure 1). Addition of the electro-diffusive phenomena resulted in a decrease in the leaching rates for all water compositions when compared to the leaching rate with a single diffusion rate (Cemdata18 vs. Cemdata18 + Diffusion, Table 1). Leaching rates were 18%, 24%, 36% and 43% lower for Vitens, PWN, Oasen and WMD respectively (Table 1). The results show that choice of database and the addition of individual diffusion rates does affect the progress of leaching, although the absolute difference is small: 0.5 mm over a 10 year simulation (Figure 1). More importantly though, differences in the database had effects on the total moles of calcite precipitated, the order of fastest to slowest leaching and the total leached distance. For example, with Cemdata07, the Oasen water composition had the smallest total leached distance, while with Cemdata18 the same composition had the largest and with the addition of the individual diffusion rates the same composition was again the smallest. This shows that the leaching rates are difficult to predict *a priori* and there are complex reaction and relationships which the model is able to simulate but are not captured by, for example, index parameters which remain the same no matter the database chosen. The Cemdata18 database with individual diffusion coefficients (Cemdata18_Diffusion) was deemed the preferable approach and used in the remainder of this research as it is the current state-of-the-art regarding thermodynamic cement modelling and the individual diffusion rates were shown in the simulations to have substantial effects on the overall leaching rates.

Table 1 The leaching rate for the different simulations results, for the previous cement database (Cemdata07), the latest cement database (Cemdata18) and the latest cement database with the addition of individual species diffusion rates (Cemdata18 + Diffusion).

	Leaching rate (mm/yr$^{0.5}$)		
	Cemdata07	**Cemdata18**	**Cemdata18_diffusion**
OASEN	0.55	0.80	0.51
VITENS	0.56	0.53	0.43
PWN	0.69	0.74	0.56
WMD	0.85	0.95	0.54

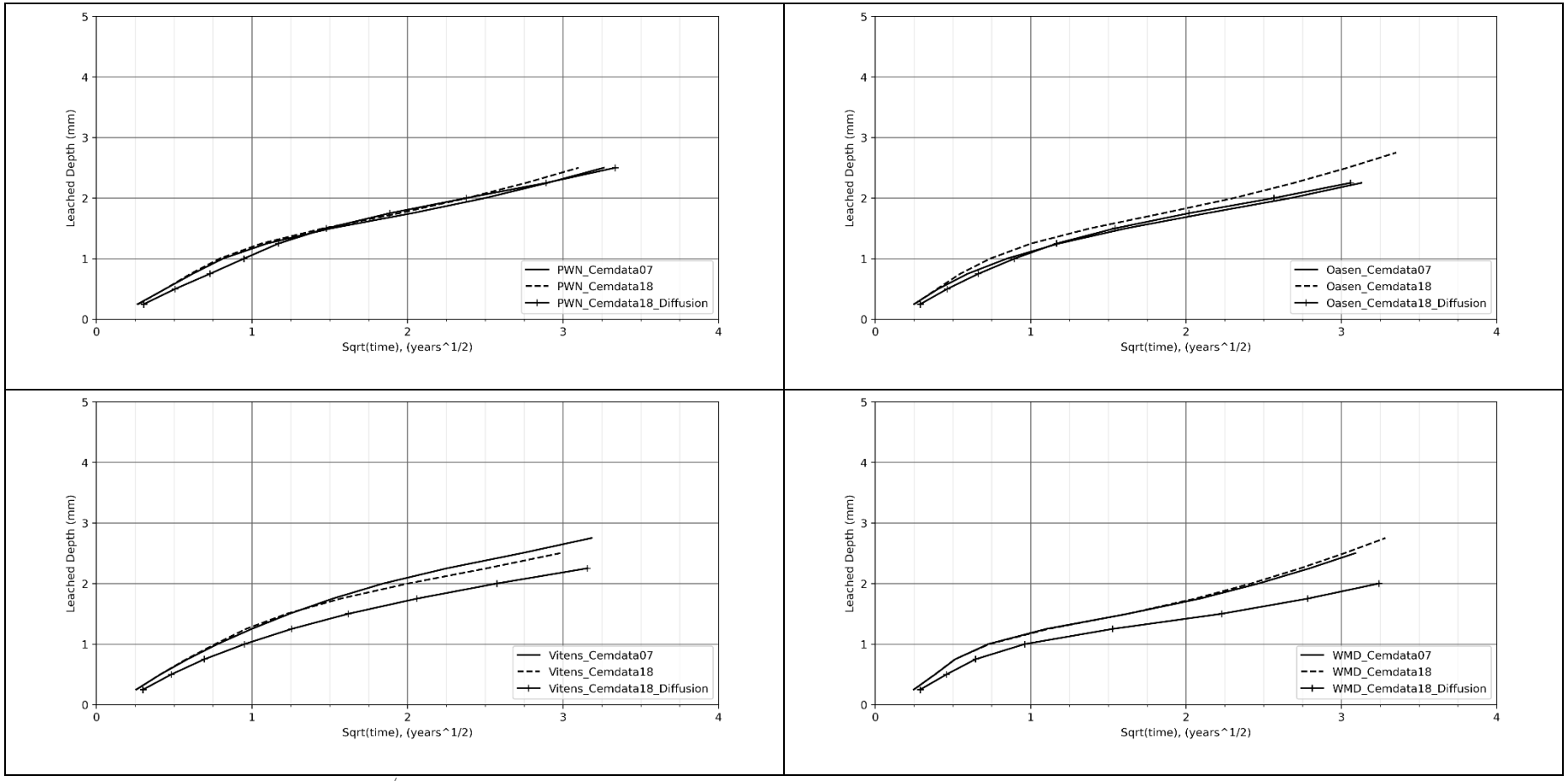

Figure 1 The difference in the leaching rate (as mm/√year) for the three databases tested: Cemdata07 (solid line), Cemdata18 (dashed line) and Cemdata18 with individual diffusion rates (solid line with cross-hashes). The results show that the Cemdata18 database results in little difference in the overall leaching rate compared to Cemdata07, while the addition of individual diffusion rates decreases the overall leaching rates for the Vitens and WMD water compositions, though little difference was observed for the PWN and Oasen water compositions. Note: in the previous project (Hockin et al., 2021) *an error in the PCO_2 resulted in different results than presented here. The error has been corrected and the results presented here are correct.*

2.3 Effect of calcite on porosity and leaching rate

In the previous work, a deviation of regular, diffusion limited leaching was observed to coincide with the precipitation of calcite. This was thought to be caused by the precipitation of calcite resulting in decreased porosity. This is a reasonable assumption since in the context of the model, the porosity is calculated based on the molar volumes of the different minerals. When calcite precipitates, the model assumes a solid precipitate which occupies a volume calculated from the molar volume of the mineral. Therefore when calcite, or any other mineral precipitates, it occupies the available pores in the cement cell, effectively blocking diffusion.

This explanation is critical to further verify, because it is the part of the model that embodies the general strategy of the water utilities to protect pipes against leaching: promoting the formation of protective scaling layers. To test the contribution of calcite scaling to the effect of leaching, the model was altered to exclude the effects of calcite precipitation on the calculation of porosity. This was done in the model by storing the minimum calcite mineral concentration per cell, such that while calcite was allowed to precipitate freely in the model, only the minimum calcite (the original calcite present in the cement) was included in the calculation of the porosity. This change in the model results in calcite being free to precipitate without contributing to the calculation of porosity. This modified model was run for 10 years for each of the four water compositions provided (Appendix IV). Cement cells were 0.25 mm with a total length of 5 mm of cement, the temperature was set at 10 degrees, and a w/c ratio of 0.5.

Figure 2 shows the difference between the simulations for the water composition when calcite was (solid line) and was not (dashed lines) included in the calculation of porosity. When precipitated calcite is ignored for the purposes of calculating porosity, the depletion of portlandite is substantially faster. Comparing the time to deplete the first 2 mm of the cement between the two simulations, neglecting calcite in the porosity resulted in depletion which was 3.6, 3.7, 5.6 and 10.9 times faster for Vitens, PWN, Oasen and WMD respectively (Table 2). In addition, the linearity of the fit increased when calcite is neglected (Table 2), as is expected for purely diffusive processes that are not modified by changes in diffusivity (porosity) over time. This non-linearity can be seen in the four water compositions including calcite (Figure 2).

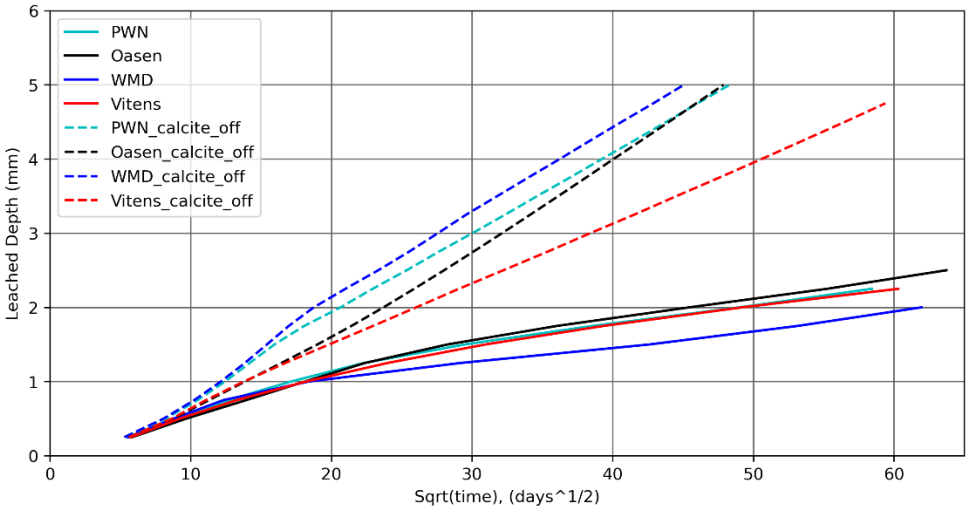

Figure 2 The difference in the leaching rate (as mm/sqrt(year)) for the four water compositions provided from PWN, Oasen, WMD and Vitens. The results show that when calcite is not included in the calculations for porosity ('calcite off'), the depletion of portlandite occurs faster.

*Table 2 Differences in the time to deplete portlandite, the linearity and the total moles of calcite precipitated in the 10 year simulation for the normal model (including calcite in porosity) and when calcite was neglected ('calcite **Neglected in porosity**').*

	Time to 2 mm depletion (years)		Linearity, R^2 [-]		Calcite (moles)	
	Normal	Calcite Neglected in porosity	Normal	Calcite Neglected in porosity	Normal	Calcite Neglected in porosity
Oasen	6.59	1.17	0.959	0.999	7.2	76
Vitens	6.63	1.86	0.965	0.999	2.3	37
PWN	5.66	1.54	0.966	0.996	7.1	143
WMD	10.52	0.96	0.959	0.998	3.9	180,005

Changes in the calcite precipitation were also observed when calcite was neglected (Figure 3). All four water compositions had substantially more calcite precipitation in the first few cement cells when compared to the simulations where calcite was included in the porosity. It should be noted that since calcite was decoupled from the porosity, unrealistically high values for calcite precipitation were calculated in those simulations (Table 2). In reality, calcite contributes to the porosity and therefore there is a feedback loop of precipitation, resulting in decreased porosity which restricts the diffusion through the cement altering the progression of leaching and calcite precipitation.

The results suggest that calcite precipitation leads to protection of the cement by decreasing the porosity, restricting leaching. It should be noted, however, that the current model for the porosity changes and their effects is still very rough. In particular, the translation of the resulting porosity to the diffusivity of the leachate assumes a lower boundary for diffusion that may be far too high (in effect, pores can never be completely blocked, no matter the amount of calcite precipitation, because the diffusivity associated with the gel pores is enforced as a lower boundary). Future research could investigate the microstructural properties of calcite precipitation in drinking water pipes to better estimate the changes in porosity as a result of calcite precipitation.

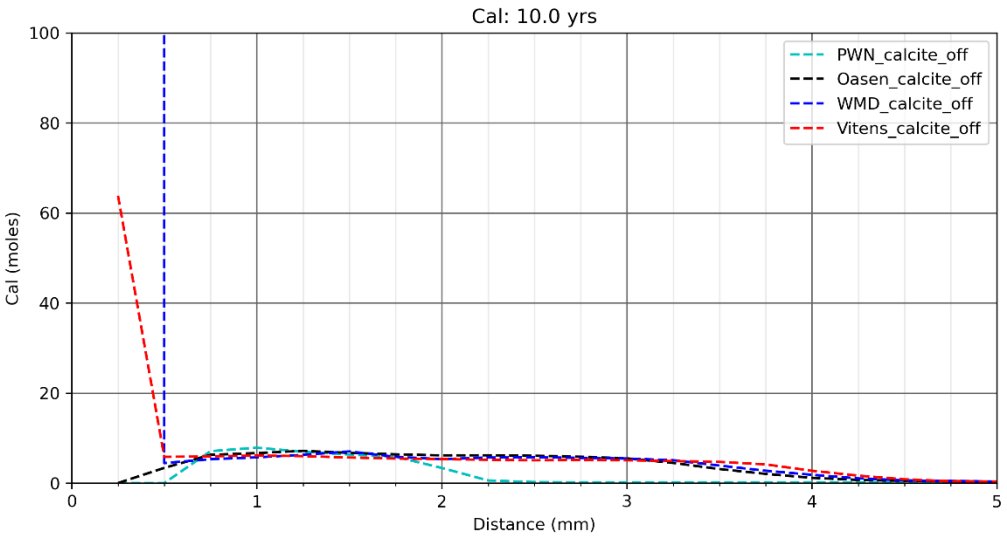

Figure 3 Total calcite precipitation for each cement cell for the four water compositions when calcite is neglected in the calculations for the cement porosity. In the case of WMD, the simulation resulted in (unrealistically) high precipitation of calcite at 180,000 moles in the first 0.5

mm of the cement. For the PWN water composition, calcite precipitation occurred followed by dissolution, resulting in the low calcite precipitation seen in the final cement composition after 10 years.

2.4 Specific production conditions of asbestos cement pipes

The historic production process of asbestos cement pipes deviated from 'regular' current mixing of cement clinker and water. Documents from Eternit, one of the most important producers of AC in the Netherlands, suggest that some of the production conditions were chosen specifically with the aim of influencing the cement microstructure (Bijleveld, 1974). The cement microstructure influences the rates of diffusive transport during leaching. Therefore, in this verification step, it was attempted to learn as much about the specific microstructure of AC as possible. Experts with first-hand experience with the historic production conditions were not available. From the literature, the following relevant properties specific to AC were found:

- AC was required to be produced with CEM I, i.e. regular Original Portland Cement (EN 197-1, 2000; Eternit, 1980; NEN 3262, 1988). This means the CEM I chemical compositions initially assumed in the model are likely to be appropriate.
- Eternit gives inconsistent reports of the water cement ratio used for the production of the cement: 0.25 (Bijleveld, 1974), 0.27 (Eternit, 1980) and 0.5 (Elzenda et al., 1974) are reported. Given the peculiar porous properties reported (see below), a w/c ratio 0.25-0.27 is assumed to be most likely.
- A weight percentage of 10-15% asbestos fibres is reported for the initial mixture of cement, asbestos and water (Eternit, 1980), resulting in around 12% weight percentage asbestos in the hardened asbestos cement (Elzenda et al., 1974).
- The AC is reported to have pore sizes with a typical length scale of 25 nm (Bijleveld, 1974), realized through a very low water cement ratio and production under high pressure. This suggests that, effectively, all pores in the initial AC are gel pores rather than capillary pores (also see section 2.5).
- The AC is reported to have a pore volume fraction of around 13% (Eternit, 1980). This is quite low compared to regularly mixed cement. This is consistent with the assumption that the pore volume is largely comprised of solely gel pores. Based on the Powers models (also see section 2.5), the gel pore volume is directly tied to the amount of CSH-gel, meaning that cement of a regular composition with a w/c ratio of 0.5 has a gel pore volume fraction of around 23%. The discrepancy between this somewhat fundamental lower limit on gel porosity and the value reported for AC could possibly be explained by traditional methods for measuring porosity are not fully effective when it comes to measuring the smallest pore sizes, see Haga et al. (2005). For the purposes of this study, it will be assumed that AC has an initial pore volume that consist solely of gel pores, calculated according to Powers.

To further refine the assumption with respect to the AC microstructure properties, laboratory measurements will be needed.

2.5 Modelling the (degrading) transport properties of cement

A more refined way of calculating the initial porosities and for updating them as the cement changes during leaching was implemented. The key change was to incorporate the established models of Patel et al. (2018) that relate the mixing conditions of the cement to the resulting gel porosity and capillary porosity. In the updated model, the following steps are used to initialize and update the porosities and cement component volumes.

Initialization

- Amounts of cement clinker, m_{cem}, asbestos fibers, m_{asb}, and water, m_w, for the initial mixture are chosen in terms of their respective weights. Their relative proportions can be based on for instance information on specific production conditions (see section 2.4).
- The volume of the added asbestos, V_{asb} is calculated from the chosen mass and the density of asbestos (in our case: 2.53 g/cm^3 for chrysotile asbestos).
- The initial volume of the resulting hydrated (cured) cement minerals, V_{cem}, is derived from the chosen amount of cement clinker through a reference case from literature that reports that 350 g cement clinker with 175 g water (i.e. w/c = 0.5) results in 202 cm^3 of hydrated cement minerals (Jacques et al., 2010). This relation is used irrespective of the chosen w/c, which is appropriate as long as it can be assumed that the mixing process leads to well-hydrated cement (which is the case for AC, see section 2.4).
- The initial volume of the gel pores that are present in between the CSH-gel molecules, V_{gp}, is calculated as follows:
    - A review by Brouwers (2004) of the Powers et al. (1946) model for cement microstructure points out that the volume of the gel pores is equal to around 38% of V_{cem} for cement with w/c = 0.5.
    - In the reference case, it is also reported that around 41.5% of V_{cem} consists of CSH-gel (Jacques et al., 2010). From this, the volume of the CSH-gel, V_{csh}, is calculated.
    - The two points above also give the information needed to conclude that the volume of the gel pores is equal to around 91% of the volume of the CSH-gel. This factor, f_{csh} = 0.91, is important because the gel pores are inherently tied to the CSH-gel. When V_{csh} changes (due to leaching), this relation defines how V_{gp} changes as well.
- The initial volume of possible capillary pores that are present between the various hydrated cement crystals, V_{cp}, is highly dependent on the specific mixing conditions during the production of the cement. It is best for this volume to be measured and then manually defined in the model accordingly. If no such measurements are available, V_{cp} can be estimated with the following empirical relation reported by Patel et al. (2018) and Powers et al. (1946) for regularly mixed cement which gives $\emptyset_{cp}$, the capillary porosity of the cement:

$$\emptyset_{cp} = \frac{wc - 0.36\alpha}{wc + 0.32} \qquad \text{Eq. 2}$$

Where α is the degree of hydration, assumed to be 1 indicating full hydration in our model and wc Is the w/c ratio.

Updating during leaching

- During the simulations, PHREEQC keeps track of the volumes of all individual minerals. Whenever a volume of minerals dissolves or precipitates, the model assumes that an equal volume of capillary pore volume is created and V_{cp} is updated accordingly.
- In the model, the CSH-gel is represented by the minerals jennite and tobermorite. Therefore, when these minerals dissolve/precipitate, not only is the V_{cp} adjusted as described in the previous point, but it is also assumed that a proportional volume (equal to $f_{csh} * \Delta V_{csh}$) of gel pores is converted to capillary pore volume or vice versa.

Over the course of a simulation, the model uses the collection of volumes described above to determine the current transport properties of the cement. First, the current capillary porosity is calculated by dividing V_{cp} by the total volume (the sum of V_{cp}, V_{gp}, V_{cem}, and V_{asb}). Then, that current capillary porosity is used to determine the current effective diffusivity of the dissolved species through the porous material, according to the methods previously described (Hockin et al., 2021).

3 Validation

The verified and refined model was validated from literature and practice, the results of which are presented in this chapter. Two approaches were followed. Firstly, validation by using the model to simulate experiments reported in the literature and comparing the outcomes. The advantage of this approach is that the controlled, reported circumstances of the experiments allow for a well-defined simulation that is suitable for such a comparison. Secondly, validation by using the model to simulate the leaching of real pipes and compare the outcomes with condition assessments of those pipes. A disadvantage of this approach is that the historic circumstances in the field are far less controlled and less well documented than is the case for lab experiments. An advantage of this second comparison, however, is that it allows the model to be tested against 'experiments' with realistic conditions and relevant timescales (multiple decades), which are unattainable in the lab.

3.1 Validation from the literature

3.1.1 Selection of cases

The literature was scanned for a suitable case study to use to further validate the model. In order for published leaching experiments to be suitable as a case study for model validation, the experiments need to be reported with sufficient level of detail. Ideal is:

- Measured and reported cement porosities;
- Leaching is measured and reported in terms of a time-series;
- The experiment concerns the leaching of regular cement (not concrete, mortar, no additives etc.), and the chemical composition of the cement is reported;
- The experiment concerns leaching due to exposure to (constantly refreshed) water of an appropriate, reported composition (e.g. tap water or demi water).

Two studies were deemed suitable to use for validation: the study reported in Moranville (2004) and the study reported in Carde et al. (1997).

3.1.2 Validation approach

Moranville simulation set up

For a more detailed explanation of the set-up the Moranville experiments see BTO 2021.052 (Hockin et al., 2021) or (Moranville et al., 2004). Three of the reported scenarios were modelled:

1. Leaching due to contact with pure water (Table 4) for cement mixed with a w/c ratio of 0.5;
2. Leaching due to contact with pure water for cement mixed with a w/c ratio of 0.4;
3. Leaching due to contact with mineral water (Table 4) for cement mixed with a w/c ratio of 0.4.

The reported w/c ratios can be used to estimate the cement porosity, as discussed in 2.5. However, Moranville also reports porosities that were directly measured. To investigate the differences between the w/c-based estimate and the direct measurements, the model was run using the given w/c ratio and then again using the total porosity reported (as described in section 2.5). The gel porosity was not altered as this is a fixed ratio to the volume of the CSH-gel in the cement. For an overview of the simulation parameters, see Table 3. In all cases the simulation settings were: temperature at 26 °C in the simulations, cement cells at 0.1 mm and simulation length of 114 days. The mineral water composition is listed in Table 4.

Table 3 Model simulation settings for porosities, given as percent, for each scenario.

	MODEL POROSITIES			MORANVILLE POROSITIES	INPUT MODEL POROSITIES
W/C	Gel	Capillary	Total	Total	capillary
0.4	25.9	5.6	31.4	39	16
0.5	22.7	17.1	39.8	44	23

Table 4 Pure and Mineral water composition used in the validation of the diffusion model (Moranville et al., 2004).

	PURE WATER	MINERAL WATER	UNIT
Ca	-	11.5	mg/L
Si	-	31.7	mg/L
Mg	-	8	mg/L
Na	-	11.6	mg/L
K	-	6.2	mg/L
Cl	-	13.5	mg/L
SO_3	-	8.1	mg/L
HCO_3	-	71	mg/L
pH	7	7	[-]

Carde simulation set-up

The Carde experiments were similar to the Moranville experiments: cement samples were suspended in constantly refreshed acidified (pH = 4.5) demi-water and the depth of degradation was measured at two points in time (t = 90 days & 210 days). The simulations were run at the reported temperature of 20°C and cement cells were set at 0.1 mm. Unfortunately, no porosities were reported in the study, so it was necessary to estimate porosities with the Powers model, based on the reported w/c ratios (see section 2.5). As the estimated porosity of the cement could not be verified, two w/c ratio were used: w/c =0.5, 0.525 and 0.55, to observe the spread in the solutions for two similar w/c ratios.

3.1.3 Results and discussion of the validation from the literature

Figure 4 shows the progress of the leached depth of portlandite for each simulation of the Moranville experiments. The simulated times series are compared to the reported measurements. It can be seen that the simulations based on the measured porosity match the reported leached depths reasonably well. The leached depth was within 0.1 mm and 0.3 mm for the cement with w/c = 0.5 and 0.4 for the pure water simulations and within 0.2 mm for the mineral water simulation of Moranville for the cement with w/c= 0.4 (Figure 4). The simulations based on the w/c-estimated porosity seem to underestimate the measurements. As the measured porosities reported by Moranville are consistently higher than the ones estimated through the w/c, this difference in result is to be expected, as a higher initial porosity results in faster initial diffusive transport. This, firstly, demonstrates the sensitivity of the

model for the initial porosities, especially the initial capillary porosities. Secondly, this demonstrates that this sensitivity to porosity is so severe that an estimate of porosity based on the Powers model may not be sufficient.

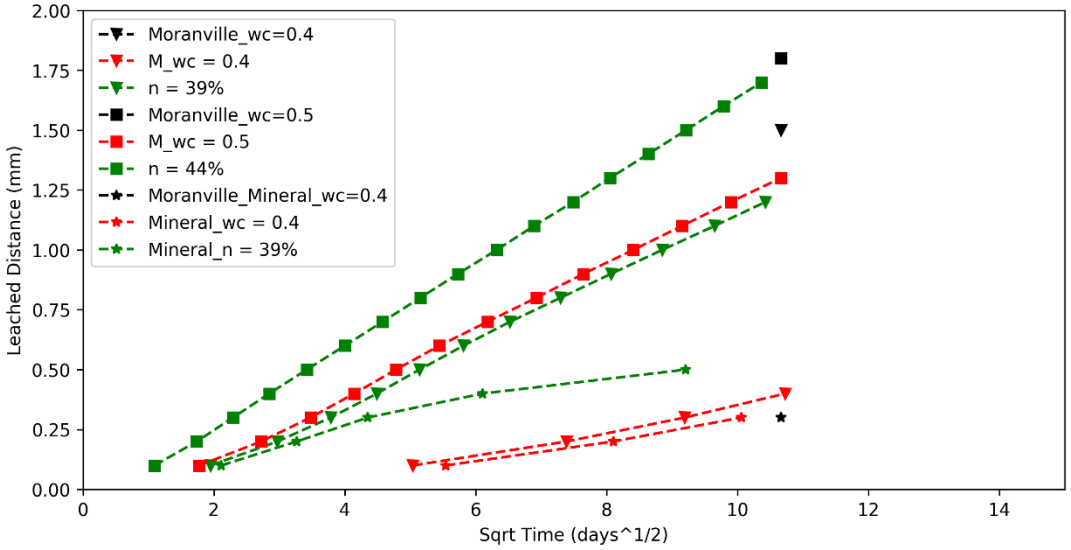

Figure 4 The progress of leaching over time, shown for the different input parameters for the model for the Moranville validation study. Red indicates the cement was initialized using the w/c ratio while green shows the initialization of the cement for the given total porosity. Black indicates the reported leached depths at the end of the simulations. The different symbols indicate which scenario was modelled.

Figure 5 shows the leached depth reported in Carde (black), the simulations with w/c =0.5 (blue), w/c = 0.525 (green) and w/c=0.55 (red). The results show reasonably good agreement with all three models, with closer results for the simulations with the high w/c ratio (w/c = 0.525, 0.55). As we have already shown in the results from Moranville, the model is sensitive to the initial capillary porosity, therefore without reported porosities to validate the initial porosity it is more difficult to get a very good fit. However, even the simulations with the w/c of 0.5 (reported value) the simulations are within 0.2 and 0.3 mm of the leaching after 90 and 210 days respectively. This is improved to 0.1 mm in the simulation with w/c = 0.525 and 0.55 for both the leached depth after 90 and 210 days. The initial capillary porosity for w/c 0.5 and 0.55 are, respectively, 17 and 21.8 %. Again, this comparison emphasizes the model's sensitivity to the cement porosity and the fact that care must be taken when estimating that porosity instead of measuring it directly. Even when using the estimate, however, the model matches the magnitude and trend of the measurements very well.

The take-aways from the validation from the literature are that the model is sensitivity to the input porosity and therefore, using the Powers relationship between the w/c ratio introduces some error as the relationship is an empirical relationship and not a particularly accurate predictor of the initial capillary porosity. However, using report porosities also has some disadvantages, because the method used to measure the porosity of the cement

influences the value reported. Moreover, the method used to determine the porosity of cement is not always reported.

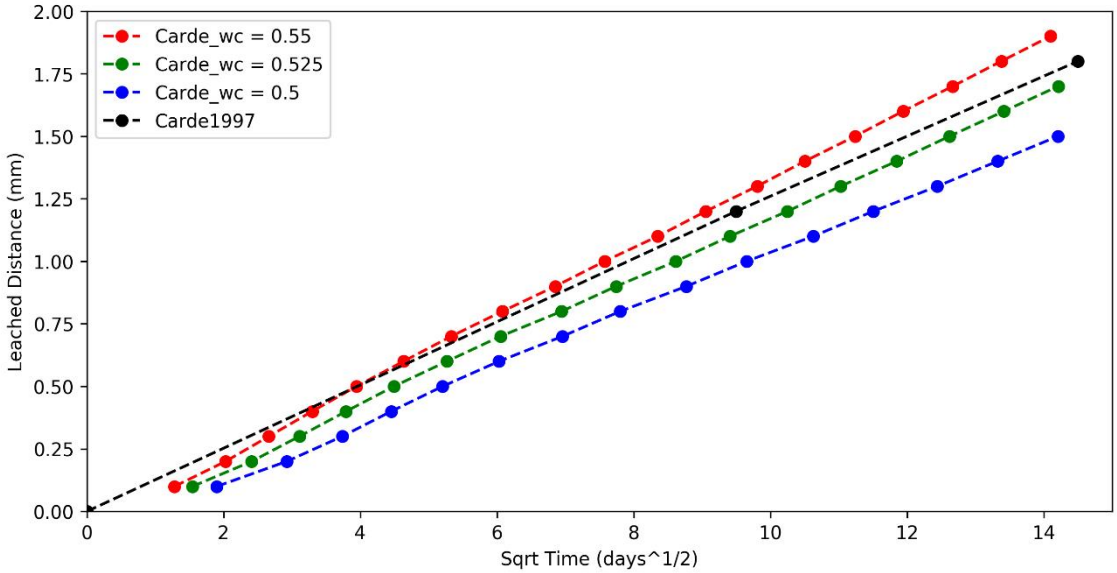

Figure 5 The progress of leaching over time, shown for the reported degradation depths in Carde (1997, (black), the simulations with a w/c ratio of 0.5 (blue), w/c = 0.525 (green) and w/c = 0.55 (red).

3.2 Case study from Practice

3.2.1 Selection of the case study

To validate the model from practice, various drinking water companies were asked for a suitable case study. Sufficient water quality and asset data, describing the case study, is needed for the case study to be suitable. The requirements for a suitable case study are:

- Available data on a minimum of two measurements of the leached depth (with e.g. phenolphthalein or thymolphthalein staining or a suitable radar/ultrasound technique) at different moments in time, performed in the same vicinity, or ideally in the same pipe,
- available data on the water compositions supplied to the location of the condition assessments during the time between the exit tests.

The availability of this required data turned out to be limited. Of the asked water utilities (Brabant Water, Oasen, WMD, Vitens, PWN), only PWN had the means to provide a part of the required data. In the end, a suitable case from Texel was provided. The initial exit tests were performed in 2005 (Mesman, et al. 2005), Table 5.

*Table 5 The reported exit (phenolphthalein) tests performed in Texel in 2005, from (Mesman, et al. 2005), *Indicates that the LSI was negative until 1992. – indicates no measurement value was available.*

2005 TESTS				
Street	Location	Diameter (mm)	LSI	Reported Degradation (mm)
Emmalaan	Den Burg	50	Neg*	-
Jonkerstraat	Den Burg	100	Neg*	0
Laagweelderweg	Oudeschild	50	Neg*	2.9
Californieweg	De Koog	100	Neg*	3.2
Zuid-haffel	Den Burg	100	Neg*	3.4
2022 TESTS				
Street	Location	Diameter (mm)	LSI	Reported Degradation (mm)
Willem van Beierenstraat	Den Burg	100	-	0 (Test 1) 5 (Test 2)

A second set of exit tests were done in the vicinity of the Jonkerstraat in February 2022. The degradation was 0 mm and 5 mm (AC test 1, AC test 2 respectively) along the Willem van Beierenstraat (the Jonkerstraat has been highlighted in yellow in Figure 6).

The two exit tests were performed on a similar section of pipe located approximately 1.1 km from the Den Burg pumping station. The pipes were installed between 1955 (AC test 2) and 1957 (AC test1), with pipe wall thicknesses of 15 mm. In the intake form, it is indicated that there is a protective bitumen coating on the outside of the pipe and no degradation on the outside of either pipe was reported. This is somewhat in contrast to the photo of AC test 2, where it appears there is degradation on the outside of the pipe (Appendix V, Figure 30).

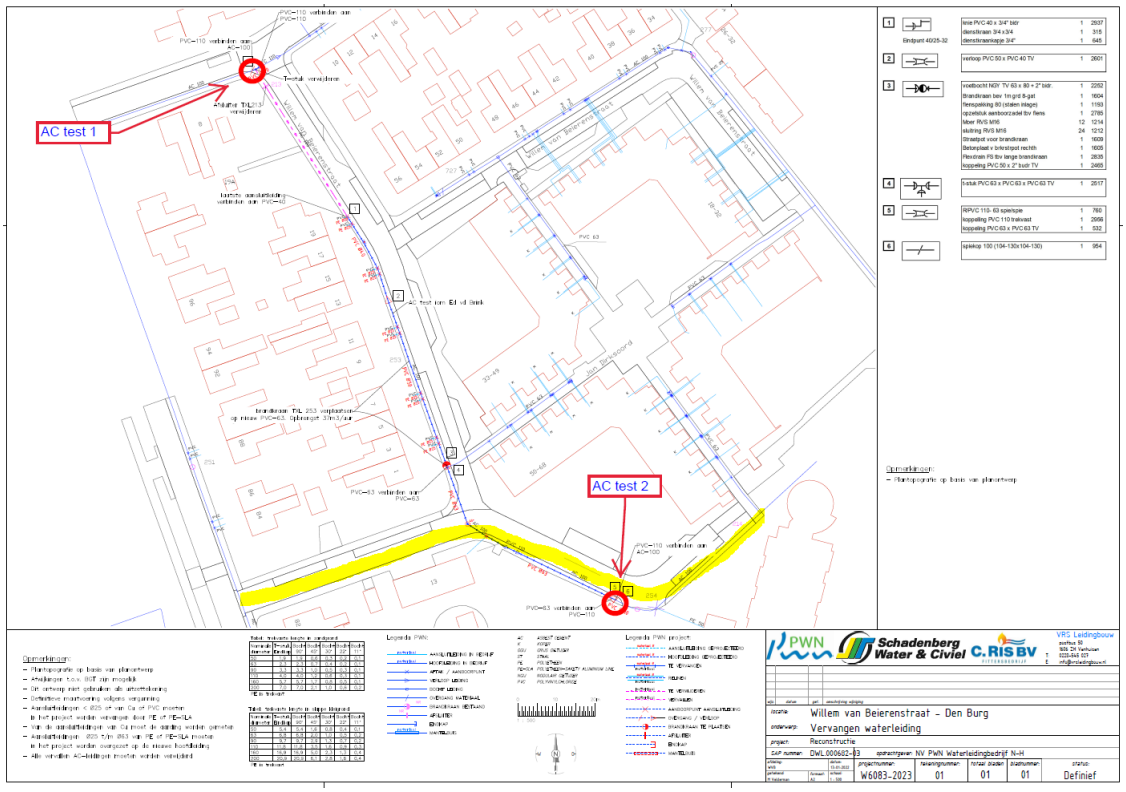

Figure 6 Location of second set of exit tests done in Texel. The Jonkerstraat (highlighted in yellow) is the location of the first exit test done in 2005, reported in (Mesman et al., 2005).

3.2.2 Validation approach

The model was used to simulate the period of leaching between the exit tests from 2005 and those from 2022. The simulations were performed with a w/c ratio of 0.27. This is lower than previous tests and based on the value reported by asbestos cement manufacturers in the Netherlands (Eternit, 1980). At such a low w/c ratio, the initial capillary porosity is zero. Cement cells were 0.25 mm thick. The historical water composition from 2004-2022 was obtained from PWN and the mean composition over the time period was used (Table 6). Temperature was set at 12.1 °C, the average temperature measured over the period between 2004-2022 (Table 6). Since the exit tests from 2005 showed zero leaching in the Jonkerstraat (the closest street to the Willem van Beierenstraat , the cement was initialized as completely intact at the start of the simulation.

Table 6 Mean water composition used in the validation from practice for the Texel case study. Water composition obtained from PWN for 2004-2022. Index parameters calculated with PHREEQC for the given water composition, see Appendix VI for explanation of index parameters.

	VALUE	UNIT	INDEX PARAMETERS	VALUE	UNIT
Al	0.0024	mg/L	EC	534	µS/cm
Ca	46.7	mg/L	SI	0.137	[-]
Cl	76.1	mg/L	Langelier SI	0.122	[-]
Mg	6.7	mg/L	CCPP	0.024	mmol/L
HCO_3	148	mg/L			
NO_3	2.5	mg/L			
Na	53.1	mg/L			
S	38.1	mg/L			
Si	5.28	mg/L			
pH	8	[-]			
Temp	12.1	°C			

Additional simulations were run increasing the initial capillary porosity to 30% in steps of 5%. The value of 30% corresponds to a w/c ratio of ~0.65, which is an extreme upper limit to what we would expect to be used for cement, far higher than expected for asbestos cement used for drinking water purposes. These simulations were performed to determine what the initial capillary porosity would have had to have been in order to have 5 mm of degradation measured in the 2022 exit test.

3.2.3 Results and discussion of the validation from practice

The simulations show in Figure 7 minimal degradation of the cement in the 17 years since the exit test of 2005. Figure 7 shows the portlandite depletion per cell with a total depletion of 0.75 mm of the cement.

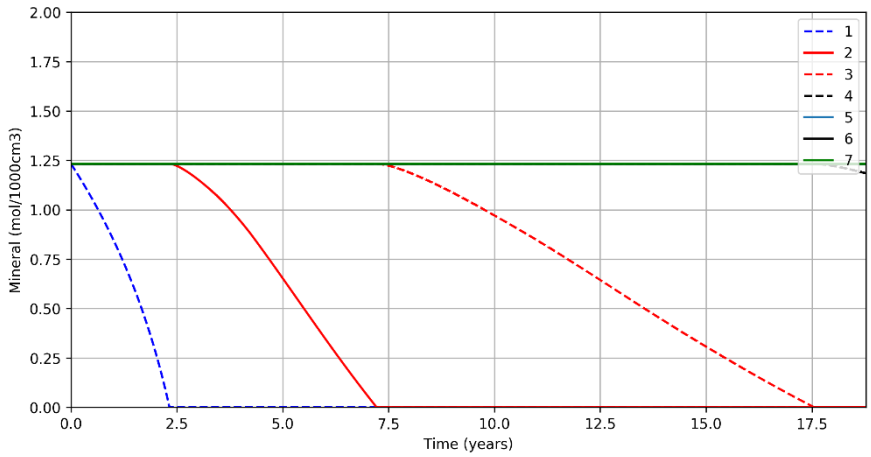

Figure 7 Texel case study results showing the amount of portlandite per cement cell (0.25 mm thick, colored lines) for the time in years since 2005. The results show the first three cells are depleted in the 17 years since 2005, for a total depletion front of 0.75 mm. The fourth cell is just starting to deplete at that moment.

The low degradation of the cement is possibly attributed to the low w/c ratio (and therefore an initial capillary porosity of zero) and the positive SI and Langelier SI (0.137 and 0.122, respectively). Also, the positive SI (Table 6) leads to substantial calcite precipitation in the first cement cell (Figure 8). Accordingly, the total porosity in the cement remains low during the simulation (<35%, with a maximum capillary porosity of 11.7%), which restricts the diffusion of incoming water and therefore degradation of the cement.

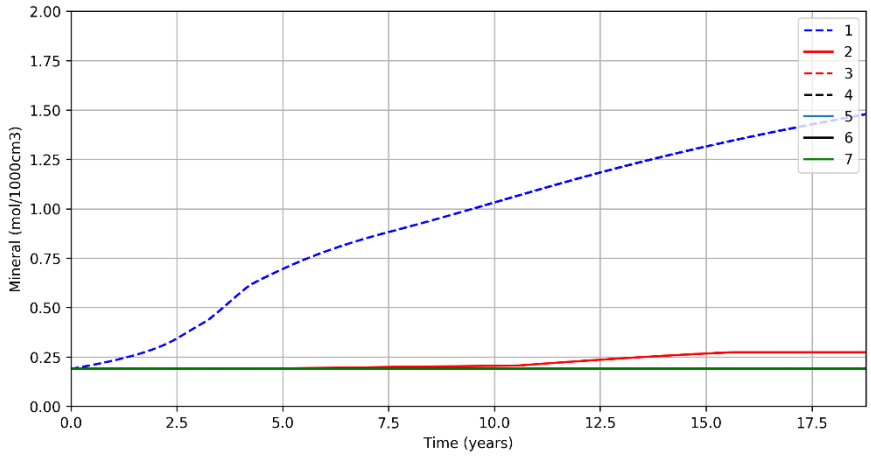

Figure 8 Texel case study results showing the amount of calcite per cement cell (0.25 mm thick, colored lines). The results show substantial calcite precipitation in the first cell over time.

The exits tests done in 2022 in the Willem van Beierenstraat showed degradation of 0 mm in AC test 1 and 5 mm in AC test 2 (Figure 6). It is not known why there is such a large difference between the two exit tests but given that the pipes were installed in different years (AC test 1: 1957, AC test 2 1955) it is possible that the pipes come from different manufacturers, or in the least, were not manufactured in the same batch. Differences in the initial conditions of the pipes, especially differences in the initial porosity, can affect the progress of degradation.

To model the influence of differences in the initial capillary porosity of the cement, a range of initial capillary porosities from 0-30% were modelled. The results are shown in Figure 9. The simulations show that only for the highest initial capillary porosity (30%) is there 4.5 mm of portlandite depletion in the 17 years between the two exit tests. This initial capillary porosity is very high, however, and asbestos cement used for drinking water pipes is not expected to have such a high initial capillary porosity. It needs to be considered, however, that if this pipe truly had different porous properties, its leaching behaviour since installation would have been different as well. A less

extreme difference in initial porosity might then explain the difference in leaching since installation. This part of the pipe lifetime cannot be simulated, however, since the required data on the water quality during that period is not available. Since both pipes must have been exposed to similar water qualities, however, differences in the pipes are still the most likely explanation for the differences in the leaching behaviour. Measuring the porosity/permeability of (the remaining intact material of) pipes might be a promising way to further elucidate these differences.

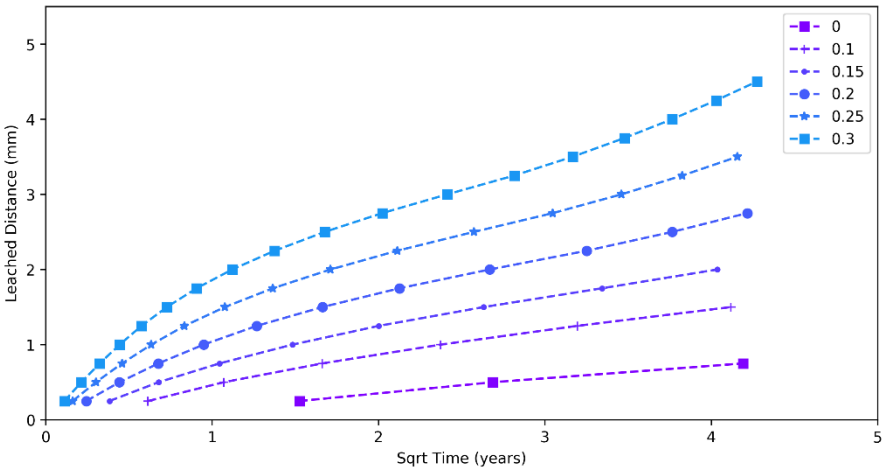

Figure 9 Influence of initial capillary porosity on the degree of degradation (given as portlandite depletion) for the Texel case study. The results show that

In addition to variations in the initial capillary porosity, it is also possible that there is some influence of the distribution network on the different pipe locations. For example, differences in flow rates, residence times and influence of areas of stagnant water etc. can all potentially influence the progress of leaching. The influence of the distribution network was not explored further in this project, though it is an interesting area of further research. Finally, the water composition used in the simulation was constant, as valid between 2004-2022. The influence of differences in water composition over time was not explored in the current project but is interesting to research in a follow up.

4 Sensitivity Study

The sensitivity of the model to various physical and chemical parameters was tested. The physical parameters tested were the influent water temperature and the initial capillary porosity. The chemical water composition parameters tested were the major elements in drinking water regulated in the *Drinkwaterbesluit* (2011) , covering a range typically found in drinking water. The sensitivity of the model for the different parameters was assessed based on the leaching rate, amount of calcite scaling and the index parameters used for conditioning drinking water (LSI and CCPP).

4.1 Range of parameters for sensitivity analysis on leaching and scaling

To get a first insight into the influence of different water compositions on the calculation of different index parameters and on leaching, we created a matrix with a reasonable range of the major elements in drinking water in the Netherlands (Table 7). The ranges were based on the *Drinkwaterbesluit* (2011) and expert judgement. From this a 'base-case' water composition was established and used in subsequent simulations. First. physical factors including the initial capillary porosity of the cement and the water temperature were also varied in separate simulations, followed by variations in the water composition.

Table 7 Water composition ranges used in the sensitivity study. Norms were obtained from the Dutch Drinkwaterbesluit *(2011).*SiO_2 given as a typical groundwater value.*

Parameter	Norm	Base case	Min	Med	Max	Unit
Alkalinity	>60	150	60	165	270	mg HCO_3/L
Ca	1 mmol/l	36	20	46	72	mg/L
pH	6-9.5	7.5	6	7.5	9	-
Al	<0.2	0.03	0	0.1	0.2	mg/L
NO_3	<50	25	0	25	50	mg N/L
Cl	<150	50	10	80	150	mg/L
Mg	1 mmol/l	10	0	10	20	mg/L
Na	<150	100	10	80	150	mg/L
S	<150	100	10	80	150	S as SO_4 mg/L
SIO_2	10-12 mg/l*	12	4	12	20	mg Si/L
O_2	>2	5	2	5	8	mg O_2/L
Index parameters						
EC	<1250					µS/cm
LSI	>-0.2					[-]
Temperature	< 25°C	16°C	10°C		25°C	°C

4.1.1 Influence of temperature and initial capillary porosity

The temperature was varied over a range of 10-25 °C, representing a reasonable range for water temperatures in the distribution network, with an upper limit of 25 °C. In addition, the initial capillary porosity was varied from 0-30%. The initial capillary porosity is determined by the total volume of water (w/c ratio) used to create the cement, see section 2.5 for more detail.

For the initial capillary porosity, the lower limit of 0% represents the expected, low w/c ratio of < 0.3 likely found for asbestos cement used in the distribution network (see section 2.4, Eternit, 1980), while the upper limit of 30% is a

very high w/c ratio (w/c > 0.6) and not expected in practice. Results with this initial capillary porosity therefore give an impression of the largest possible influence of the initial porosity to indicate its influence will not be larger than this.

4.1.2 Influence of the effect of water composition on leaching and scaling

A subset of the water compositions were run in the model for 10 years to determine which parameters have an effect on the scaling and leaching behavior of the cement. It was not computationally feasible to run all 177 147 combinations of the water compositions in the model, therefore a subset of the combinations were chosen. Twenty-three water compositions were created using the minimum, maximum and base-case values for the parameters given in Table 7. For each simulation, one parameter at a time was changed from the base-case value to either the minimum or the maximum. This results in n=11 compositions at the minimum, n=11 at the maximum and one composition with all parameters at the base-case for a total of 23 compositions. The simulations were run for 10 years, with a w/c ratio of 0.5 and cement cells of 0.25 mm. A base-case temperature of 16 °C was used for each simulation.

4.1.3 Extended sensitivity analysis on water composition for leaching and scaling

Based on the results from the initial sensitivity analysis (section 4.2.2), an extended sensitivity analysis was performed for the parameters which were found to affect the leaching, scaling and index parameters. The six parameters of interest (Alkalinity, pH, Ca, Mg, SiO_2 and S) were varied from high to low to create 64 ($n=2^6$) unique water compositions. These compositions were run for 10 years, with a temperature of 16 °C, w/c ratio of 0.5 and cement cells of 0.25 mm with a total 2 mm of cement. The total cement length was reduced from the standard 5 mm to 2 mm in order to save computational time.

4.2 Results of sensitivity analysis on leaching and scaling

4.2.1 Temperature & Initial capillary porosity

The influence of physical water quality parameters, including the water temperature and the initial capillary porosity of the cement were modelled. Influent water temperatures were ranged from 10 to 25 °C. Figure 10 shows the influence of temperature on the leaching rate, given as the leached depth plotted versus the square root of time. An increase in the temperature from 10 to 25°C results in a total increase in the leached depth of only 0.25 mm (20%) over 10 years and an increase in the leaching rate of 17% (Figure 10).

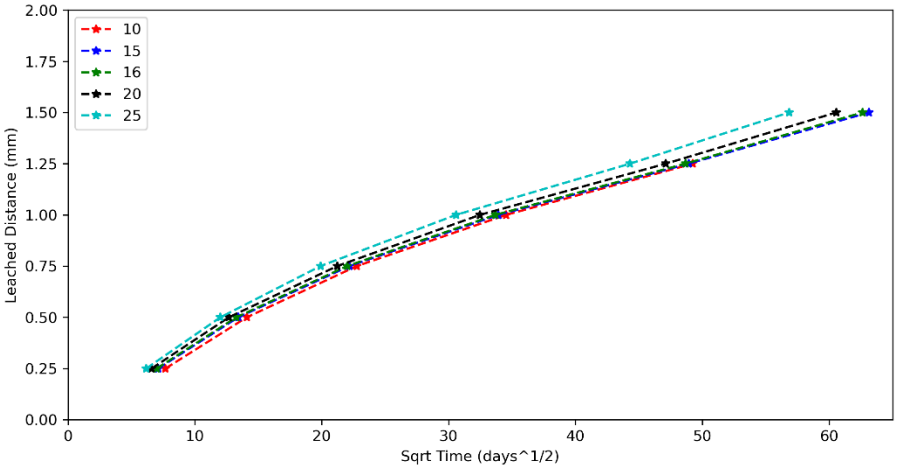

Figure 10 Influence of temperature of the water in the distribution network on the degree of degradation (given as portlandite depletion) for the base case water composition.

According to Jacques, Wang, et al. (2011) the rate of leaching of cement depends on (1) the amount of Ca in the cement, (2) the chemical composition of the influent water and (3) the flow rate through the cement. In the case of the temperature simulations, both the cement and water composition was kept constant between the simulations, however the temperature of the water influences the rate of diffusion through the cement. An increase in temperature from 10 to 25 °C results in a 54% increase in the diffusion coefficient. In addition to the increase in the diffusion constant, temperature also affects the equilibrium for minerals. Cemdata18 is able to take into account the changes in the mineral equilibria over a range of temperatures from 0-100 °C (Lothenbach et al., 2019). As can be seen in Figure 10 the difference in the diffusion rate and mineral equilibrium when the temperature is increased from 10 to 25 °C is minimal. Table 8 summarizes the changes in the index parameters and the total calcite precipitated as a result of the changes in temperature.

The influence of the initial capillary porosity of the cement was tested over a range from 0-30% (Figure 11). In contrast to the changes in temperature, increasing the initial capillary porosity results in substantial changes in the leaching rates. Increasing the initial capillary porosity from 0% to 10% resulted in the first cell (0.25 mm) leaching 6.24 times faster (0.54 years at 0% vs. 3.35 years at 10%), while an increase to 30% resulted in 236 times faster leaching (0.014 years, Figure 11).

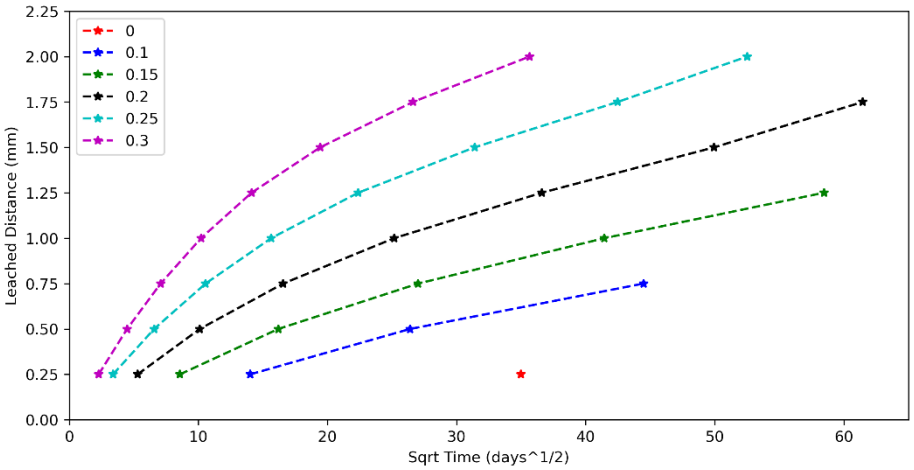

Figure 11 Influence of initial capillary porosity of the cement on the degree of degradation (given as portlandite depletion) for the base case water composition. The results show that increasing the initial capillary porosity of the cement has a substantial effect of the leaching of the cement when simulated over 10 years.

Higher porosity means larger pore sizes which means faster diffusion and thus leaching. This is a positive feedback loop, where an increase in diffusion allows dissolution products to be transported out of the inner cement pipe wall, which induces more dissolution of the remaining minerals. As expected, there was no change in the index parameters for the porosity simulations, since the same 'base-case' water composition was used in each simulation (Table 9).

Table 8 Water composition index parameters for the different temperatures simulated in the model. A temperature of 16 °C indicates the base case.

		Temperature (°C)				
Parameter	Unit	10	15	16	20	25
EC	µS/cm	835.9	957.1	982.1	1084.8	1218.4
SI	-	-0.58	-0.51	-0.50	-0.44	-0.37
LSI	-	-0.48	-0.42	-0.41	-0.36	-0.30
CCPP	mmol\L	-0.14	-0.12	-0.12	-0.10	-0.09
Aggressive CO_2	mg/L	6.32	5.35	5.17	4.51	3.75

Calcite precipitation	moles	2.18	2.19	2.20	2.28	2.37

Table 9 Water composition index parameters for the different initial capillary porosities simulated in the model were the same for each initial capillary porosity (EC: 982.1 µS/cm, SI: -0.5, LSI: -0.41, CCPP: -0.12 mmol/L, aggressive CO_2 5.17 mg/L) while the total calcite precipitation in the model after 10 years varied.

		Initial capillary porosity [-]					
Parameter	Unit	0	0.1	0.15	0.2	0.25	0.3
Calcite precipitation	moles	0.72	1.62	2.06	2.43	2.80	3.05

Notably, as the initial capillary porosity increased, so did the total calcite precipitation at the end of the 10 year simulation. It is commonly understood that calcite precipitation in the inner layers of the pipe wall, prevent leaching. However, this seems to contradict the observation that only with increasing leaching (high porosity) calcite precipitation increases.

It is well known that during the leaching of cement, not all minerals dissolve at the same time but in a certain order (Hockin et al., 2021; Jacques et al., 2010). This evolution of cement dissolution can be classified in 3 phases[4]. In phase 1 only Portlandite ($Ca(OH)_2$) dissolves. After it is (almost) completely dissolved, phase 2 begins because the resulting pH drop forces all minerals except calcite to dissolve as well. The end of phase 2 is determined by the complete dissolution of the CSH-gel. Phase 3 largely consists of a slow precipitation or dissolution of calcite ($CaCO_3$), depending on its SI in the feed water. This evolution of cement mineral dissolution and precipitation determines how and where calcite is formed in the cells in the model.

Calcite can form both during the dissolution of portlandite (phase 1) and/or during the dissolution of carbonate-containing minerals (e.g. monocarbonate, tricarboaluminate, phase 2). This process is illustrated schematically in Figure 12. During phase 1, the dissolution of portlandite results in free Ca^{2+} ions which can react with inorganic carbon present in the influent water as CO_3^{2-}. In phase 2, the dissolution of carbonate-containing minerals occurs after the complete dissolution of portlandite (phase 1). The dissolution of carbonate-containing minerals which produces CO_3^{2-} which can react with free Ca^{2+} ions present (for example as a result of dissolution of portlandite in phase 1 from deeper cells) and form calcite. In the simulations, the majority of the calcite precipitated during phase 2, therefore after the complete dissolution of portlandite. This results in the greater calcite precipitation observed in simulations with greater degradation, as the dissolution of portlandite followed by the carbonate-containing minerals (monocarbonate, tricarboaluminate) provide the necessary Ca^{2+} and CO_3^{2-} to precipitate calcite (Table 9).

[4] Note that these phase numbers are different from those of Jacques et al. (2010) and in the previous project (Hockin et al., 2021). In those references, phase 1 refers to the dissolution of sodium and potassium minerals (Na_2O and K_2O), phase 2: portlandite dissolution, phase 3: CSH, AFm and Aft phases, phase 4: calcite. As we do not include the sodium and potassium minerals in the current model we refer to a new phase numbering system here.

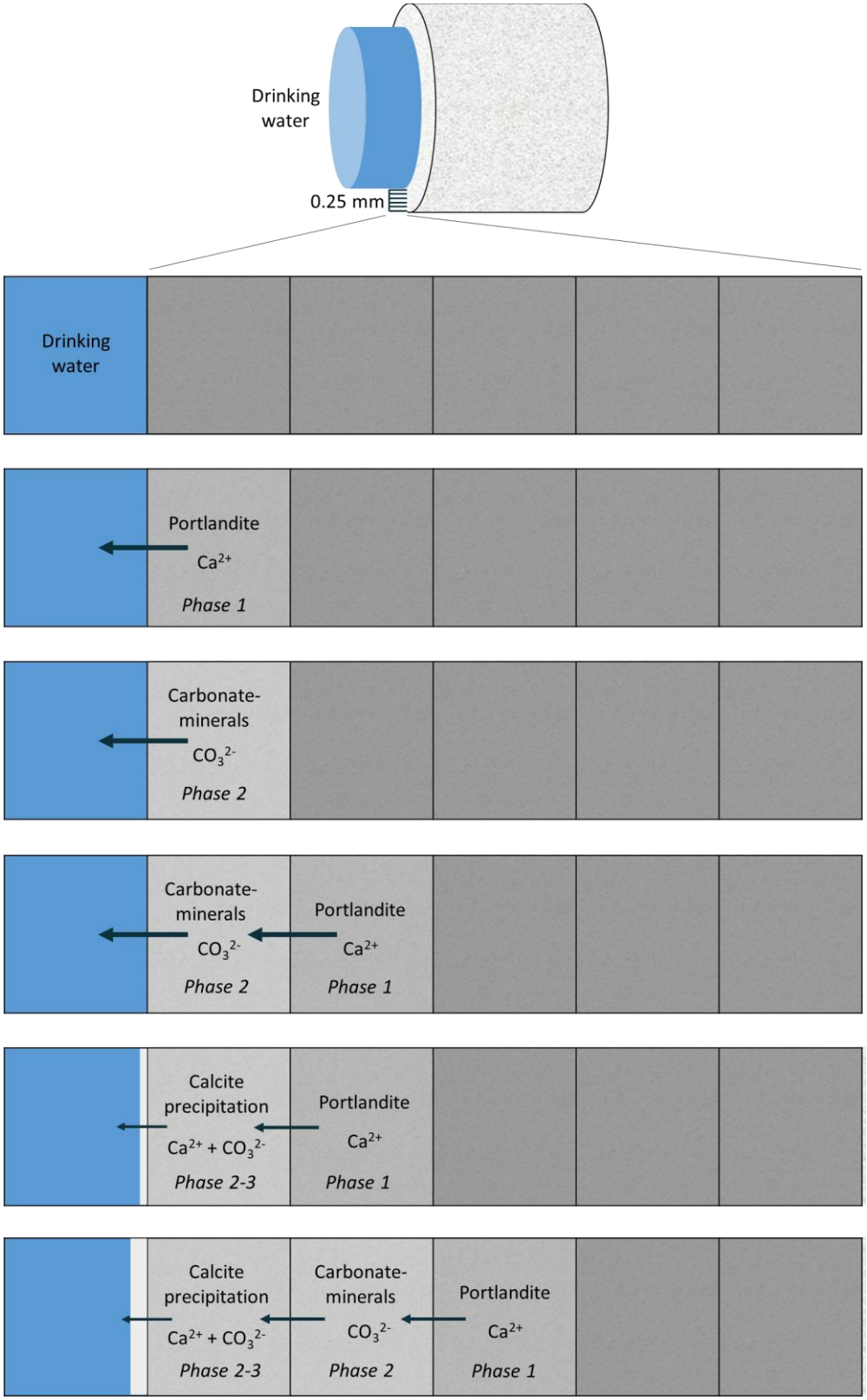

Figure 12 Illustration of the formation of calcite due to the dissolution of Ca^{2+} (Portlandite) and CO_3^{2-} (monocarbonate, tricarboaluminate) containing minerals in the different layers of the cement model. The model shows 5 cement cells (grey) and the influent drinking water in contact with the cement pipe on the left-hand side. First portlandite depletes in the inner cells or layers of the pipe wall. After portlandite depletes, carbonate-containing minerals dissolve. At the same time, portlandite dissolves in the deeper layers of the model. Due to diffusion of the Ca^{2+} from deeper cells and the co-incident release of CO_3^{2-} in the inner cells, calcite can form (light grey scaling on boundary between cement and drinking water). However, in the majority of cases calcite is only formed after the complete dissolution of portlandite in the inner cement layers.

4.2.2 Effect of water composition parameters on leaching and scaling

Leaching rates for each of the 23 water composition can be seen in Figure 13. It is clear that some parameters have little to no effect on the progress of leaching within 10 years (Al, NO_3, Cl, Na and O_2), while others had substantial effects on the index parameters and/or the leaching rate (Alkalinity, Ca, pH, Mg, S and SiO_2). The effect of each parameter on the leaching, scaling and the calculations of the index parameters is summarized in Table 10.

The lack of effect of Al, NO_3, Cl, Na, O_2, Mg and SiO_2 on the index parameters is expected, as these elements are not involved in the reactions of calcite. However, the influence of Mg, S and SiO_2 on the leaching rate and scaling was unexpected. These parameters, along with the usual suspects that influence leaching rates (Ca, pH and alkalinity) were explored further in the extended sensitivity analysis (section 4.2.3).

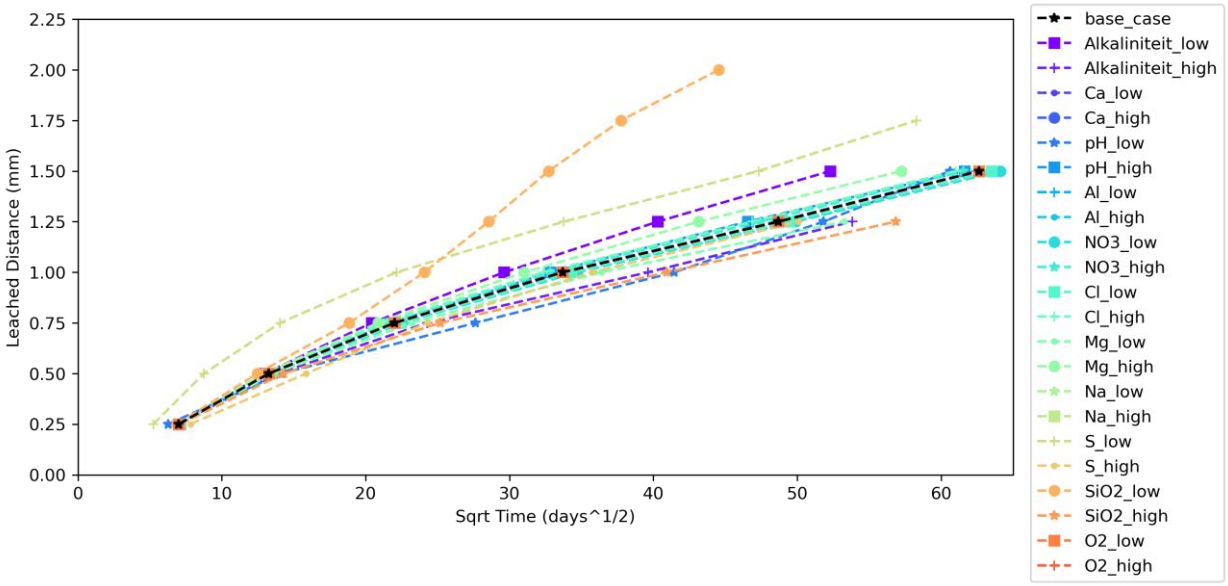

Figure 13 Differences in the leaching rates shown here as the leached depth as a function of the square root of time in days.

*Table 10 Summary of the effect of the different water composition parameters on the leaching-and scaling rates and the calculation of the various index parameters. Symbols (*) indicate if the absolute difference in value for the leaching/scaling/index parameter when the parameter of interest was set at either the minimum or maximum compared to the base case: - = no effect (0-5%), *<10%, ** (>10%), ***(>100%).*

			INDEX PARAMETERS	
Parameter	Leaching	Scaling	LSI	CCPP
Alkalinity	**	**	**	**
Ca	-	-	**	**
pH	-	***	***	***
Al	-	-	-	-
NO_3	-	-	-	-
Cl	-	-	-	-
Mg	**	**	-	-
Na	-	-	-	-
S	**	*	**	**
SIO_2	**	***	-	-
O_2	-	-	-	-

4.2.3 Extended sensitivity analysis on water composition for leaching and scaling

Based on the results from the initial sensitivity simulations, an extended set of simulations (n=64) was performed. They consist of the parameters that have shown an effect on the leaching, scaling and/or index parameters (Alkalinity, Ca, pH, Mg, S and SiO_2; see section 4.2.2). The resulting leaching rates of all 64 simulations are summarized in Figure 14, it shows extensive variation in the leaching rate depending on the water composition. The graph gives a nice overview of the results, but is too complex to be discussed in itself. Therefore, the 64 simulations are discussed by looking at the influence of alkalinity, calcium, pH, Mg, SO_4 and SiO_2 on the leaching rate; each of which are discussed separately below. The water compositions for each of the 64 simulations is given in Table 16 (Appendix VIII).

In addition, in Figure 15 the leached distance as a function of the square root of time have been plotted for the four drinking water compositions and the base-case, superimposed over the results of the extended sensitivity simulations. The results show that the leaching for the four drinking water compositions is within the range of the leaching for the water compositions simulated, therefore the simulations are demonstrative of the leaching rates expected for drinking water compositions from practice. The base-case composition leaching rate is below that of the four drinking water compositions.

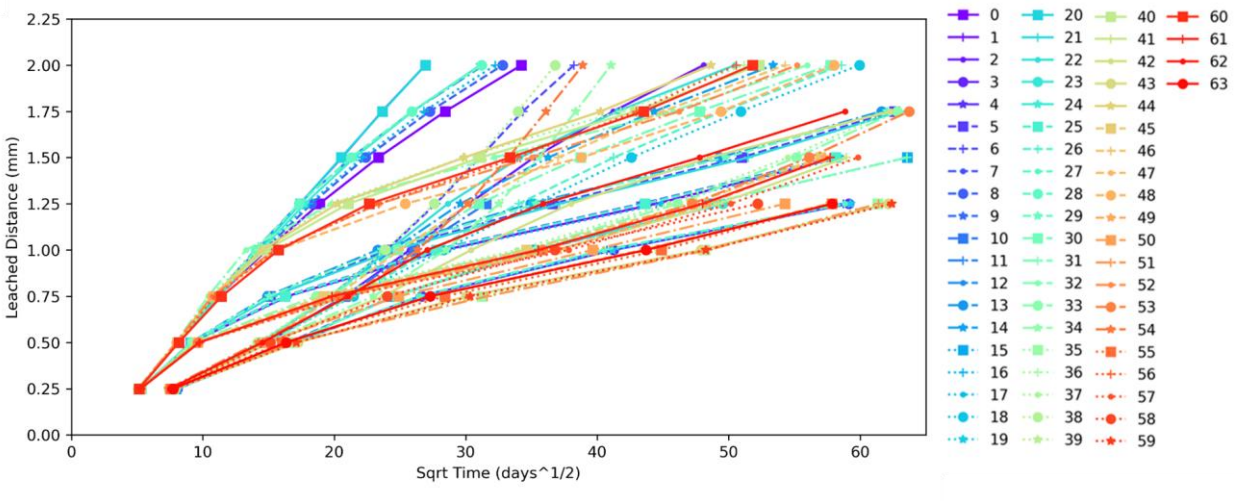

Figure 14 Leaching rates shown here as the leached depth as a function of the square root of time in days for the extended sensitivity analysis. The water compositions for each of the 64 simulations is given in Table 16 (Appendix VIII).

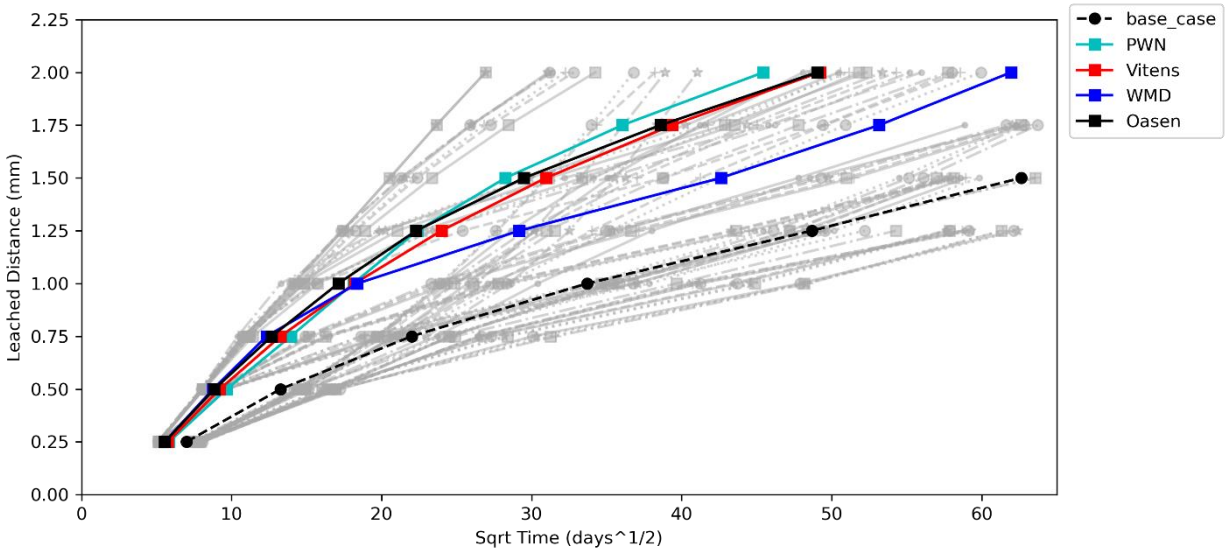

Figure 15 The 'base-case' (black dashed line) and the four drinking water compositions have been added to the graphic for comparison to all 64 the simulations shown in Figure 14. The simulations there are representative of the water compositions which can be expected in practice.

SiO_2

The extended sensitivity analysis show substantial differences in the leaching rate of the cement when SiO_2 concentrations were low (4 mg/L as Si) compared to high concentrations (20 mg/L as Si). This is illustrated in Figure 16 where all 64 simulations are plotted as one dot each; the dot indicates their LSI and leaching rate after 10 years. SiO_2 pairs are connected by a black line. Here each pair refers to the fact that for every simulation there exists exactly one simulation which has the same water composition, except for the SiO_2 concentration; after all, the 64 simulations consist of the linear combinations of two concentrations of amongst others, SiO_2. The graph shows that for all 32 SiO_2 pairs, the lower SiO_2 concentration (4 mg/L) has faster leaching compared to its high SiO_2 counterpart. This difference is sometimes small with a 2 fold increase of the rate, but sometimes the same change in SiO_2 concentration gives a 10 fold increase in leaching rate. Changing the SiO_2 concentration has no effect on the LSI, which was already shown in Table 10 in section 4.2.2. The influence of different water composition parameters on the different index parameters is discussed separately in section 4.3.

Another observation from Figure 13 is that all simulations with higher SiO_2 have leaching rates that have a minor variation (roughly between 0.1 and 0.2 mm/yr) while their lower SiO_2 counterparts show much larger variations (0.15 – 1 mm/yr). Apparently, when sufficient SiO_2 is in the water (at least more than 4 mg/L, maybe up to 20 mg/L) leaching is significantly suppressed. Or in other words, when insufficient SiO_2 is in the water (4 mg/L), leaching is promoted.

A big influence of dissolved SiO_2 on the leaching of cement is not common knowledge. Not in the (Dutch) drinking water sector, but also more general; no papers were found that discuss this topic (after a brief scan). Therefore, it is required to look deeper into what are the mechanism that explain the influence of SiO_2 on the leaching rate. To this end, we look in more detail at the simulation with the fastest and slowest leaching which are water composition number 4 and 43 respectively. Their SiO_2 pairs are composition 5 and composition 42, respectively.

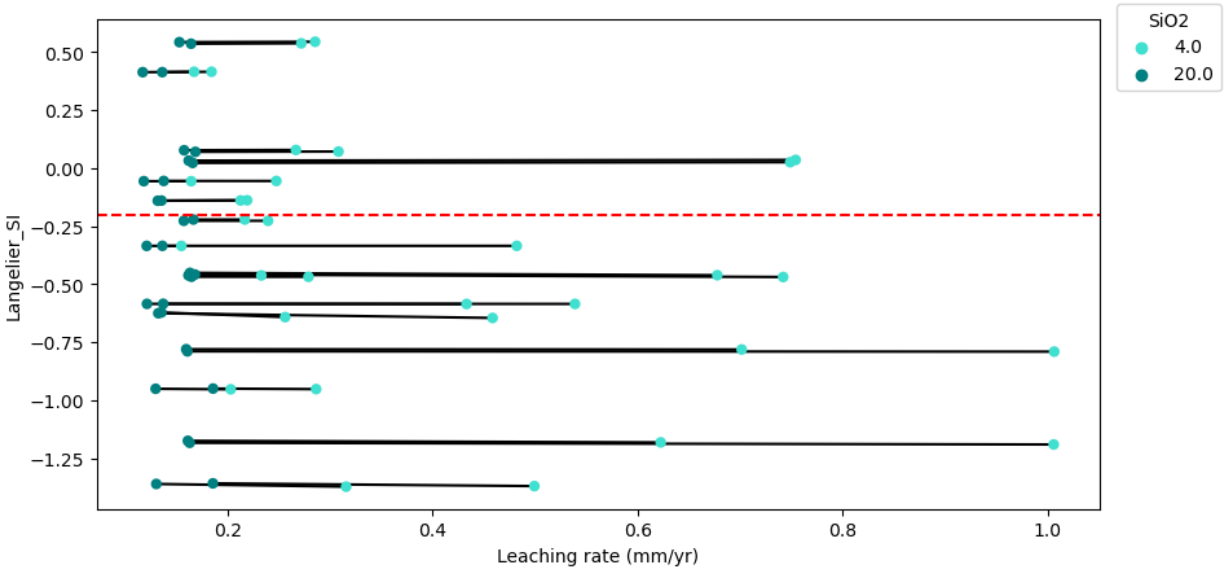

Figure 16 Leaching rate in mm/yr after 10 years versus the Langelier SI for different SiO_2 concentrations. The black lines join matching pairs of water compositions where the only difference is the concentration of SiO_2. The results show higher leaching rates for each composition with the low SiO_2 concentration.

Examination of these pairs shows that low SiO_2 results in the complete dissolution of the CSH-gel (Figure 17), consisting of jennite and tobermorite (Tob-II) which constitute the full CSH-gel in our cement model. The high SiO_2 composition (Figure 18) shows an increased precipitation of jennite during portlandite dissolution (phase 1, see section 4.2.1 for an explanation of the phases). This decreases the capillary porosity and extends portlandite dissolution (phase 1) slightly. In both cases, once portlandite is fully dissolved in the first cell, monocarbonate and jennite dissolve and tobermorite, ettringite and straetlingite precipitate (phase 2). When all monocarbonate is dissolved, tricarboaluminate and jennite dissolve further. Once jennite is low, tobermorite begins to dissolve. In the case of the low SiO_2 composition, jennite depletes completely, resulting in the complete dissolution of tobermorite, followed by the complete dissolution of ettringite (Figure 17). The complete dissolution of the CSH-gel signals the end of phase 2 and the start of phase 3. In contrast, for the high SiO_2 composition, the amount of jennite increases, stabilizing the tobermorite concentrations (Figure 18) to such an extent that it never depletes and phase 3 is never entered. The only difference between these simulations is the difference in SiO_2 concentration in the influent water.

We speculate that the high SiO_2 in the influent water, causes the precipitation of jennite which stops the evolution of cement leaching such that it never enters phase 3 and, as such, prevents further leaching. This influence can explain the major impact seen in Figure 16, because the complete loss of the CSH-gel (in the low SiO_2 simulations) results in a (large) increases in the capillary porosity, resulting in a positive feedback loop of increased dissolution due to increased diffusion (which increase leaching etc.).

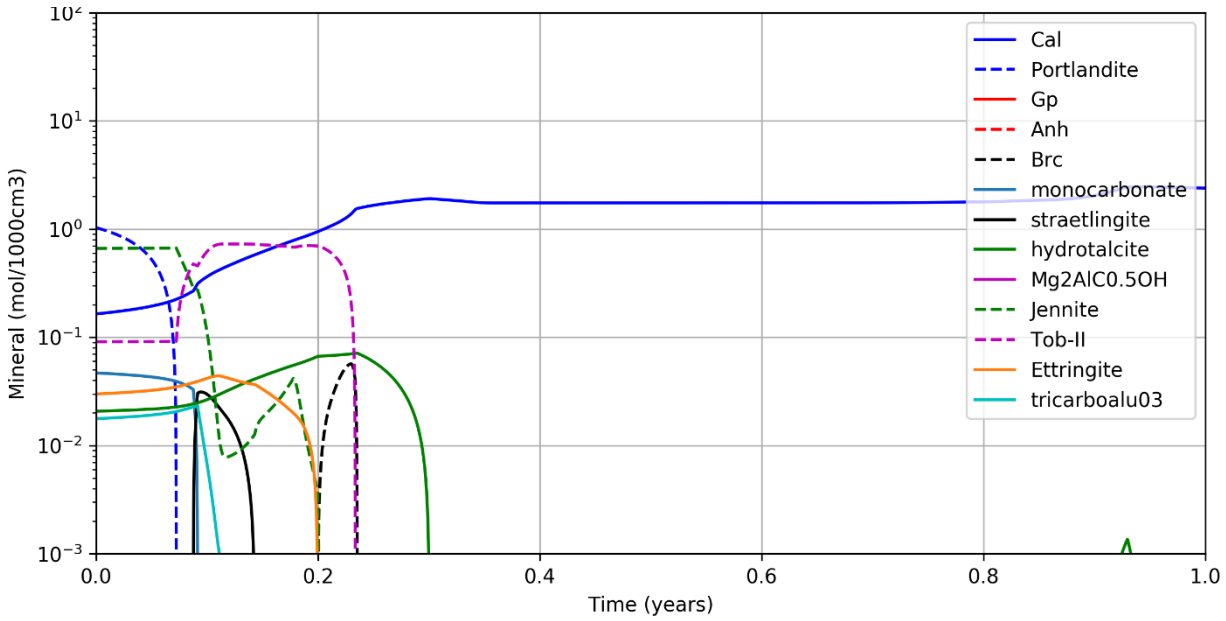

Figure 17 Composition 4 which has low (4 mg/L) SiO_2. The low SiO_2 results in the complete dissolution of the CSH-gel which consisting of jennite and tobermorite (Tob-II).

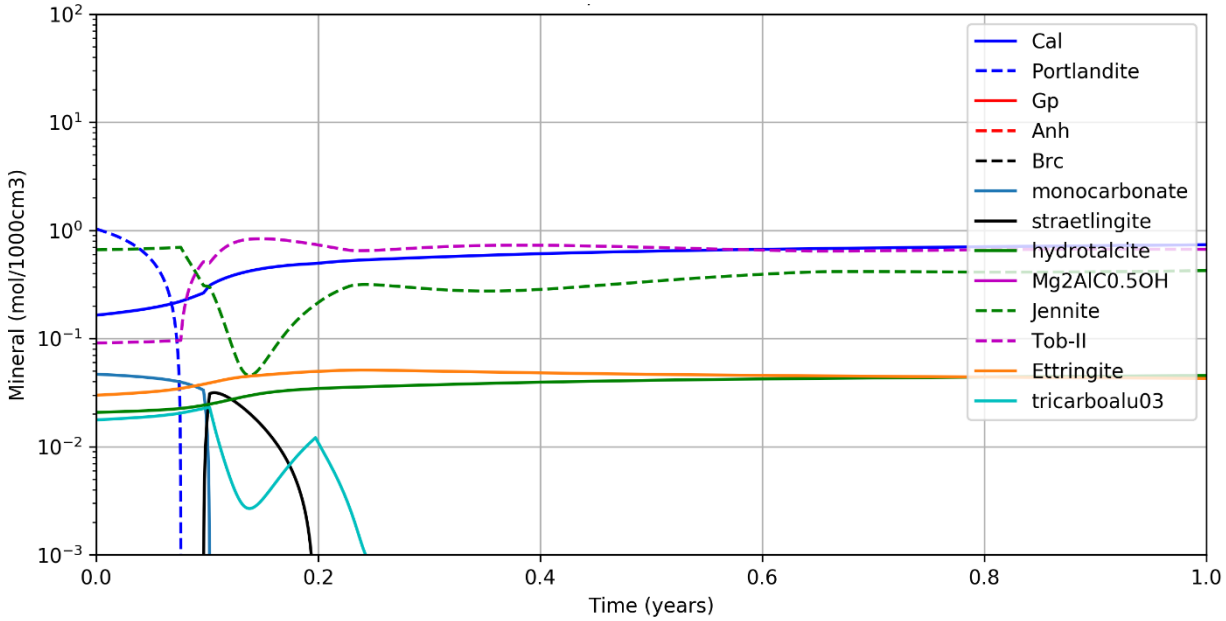

Figure 18 Composition 5 has a high SiO_2 composition (Figure 18 mg/L) and shows an increased precipitation of jennite during portlandite dissolution phase. The increased dissolution of jennite is difficult to see in the graphic due to the log scale.

As discussed in section 4.2.1, a somewhat paradoxical result is that in some simulations, the increase in degradation results in increased calcite precipitation as a result of more free Ca^{2+} coming from the deeper parts of the pipe wall that interact with CO_3^{2-} that occurs due to the dissolution of carbonate-containing minerals. This is also observed in the simulations with low SiO_2 – increased degradation results in the increased scaling (of the pores) due to precipitation of calcite (dark blue line in Figure 17 and Figure 18, see also Figure 32 in Appendix IX).

Mg

The results show that increasing the concentration of Mg, has either very little effect or increases the rate of leaching (Figure 19). When the concentration of SiO_2 is low increasing Mg results in increased leaching. When SiO_2

is high, there is little effect of increased Mg-concentrations on either the leaching or scaling. The influence of SiO_2 on leaching and scaling are discussed in the section above. Focusing on the changes as a result of Mg, hydrotalcite, a Mg-containing mineral, precipitates during phase 2 in high-Mg compositions (Figure 20), while the mineral concentration remains constant in low-Mg compositions (Figure 21). While hydrotalcite precipitates in high Mg compositions during phase 2, there is also increased dissolution of the CSH-gel minerals jennite and tobermorite, shortening phase 2. As the only difference between the simulations is the increased Mg-concentration in the influent water, this should be the cause of the increased hydrotalcite precipitation, increased dissolution of the CSH-gel and subsequent stable calcite precipitation. We speculate therefore that the low Mg concentrations lengthen phase 2 of the cement and prevents further leaching. This can be seen in the lack of stable calcite precipitation observed in the low Mg compositions. As was explained in section 4.2.2 and illustrated in Figure 12, increased calcite precipitation can result from increased leaching which dissolves of portlandite and carbonate-containing minerals in deeper cells. This is also visible in Figure 33 and Figure 34 (Appendix IX) where the moles of calcite precipitated increase but only for water compositions with low SiO_2. As can be seen in Figure 19, changes in Mg have little on the LSI.

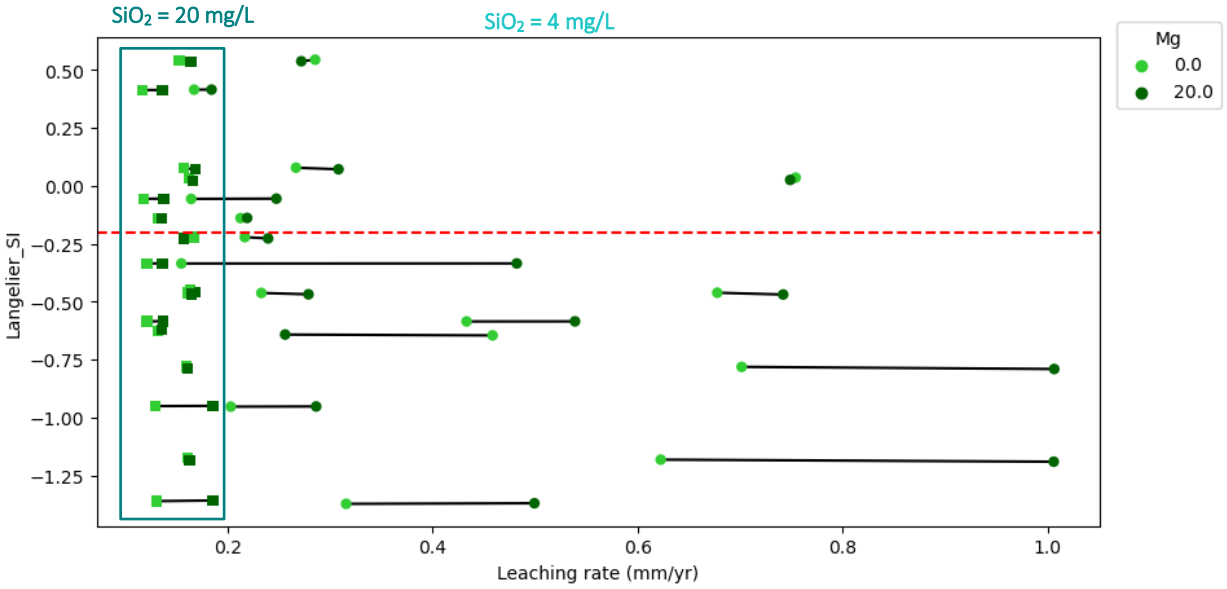

Figure 19 Leaching rate in mm/yr after 10 years versus the Langelier SI for different Mg concentrations. The black lines join matching pairs of water compositions where the only difference is the concentration of Mg. The square symbols indicate water compositions with high SiO_2 concentrations (20 mg/L) while the round symbols indicate low SiO_2 concentration (4 mg/L).

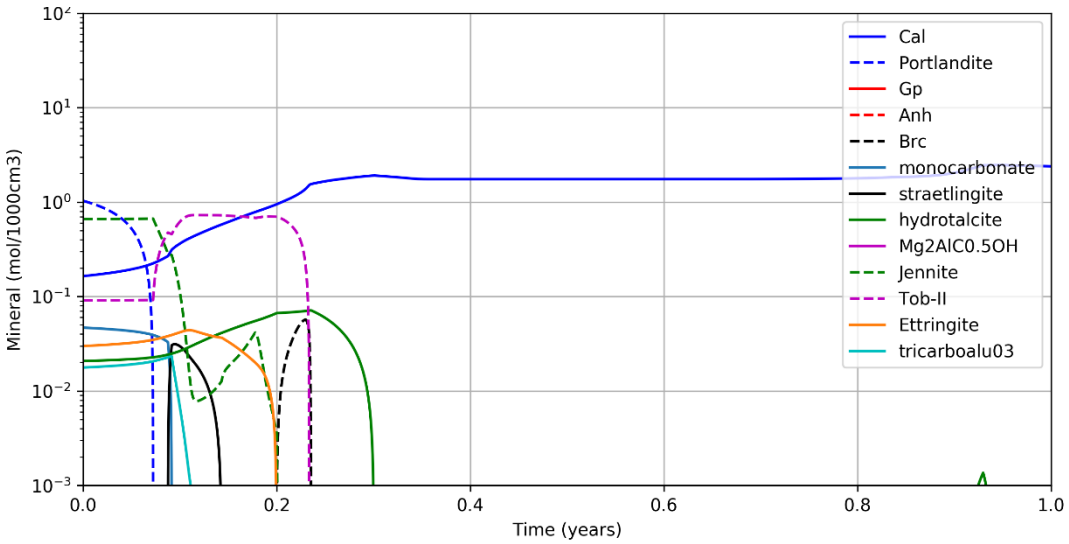

Figure 20 The mineral concentration of the first cement cell as a function of time for Composition 4 which has high Mg (20 mg/L) and show increased precipitation of hydrotalcite, a Mg-containing mineral, during phase2. As a result, calcite precipitation appears to be stable in the first cell. Increased calcite precipitation has been shown to be related to increased dissolution of portlandite in deeper cells of the cement, as illustrated in Figure 12.

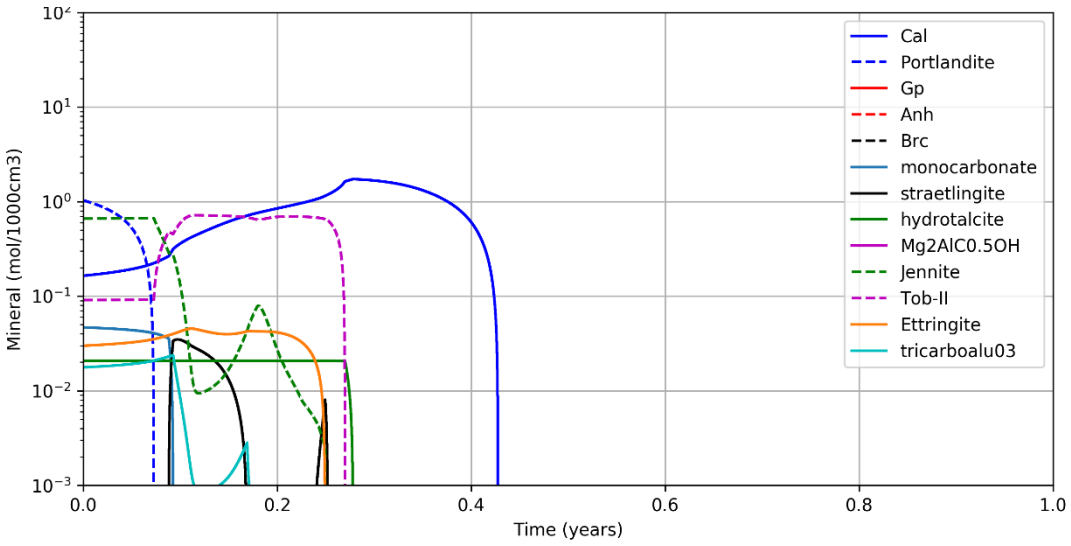

Figure 21 The mineral concentration of the first cement cell as a function of time for Composition 0 which has low Mg (0 mg/L). Calcite is not stable in the first cell, which may be due to a lack of Ca^{2+} or CO_3^{2-} from increased dissolution of portlandite or carbonate-containing minerals in deep cells, as illustrated in Figure 12

S

Figure 22 shows the change in the leaching rate for the extended sensitivity analysis for the pairs of simulations where only S is changed. Similar to the Mg results described in the section above, the effect of increased S depends on the SiO_2 concentration of the water: when SiO_2 is low (round symbols), increasing the S concentration decreases the leaching rate, while when SiO_2 is high (square symbols), changing the S concentration has much less effect on the leaching rate. Five water compositions are exceptions, where increasing the S concentration increases the leaching rate, regardless of the SiO_2 concentration. However, no clear pattern in the water compositions could be determined to explain why these pairs differed in their behavior. The pairs of S water compositions are composition 4 with low S (10 mg/L, Figure 17) and composition 6 with high S (150 mg/L, Figure 23). Examination of the S pairs of water compositions shows that high S concentrations result in increased precipitation of ettringite (a S-containing mineral) during phase 2. This increased ettringite precipitation promotes the precipitation of

tobermorite, a component of the CSH-gel. In contrast, when S is low, there is no increased ettringite or tobermorite precipitation and there is complete dissolution of the CSH-gel, shortening the length of phase 2 which in turn promotes further leaching of the cement.

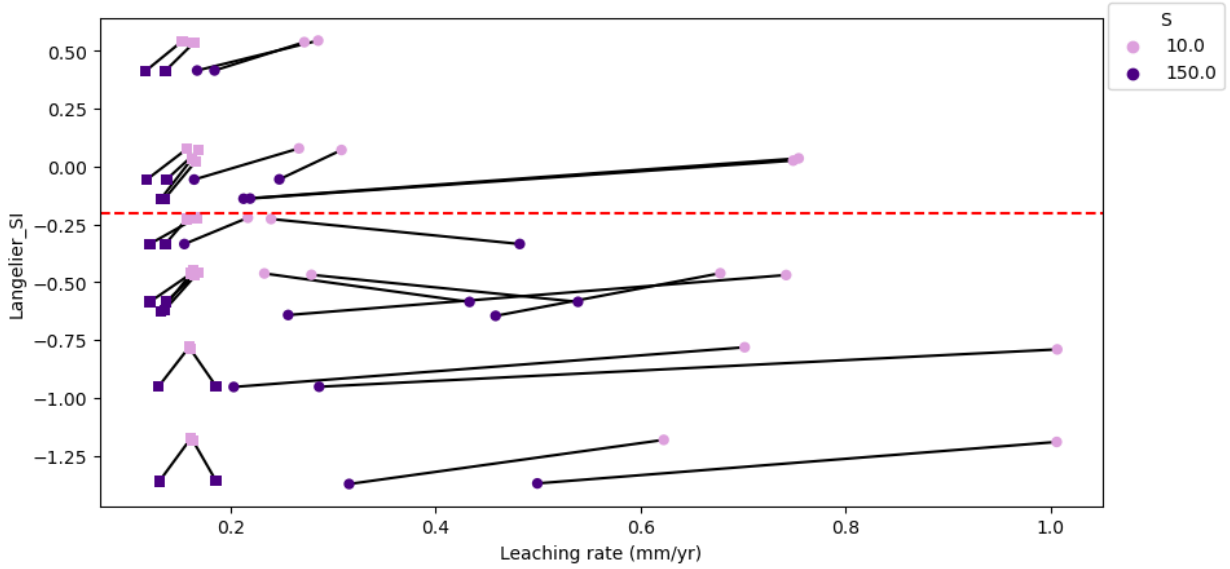

Figure 22 Leaching rate in mm/yr after 10 years versus the Langelier SI for different S concentrations. The black lines join matching pairs of water compositions where the only difference is the concentration of S, indicated by the color of the symbol. The square symbols indicate water compositions with high SiO_2 concentrations (20 mg/L) while the round symbols indicate low SiO_2 concentration (4 mg/L). The results show higher leaching rates for low S concentrations, dependent on the SiO_2 concentration.

Scaling (calcite precipitation) was also found to be dependent on the SiO_2 concentration, with little differences in calcite precipitation when SiO_2 concentrations were high (Figure 34, Appendix IX). When SiO_2 concentrations are low, however, no discernable pattern in the change in calcite precipitation was found for changes in the S concentrations.

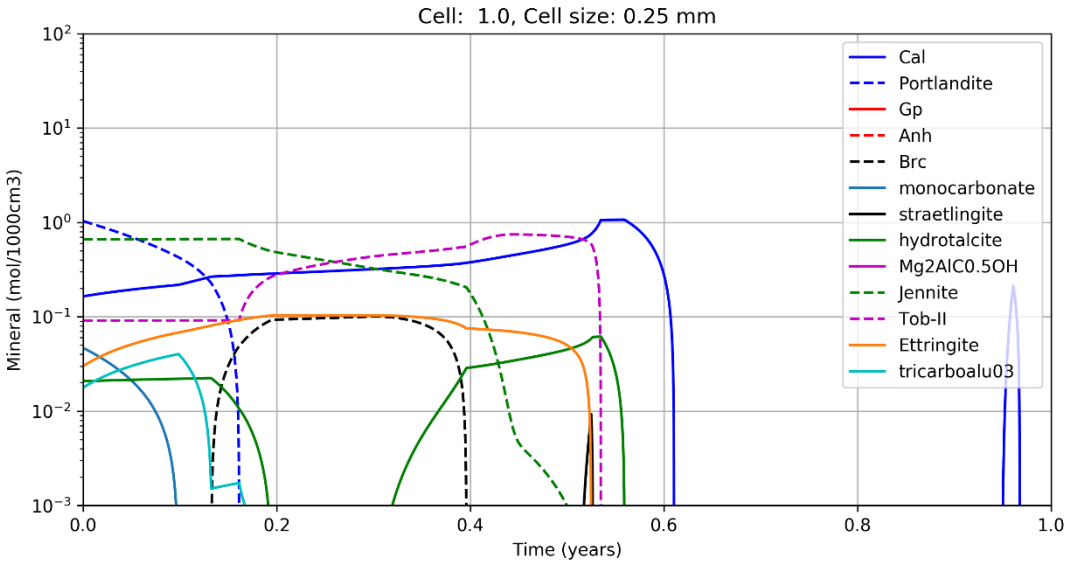

Figure 23 The mineral concentration of the first cement cell as a function of time for Composition 6 which has high S (150 mg/L). When compared to the low S composition pair (Figure 17), phase 2 is lengthened as a result of high S, signaled by the complete dissolution of the CSH-gel (jennite and tobermorite).

Ca

Figure 24 shows the change in the leaching rate for the extended sensitivity analysis for the pairs of simulations where only Ca is changed. The effect of Ca on the leaching rate was found to be dependent on the SiO_2 concentration, as has been shown in the sections above for Mg and S. When SiO_2 is low (round symbols Figure 24), increasing the Ca concentration has practically no effect on the leaching rate, while when SiO_2 is high (square symbols Figure 24), increasing the Ca concentration decreases the leaching rate. There are five exceptions to this, where increasing the Ca concentration increases the leaching rate (four pairs of compositions with leaching rates greater than 0.6 mm/yr and one pair with leaching in the range of 0.3 mm/yr in Figure 24). The interconnected effects of changing multiple water composition parameters at once are too complex to discuss here. Examination of the Ca water composition pairs shows that low Ca compositions have a shorter phase 2, due to faster dissolution of jennite, a component of the CSH-gel, compared with compositions with high Ca. A shorter phase 2, results in faster leaching of the cement. Interestingly, no substantial differences in the scaling of calcite were observed for most water compositions when Ca concentrations were changed (Figure 35, Appendix IX). For the compositions where there was a substantial differences in the moles of calcite precipitated, no pattern in the water compositions could be discerned.

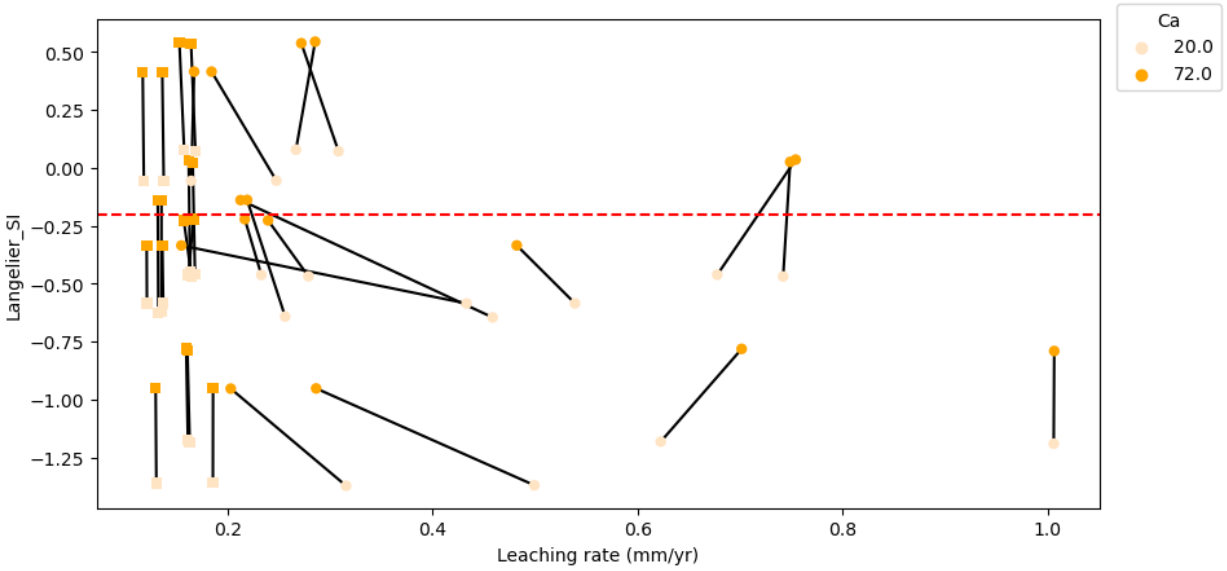

Figure 24 Leaching rate in mm/yr after 10 years versus the Langelier SI for different Ca concentrations. The black lines join matching pairs of water compositions where the only difference is the concentration of Ca, indicated by the color of the symbol. The square symbols indicate water compositions with high SiO_2 concentrations (20 mg/L) while the round symbols indicate low SiO_2 concentration (4 mg/L). The results show no little or no difference in leaching when SiO_2 concentrations are high, while when SiO_2 concentrations are low generally increased Ca decreases leaching.

pH, Alkalinity

Both pH and alkalinity, here given as the concentration of HCO_3^-, affect the leaching and scaling rates. However, there is no consistency in the magnitude or direction of the effect, as is visible in Figure 25 and Figure 26 (below)and Figure 36 and Figure 38 (Appendix IX). The influence of SiO_2 on the leaching rate (square symbols, as discussed in the sections above) is visible in the graphics, with lower leaching rates for the high SiO_2 concentrations, regardless of the pH or alkalinity (Figure 25 and Figure 26). The influence of SiO_2 with pH and alkalinity is less dominant for calcite precipitation (Figure 36 and Figure 38, Appendix IX).

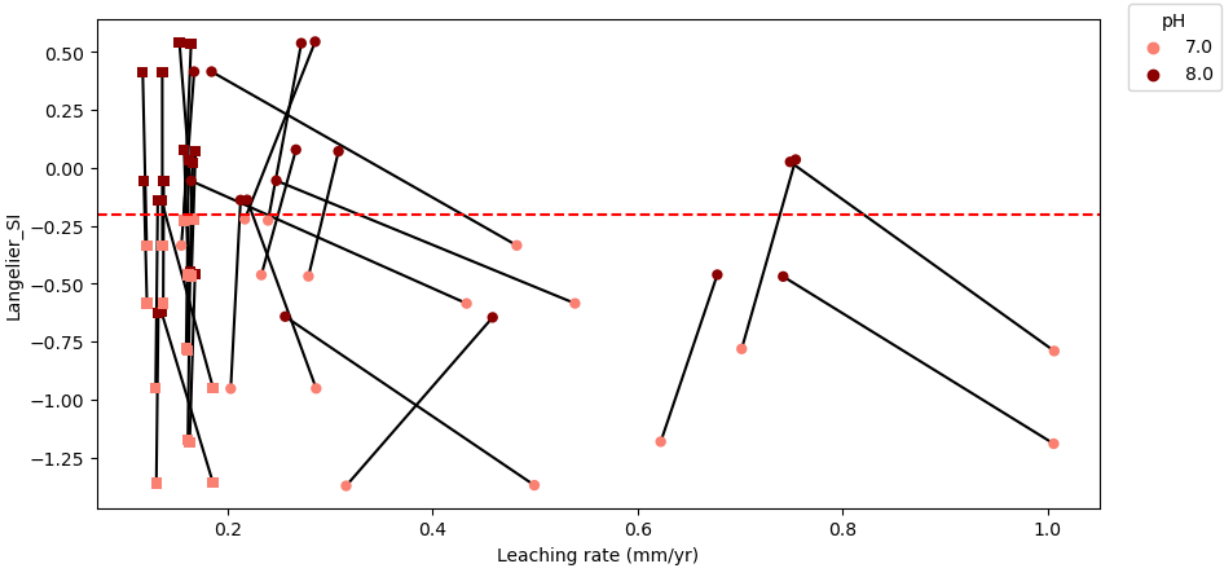

Figure 25 Leaching rate in mm/yr after 10 years versus the Langelier SI for different pH. The black lines join matching pairs of water compositions where the only difference is the pH, indicated by the color of the symbol. The square symbols indicate water compositions with high SiO_2 concentrations (20 mg/L) while the round symbols indicate low SiO_2 concentration (4 mg/L).

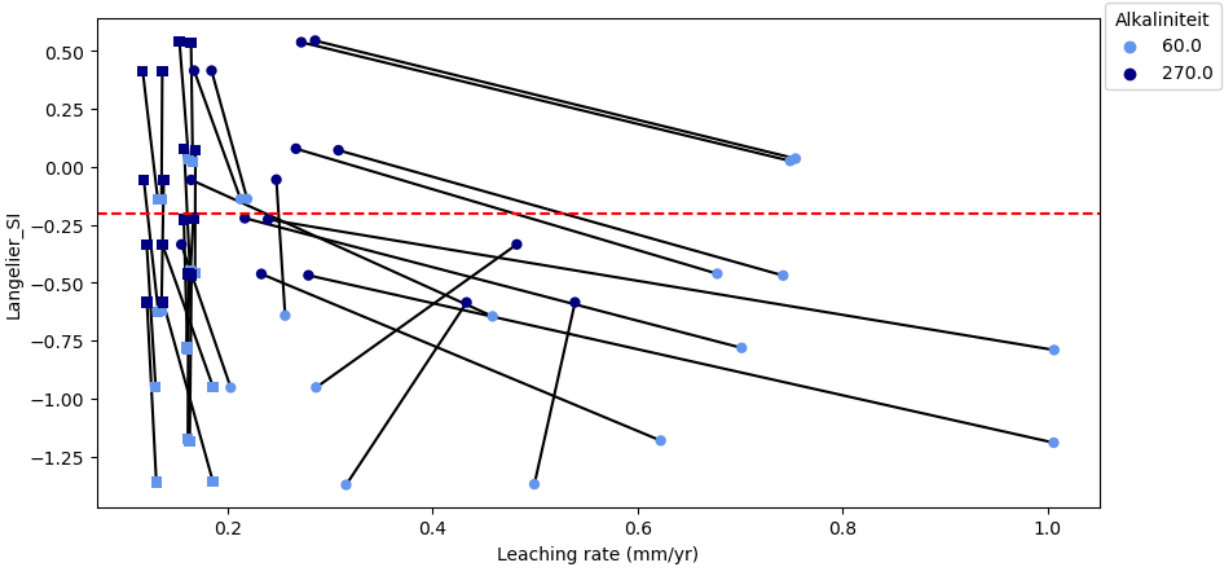

Figure 26 Leaching rate in mm/yr after 10 years versus the Langelier SI for different alkalinity concentrations (in mg HCO_3^- per L). The black lines join matching pairs of water compositions where the only difference is the alkalinity, indicated by the color of the symbol. The square symbols indicate water compositions with high SiO_2 concentrations (20 mg/L) while the round symbols indicate low SiO_2 concentration (4 mg/L).

4.2.4 Discussion of the influence of water composition on leaching and scaling

Table 11 summarized the effects on the leaching, scaling and index parameters of the different water composition parameters discussed above and possible mechanisms for these effects. What stands out from the sensitivity analysis is the effect that low SiO_2 concentrations have on the leaching and the importance of the CSH-gel for determining how quickly the cement degrades. The sensitivity analysis also highlighted that scaling in the form of calcite precipitation does not prevent leaching as initially thought.

SiO_2 influenced the leaching rate the most of all the water composition parameters. This was surprising as no literature on the subject could be found which discussed the influence of Si concentrations in influent water and no index parameter is known which is influenced by SiO_2. The low SiO_2 concentrations seem to promote the

dissolution of the CSH-gel, which shortens phase 2 of the cement degradation increasing the degradation rate. The effect of SiO_2 should be validated using experiments, for example by varying the influent SiO_2 concentration and measuring the effect on portlandite dissolution and other changes in the cement minerology and microstructure. In addition, a larger range in SiO_2 concentrations should be modelled, with input from the drinking water utilities on typical Si concentration in the water. Furthermore, it would be interesting to examine any data on problematic locations (areas with known high leaching rates) and see if there is any relationship with the Si concentration of the drinking water.

A second important insight from the sensitivity analysis is the role of calcite scaling in preventing leaching. Initially it was thought that the key to preventing leaching was to promote the precipitation of calcite layers on the inner pipe walls. The coating of the calcite layer was thought to prevent the dissolution of portlandite, thereby protecting the pipe from degradation. We have highlighted that in fact, in most cases, calcite is primarily formed only after the complete dissolution of portlandite. In fact, the dissolution of portlandite provides Ca^{2+} and the dissolution of the carbonate-containing minerals (monocarbonate and tricarboaluminate) provide the CO_3^{2-} necessary to precipitate calcite. Therefore the cement must by definition degrade to form calcite. However, as discussed in section Error! Reference source not found., the relationship between calcite, porosity and diffusion in the model could be improved. Currently, the model uses the general effective media (GEM) equation (Oh et al., 2004) to model the change in diffusion as a result of changes in porosity. However, the equation assumes a lower limit of diffusion which may be too high when calcite precipitation is taken into account – the effect is that essentially pores can never be fully blocked no matter the amount of calcite precipitation. Future research could investigate the microstructural properties of calcite precipitation in drinking water pipes to better estimate the changes in porosity as a result of calcite precipitation and to inform a better relationship between calcite precipitation, changes in porosity and changes in diffusion.

A final important insight from the sensitivity analysis is the role that the CSH-gel plays in controlling the degradation rate of the cement. During phase 2, portlandite has (mostly) already depleted and the remaining cement minerals begin to dissolve. The end of phase 2 is marked by the complete dissolution of the CSH-gel. It was found in the sensitivity analysis that for most water composition parameters the changes in leaching associated with an increase or decrease of a certain parameter could be linked back to changes in mineral dissolution/precipitation which ultimately affected the length of phase 2. The changes in phase 2 also influence the formation of calcite. As discussed, and illustrated in Figure 12, both Ca^{2+} and CO_3^{2-} are required to form calcite. Ca^{2+} is available primarily from portlandite dissolution in phase 1 and CO_3^{2-} from carbonate minerals in phase 2. It is proposed that there is an interplay between the different layers of the cement, where deeper layers are dissolving portlandite while shallower layers are dissolving carbonate-minerals. The diffusion from deeper to shallower layers results in the contact between the Ca^{2+} and CO_3^{2-}. A longer phase 2 may result in longer contact of Ca^{2+} and CO_3^{2-} and therefore more calcite formation, while a shortening of phase 2 results in both faster degradation and less calcite formation. Two important considerations here are the diffusion rates of both Ca^{2+} and CO_3^{2-} and the kinetics of the mineral dissolution and precipitation.

First, the model currently implements a multi-component diffusive transport code, where Ca^{2+} and CO_3^{2-} have different diffusion rates (Table 14, Appendix III), with CO_3^{2-} being ~1.2 times faster than Ca^{2+}.How the dynamics of the different diffusion rates, combined with the kinetics of the dissolution/precipitation rates plays out in the cement and in the model requires further investigation. For example, is one of Ca^{2+} or CO_3^{2-} the limiting parameter for calcite formation and if so what does this imply for the conditioning of drinking water to protect cement pipes?

A second important consideration is that the model assumes equilibrium reactions and does not take into account differences in the kinetics of the different mineral reactions. For example, how quickly the CSH-gel dissolved was found to be critical for determining the overall rate at which the cement degraded and in particular the effect of increasing or decreasing the SiO_2 concentration. However, if the kinetics of CSH-gel dissolution or precipitation are extremely slow compared to, say portlandite dissolution or calcite precipitation, this could have a large impact on

the leaching rates calculated in the model. It was outside the scope of this research to incorporate kinetic rates of reactions for the different cement minerals but future work should focus on investigating the kinetics for the most important cement minerals (e.g. portlandite, calcite, jennite/tobermorite (CSH-gel)).

A final important consideration for the water composition is the relationship between the water composition and the index parameters used to condition the water to prevent leaching. This is explored in the next section.

Table 11 Summary of the effect of different water composition parameters on the leaching, scaling and index parameters and the corresponding mechanisms.

PARAMETER		EFFECT	POSSIBLE MECHANISMS
SiO_2	Leaching	• ↓ SiO_2 = ↑ leaching • Low SiO_2: high degradation (> 0.2 mm/yr) • High SiO_2: low degradation (< 0.2 mm/yr)	Speculate that low SiO_2 promotes the dissolution of the CSH-gel (Si containing minerals), which shortens phase 2 and leading to faster degradation of the cement.
	Scaling	• ↓ SiO_2 = ↑ calcite precipitation • Low Mg: increase in scaling is low • High Mg: increase in scaling is high	Low SiO_2 means more degradation, which in turn leads to more Ca^{2+} and CO_3^{2-} available for calcite precipitation (see section 4.2.2, Figure 12).
	LSI, CCPP	• No effect	
Mg	Leaching	• ↑ Mg = ↑ leaching • High Mg: higher degradation • When SiO_2 low, high Mg has more effect (more degradation)	High Mg compositions precipitate hydrotalcite (Mg-containing mineral) and promotes dissolution of the CSH-gel, while low Mg appear to lengthen phase 2, decreasing the cement degradation.
	Scaling	• When SiO_2 high no difference in scaling due to changes in Mg • when SiO_2 low, ↑ Mg = ↑ scaling	High Mg leads to more degradation, leads to more Ca^{2+} and CO_3^{2-} available for calcite precipitation.
	LSI, CCPP	• No effect	
S	Leaching	• ↑ S = ↓ leaching • High S: slower first cell depletion of portlandite • Low S: faster degradation • Depends on SiO_2, when SiO_2 high differences in leaching are small	High S precipitates ettringite (S containing mineral), promotes precipitation of the CSH-gel lengthening phase 2, decreasing cement degradation.
	Scaling	• When SiO_2 high differences in scaling due to changes in S are small • When SiO_2 low, differences in scaling due to changes in in S are larger, but there is no consistent pattern	
	LSI, CCPP	• ↑ S = ↓ LSI, CCPP	High S concentrations promote dissolved $CaSO_4$ formation, reducing free Ca^{2+} in the water which lowers the LSI and CCPP.

Ca	Leaching	• When SiO_2 is high, no difference in leaching for changes in Ca • When SiO_2 low, ↓ Ca = ↑ leaching	When SiO_2 is low, low Ca leads to the complete dissolution of the CSH-gel faster than for higher Ca concentrations. The dissolution of the CSH-gel shortens phase 2, increasing degradation of the cement.
	Scaling	• No pattern easily discernable	
	LSI, CCPP	• ↑Ca = ↑ LSI and CCPP	
pH	Leaching & Scaling	• No pattern easily discernable	
	LSI, CCPP	• ↑ pH = ↑ LSI and CCPP	
Alkalinity	Leaching & Scaling	• No pattern easily discernable	
	LSI, CCPP	• ↑ Alk = ↑ LSI • High pH, ↑ Alk = ↑ CCPP • Low pH, ↑ Alk = ↓ CCPP	High alkalinity-low pH: At pH 7, some dissolved carbonate is in the form of CO_2 which reacts with H_2O to form H_2CO_3 which promotes the dissolution of calcite (lower CCPP).

4.3 Influence of water composition on index parameters

Index parameters are used to control the conditioning of drinking water in order to prevent the degradation of cement drinking water pipes with the assumption that scaling of calcite will prevent leaching. There are various index parameters used to this end. These parameters include the saturation index (SI), Langelier SI (LSI), the Calcium Carbonate Precipitation Potential (CCPP) and aggressive CO_2. Briefly, the LSI is the difference between the measured pH of the water and the pH when calcite is saturated. SI is calculated by comparing the chemical activities of the dissolved ions of the mineral with their solubility product. The LSI is essentially a simplification of the SI and in many cases the LSI is a good indicator of the SI. The CCPP (NL: Theoretisch Afzetbaar Calcium Carbonaat (TACC)) gives the amount of $CaCO_3$ which can theoretically precipitate or dissolve at a given water composition. Aggressive CO_2 is the CCPP expressed as mg/L CO_2 and has the opposite sign of the CCPP. For a more complete explanation of the index parameters, see Appendix VI. Going forward we will focus primarily on the LSI and the CCPP. In this section we examine the relationship between the different index parameters and the water composition and the relationship between different index parameters for the same water composition.

4.3.1 Range of water composition parameters for index parameter simulations

To test the effect of different water compositions on the calculation of the index parameters, combinations of the minimum, medium and maximum values for each parameter from Table 7 were created and the index parameters were calculated using PhreeqPython. In total, 177 147 (n= 3^{11}) combinations were tested for each of the four index parameters (SI, LSI, CCPP, aggressive CO_2). Furthermore, both the Cemdata18_Diffusion and the Stimela database were used. Stimela is a database developed by researchers at Delft university to model drinking water chemical reactions (de Moel et al., 2013). For calculations of index parameters such as CCPP it has been shown to produce results similar to phreeqc.dat (Tang et al., 2021). Stimela was used here as this is the database used by the drinking water companies for their own calculations of, for example, CCPP, $CCPP_{90}$, aggressive CO_2.

4.3.1 Results of the influence of water composition on index parameters

The Stimela and the Cemdata18 database were found to produce similar results for the calculation of the index parameters (aggressive CO_2/CCPP, LSI and SI), see Appendix VII. The Langelier SI (LSI) and the SI were comparable when the SI was between -0.5 and 0.5 (Figure 27). When the SI > 0.5, the LSI underestimates the SI, while when the SI < -0.5, the LSI overestimates the SI. The results also show that the pH influences the accuracy of the LSI to estimate the SI, where high pH (pH ≥ 8) water compositions have more comparable LSI and SI's than low pH (pH ≤ 7.5). From these results we can conclude that the LSI does a poor job of estimating the SI when the pH is low (pH ≤ 7.5) and/or when the SI differs substantially from equilibrium (SI ≈ 0). The *Drinkwaterbesluit* stipulates that drinking water composition must have an LSI > -0.2, therefore within the range of when the LSI is within reasonable agreement with the SI.

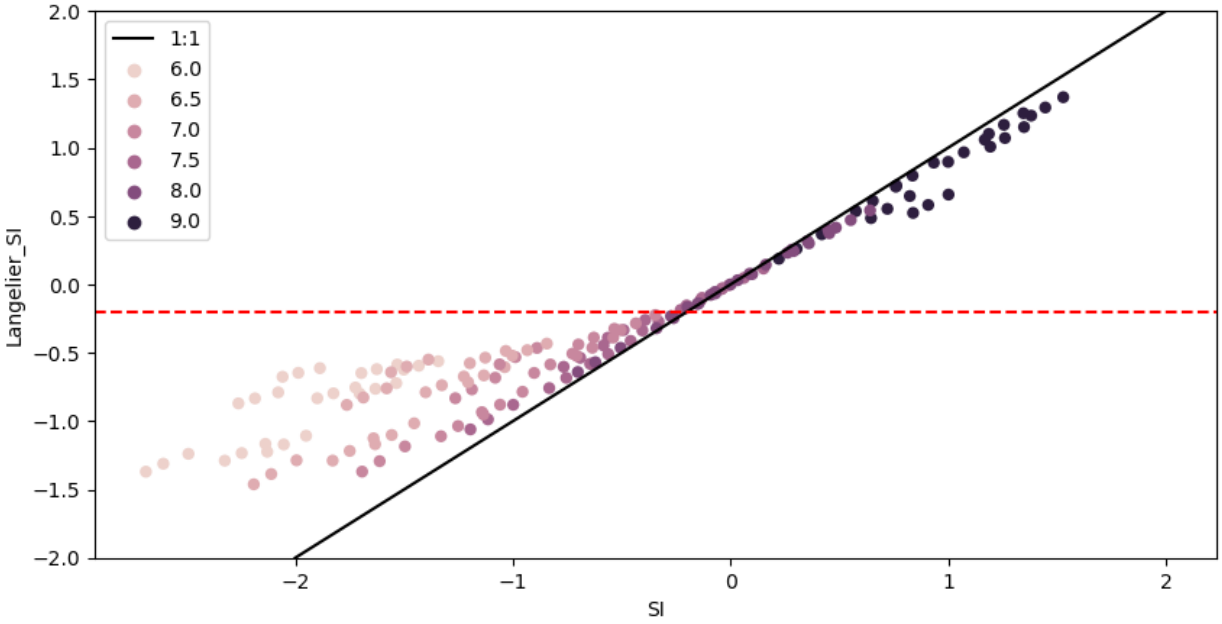

Figure 27 The relationship between the SI and the Langelier SI for different water compositions. The color of the water composition in this case indicates the pH. The red dashed lines indicate the minimum value of -0.2 for the Langelier SI on the y-axes and the black solid line indicates a 1:1 relationship between the SI and Langelier SI. As can be seen, above the norm of -0.2 the Langelier SI predicts the actual SI reasonable well.

Another indicator for the aggressiveness of water is the CCPP. Figure 28 shows the CCPP (in mmol/L) and the corresponding LSI's. The results show that for the same LSI, there can be a wide range of CCPPs depending on the water composition. For example, for an LSI = 0.6 ± 0.2, the CCPP concentration can vary from -0.06 to -3.84 mmol/L. It is also possible to meet the standard for CCPP but not for the LSI and vice versa (lower left and upper right quadrants, respectively in Figure 28). Again, the pH of the solution has an influence on the index parameters, where a pH ≥ 8 is more likely to mee the LSI and CCPP requirements than a pH ≤ 7.5 regardless of the water composition.

A similar comparison of the SI vs. CCPP was performed by (de Moel et al., 2013). In the simulations, 10 water compositions were simulated using PHREEQC and the Stimela database to assess the suitability of using PHREEQC to comply with the German standard for the calculation of calcite saturation in drinking water (DIN 38404-10, 2012). The results of the simulations performed by de Moel et al. (2013) demonstrated that for a given water composition the SI and the CCPP are qualitatively, but not quantitatively, related. This qualitative relationship is also what our simulations show.

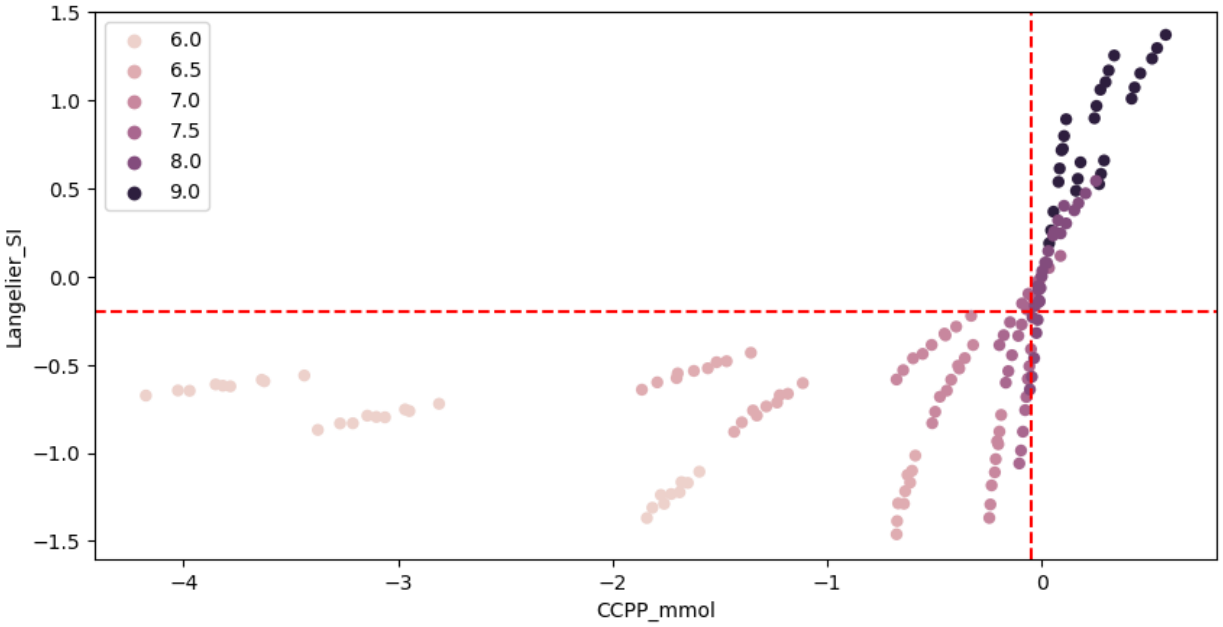

Figure 28 The relationship between the Langelier SI and aggressive CO_2 for different water compositions. The color of the water composition in this case indicate the pH. The red dashed lines indicate the minimum value of -0.05 mmol/L for CCPP and -0.2 for the Langelier SI on the x- and y-axes respectively. Within these water compositions, alkalinities of 60, 165 and 270 mg/L HCO_3 are present. A similar graph based on the SI instead of the LSI (not shown) is slightly skewed but not meaningfully different in shape and shows the same qualitative trends.

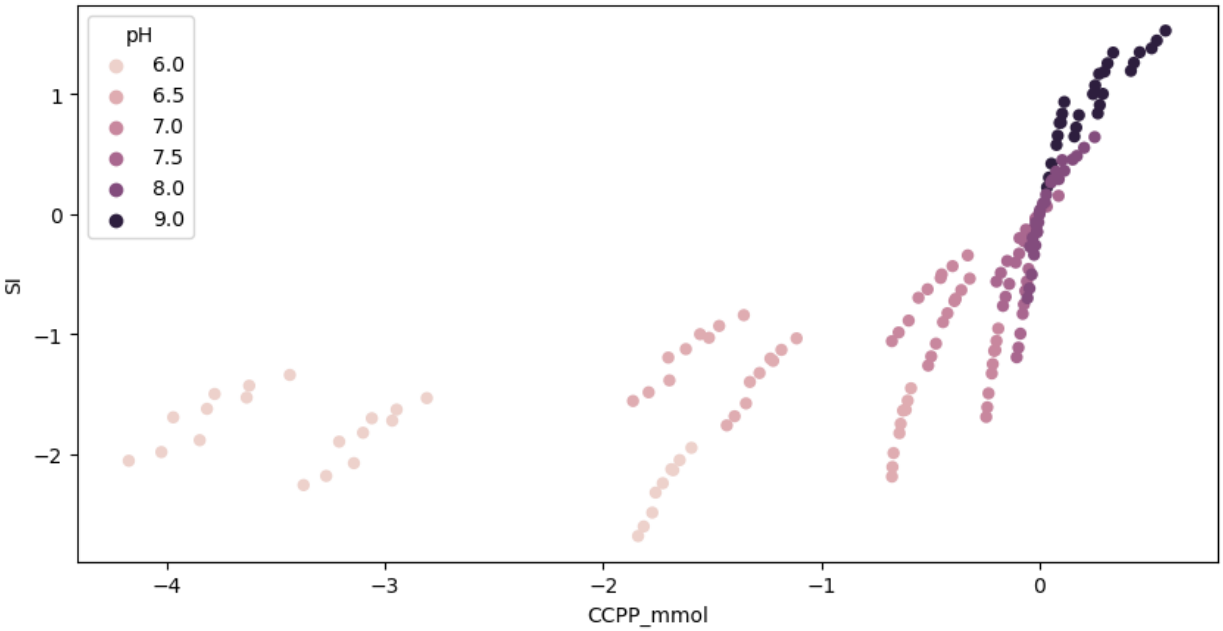

The four drinking water compositions provided by PWN, Vitens, Oasen and WMD used elsewhere in this report, along with two water compositions from pompstation (PS) Laren and Nijverdal (Vitens) are plotted in the Figure 29. The results show that PS Laren meets the LSI requirement (LSI > -0.2), but falls outside of the recommended CCPP minimum value of -0.05 mmol/L. PS Nijverdal and the water composition provided by Vitens, on the other hand, meet the CCPP requirement but fall below the LSI requirements. Finally, the water compositions provided by PWN, Oasen and WMD meet both the CCPP and LSI requirements. The results demonstrate that the range of water compositions simulated encompass the variety in water compositions which can be expected for drinking water in the Netherlands.

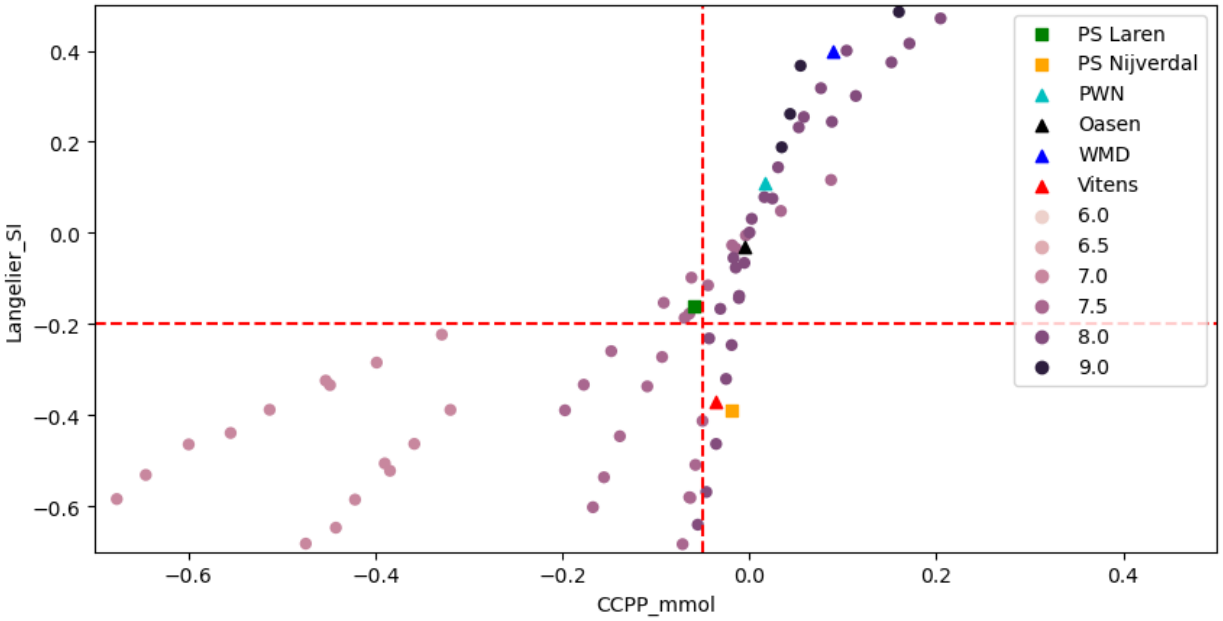

Figure 29 The relationship between the Langelier SI and aggressive CO_2 for different water compositions. The round symbols indicate the pH of the different water compositions. The red dashed lines indicate the minimum value of -0.05 mmol/L for CCPP and -0.2 for the Langelier SI on the x- and y-axes respectively. For reference, two water compositions, from PS Laren, PS Nijverdal (Vitens, square symbols), and the four references water compositions provided by the DWC (Table 15, triangle symbols) were added to the figure.

4.3.2 Discussion on the influence of water composition on the calculation of index parameters

For the initial 23 water composition simulations for the sensitivity analysis (section 4.2.2), we know that concentration of Mg and SiO_2 have no effect on the calculation of the different index parameters (Table 10). This result is expected, as Mg and SiO_2 are not involved in the reactions of calcite, which the index parameters asses. Ca, pH and alkalinity all had expected effects on the calculations for the index parameters – increases in the Ca, pH and alkalinity increased the LSI (Table 11). Increases in Ca and pH also increased the CCPP. For alkalinity, at high pH (pH = 8), an increase in the alkalinity increased the CCPP while at low pH (pH = 7) an increase in the alkalinity decreased the CCPP (Figure 38, Appendix IX). This difference in the effect of alkalinity (HCO_3^-) with pH has to do with dissolved carbonate speciation as a function of pH (Appelo et al., 2005). At pH 8, the majority of dissolved carbonate is in the form of HCO_3^-, while at pH 7, some is in the form of CO_2 (Appelo et al., 2005). This CO_2 reacts with H_2O to form carbonic acid (H_2CO_3) which promotes the dissolution of calcite, hence the lower CCPP for high alkalinity-low pH water compositions.

Possible explanation for the decrease in the LSI, SI and CCPP for high S concentrations, is that in water compositions with high S, dissolved $CaSO_4$ forms and there is reduced free Ca^{2+} in the water. This reduced Ca^{2+} could lead to lower LSI, SI and CCPP. However, this is in contrast to the effects we observe on the leaching rate, where increased S (which lowers the LSI) also lowers the leaching rate.

Overall what we observe is that the index parameters are not sufficient to explain either the leaching or scaling rates observed for the different water compositions. When the LSI is above the norm of -0.2 for the water, in general we observe low leaching rates (< 0.3 mm/yr after 10 years), with two exceptions (water compositions 24 and 28, Table 16, Appendix VIII). When the LSI is below the norm, leaching can range from < 0.1 mm/yr to more than 1 mm/yr and depends on the SiO_2 concentration.

SiO_2, which has been discussed in section 4.2.3 and 4.2.4, influences the leaching rate the most of all the water composition parameters, however SiO_2 is not captured in the index parameters. The effect of SiO_2 should be validated using experiments, as no papers could be found which discuss the influence of high or low Si in influent waters on pipe degradation. From Figure 16 what stands out is that water compositions with a high SiO_2 all have a

low leaching rate, in the order of 0-0.2 mm/yr after 10 years, regardless of the calculated LSI. This implies that water compositions with an LSI below the norm are potentially not aggressive and do not require additional conditioning so long as the SiO_2 concentration does not fall below a certain concentration.

Given that the insights into, in particular, the effects of SiO_2 but also the other parameters, could not be verified in the literature or in experiments, we cannot yet make recommendations for a bandwidth of conditioning parameters or determine with certainty that the current index parameters should be disregarded or changed. Future research should investigate – both experimentally and with the model – a larger range in SiO_2 concentrations to better determine the relationship between leaching, scaling and the SiO_2 concentration. The dependence of the leaching rate on the SiO_2 concentration, a parameter not captured in the index parameters, also highlights the utility of the model in being able to predict the potential actual aggressiveness of water. This raises the possibility of using the model directly in decision making processes in the daily drinking water practice (as opposed to or in support of decisions being made solely based on the currently used index parameters.

5 Conclusies en aanbevelingen

Dit onderzoek heeft aangetoond dat de relatie tussen de watersamenstelling en de degradatiesnelheid van cementbuizen nog gecompliceerder is dan gedacht en dat een *bottom-up* model van cementdegradatie nieuwe inzichten in cementdegradatie kan verschaffen.

Verificatie

Tijdens de verificatie zijn verschillende aspecten en modelaannames kritisch getoetst aan de laatste stand van de wetenschappelijke en praktische kennis. Een eerste stap was het implementeren van de nieuwste cementdatabase: Cemdata18 (Lothenbach et al., 2019). Aangezien het vakgebied van de cementchemie zich blijft ontwikkelen, is het belangrijk om de nieuwste inzichten te blijven gebruiken. Ook bevatte de database een aanzienlijk aantal nieuwe cementmineralen en meer keuze en flexibiliteit voor het model in de toekomst. Zo kunnen nu bijvoorbeeld verschillende keuzes van CSH-gel modellen worden geïmplementeerd. Het model is ook ge-upgrade om de effecten van elektrostatica op te nemen (verschillende diffusiesnelheden per element). De opname van elektrostatica resulteerde in veranderingen in de uitlogingspercentages voor de geteste watersamenstellingen, terwijl de uitlogingspercentages niet *a priori* konden worden voorspeld, hetgeen de noodzaak onderstreept van een model om de uitlogingspercentages te beoordelen. Ook is de relatie tussen calciet, porositeit en uitloging getest. Calciet bleek een groot effect te hebben op de uitlogingssnelheid wanneer het uit de berekeningen voor de porositeit werd verwijderd. Dit suggereerde een mogelijk beschermend effect van calciet, hoewel in latere simulaties werd aangetoond dat de relatie tussen calciet en uitloging complex is en niet zo eenvoudig als aanvankelijk werd gedacht. Tenslotte is getracht de productieomstandigheden voor asbestcement in Nederland zoveel mogelijk te karakteriseren. Dit is belangrijk omdat de productieomstandigheden bepalend zijn voor de beginvoorwaarden van de cementinvoer in het model. Er was geen expertise uit de eerste hand beschikbaar, zodat in plaats daarvan is teruggegrepen op de literatuur..

Validatie

Validatie is een belangrijke stap in de ontwikkeling van een model, omdat hiermee de nauwkeurigheid en betrouwbaarheid van het model om het gedrag van het betrokken systeem te voorspellen, worden beoordeeld. Validatie is gedaan op basis van zowel experimenten uit de literatuur als een case-study uit de praktijk. Geschikte studies uit de literatuur waren moeilijk te vinden door het gebrek aan rapportage van cementporositeiten, het gebruikte cementtype, het gebruik van geschikt uitloogwater en een gebrek aan tijdreeksgegevens van cementdegradatie. Twee geschikte studies uit de literatuur zijn gebruikt. Het model gaf een betere overeenkomst

te zien wanneer de oorspronkelijke condities van het cement werden gecreëerd aan de hand van gemeten porositeiten dan wanneer de w/c-verhoudingen werden gebruikt. Het model is gevoelig voor de gebruikte porositeiten en niet alle methoden om de porositeit te meten zijn even nauwkeurig. Daarom moet voorzichtig te werk worden gegaan bij het selecteren van studies voor validatie en/of bij het selecteren van meetmethoden voor gebruik bij validatie vanuit de praktijk.

Validatie vanuit de praktijk was ook moeilijk, vanwege een gebrek aan gegevens over de uitgangstoestand van cementbuizen en het ontbreken van goed gedocumenteerde watersamenstelling (zo waren gegevens over de watersamenstelling vóór ~2004 niet te verkrijgen). Aangezien asbestcementbuizen vaak al in de jaren 1950 zijn geïnstalleerd, is het moeilijk om de volledige levensduur van de buis, vanaf de installatie, te modelleren bij gebrek aan betrouwbare gegevens over de watersamenstelling. Als alternatief is gebruik gemaakt van gegevens van twee recente uitgangsbepalingen op dezelfde plaats, waarbij de watersamenstelling tussen de tests bekend is. Ook dit bleek erg moeilijk te zijn, aangezien er aanzienlijke verschillen (± 5 mm) waren in de uitloging voor exit tests die op korte afstand van elkaar waren uitgevoerd. Gezien de beperkingen van de beschikbare gegevens was het model toch in staat de uitlogingssnelheid in een van de twee literatuur proeven vrij goed te voorspellen. Het model is ook in staat aan te tonen dat verschillen in de uitgangscondities van de buizen een deel van de waargenomen verschillen tussen de twee uitloogtests kunnen verklaren.

Gevoeligheidsanalyse

Er is een analyse uitgevoerd van de gevoeligheid van het model voor verschillende fysische en chemische parameters. Wat de fysische parameters betreft, bleek het model relatief ongevoelig te zijn voor de temperatuur van het water, en zeer gevoelig voor de initiële capillaire porositeit. Een verhoging van de initiële capillaire porositeit van 0% tot 30% leidde tot een 236 maal sneller verlies van de eerste cementcel. Een verhoogde initiële capillaire porositeit verhoogde ook de totale hoeveelheid calcietneerslag in het model. Dit bleek het gevolg te zijn van de verhoogde toevoer van Ca^{2+} en CO_3^{2-} door de verhoogde oplossing van de cementmineralen.

Een reeks watersamenstellingen is getest waarbij de concentratie van de verschillende hoofdelementen werd gevarieerd binnen een redelijke marge die voor drinkwater in Nederland wordt verwacht. De watersamenstellingen zijn geëvalueerd op hun invloed op de uitloging, de hoeveelheid kalkneerslag en het effect op de indexparameters die gebruikt worden voor het conditioneren van drinkwater (LSI, CCPP). De parameters Al, NO_3, Cl, Na en O_2 bleken geen effect te hebben op de uitloging, de kalkafzetting of de berekening van de indexparameters, zoals verwacht. Alkaliniteit, Ca, pH, Mg, S en SiO_2 bleken wel van invloed te zijn op een of meer van de uitlogings-, neerslag- of berekening van de indexparameters. Om de effecten beter te begrijpen, is een uitgebreide gevoeligheidsanalyse uitgevoerd met alleen deze zes parameters.

Van de zes geteste parameters had SiO_2 de grootste invloed op de uitlogingssnelheid. Bij water met een hoge SiO_2-concentratie was de uitspoeling beperkt (< 0,2 mm/jaar na de eerste 10 jaar), in vergelijking met water met een lage SiO_2-concentratie. Verhoging van alleen de SiO_2-concentraties, bij gelijkblijvende andere parameters, leidde tot een 2 tot 10-voudige toename van de uitlogingssnelheid. Als mechanisme hiervoor wordt verondersteld het oplossen van de CSH-gel, die is samengesteld uit de Si-houdende mineralen jenniet en tobermoriet. Aangenomen wordt dat een lager SiO_2 in het instromende water een snellere oplossing van de CSH-gel en bevordert, waardoor de totale afbraaksnelheid van het cement toeneemt. Als gevolg van de verhoogde afbraak van het cement vertoonde laag SiO_2 water ook een verhoogde neerslag van calciet. Vergelijkbare processen die de CSH-gel beïnvloeden zouden verantwoordelijk zijn voor de effecten van uitloging en kalkneerslag die zijn waargenomen voor Mg en S: precipitatie van het Mg-bevattende mineraal hydrotalciet leidt tot snellere oplossing van de CSH-gel, waardoor de afbraak van het cement in water met een hoog Mg-gehalte afneemt, terwijl precipitatie van het S-bevattende mineraal ettringiet leidt tot langzamere oplossing van de CSH-gel, waardoor de afbraak in water met een hoog S-gehalte afneemt. De effecten van Mg en S bleken ook afhankelijk te zijn van de SiO_2-concentratie - wanneer SiO_2 hoog was, waren de verschillen kleiner dan wanneer SiO_2 laag was.

Een verrassend resultaat was dat zelfs het effect van Ca afhankelijk was van de SiO_2-concentratie - alleen bij lage SiO_2-concentraties leidde een lage Ca-concentratie tot een verhoogde uitspoeling. Bij hoge SiO_2-concentraties had de Ca-concentratie geen effect op de uitlogingssnelheid. Ook hier is gespeculeerd dat de veranderingen verband lijken te houden met de CSH-gel, waarbij een laag Ca en een laag SiO_2 leiden tot de volledige ontbinding van de CSH-gel, waardoor de uitloging wordt versneld. Het effect van pH en alkaliteit bleek geen consistent effect te hebben op de omvang of richting (toenemend of afnemend) van uitloging of verkalking.

Het model toont aan dat kalkafzetting niet alleen het gevolg is van de neerslag van calciet uit het instromende water op de cementwanden, maar dat er een complex geheel van interacties en reacties is tussen het instromende water en het oplossende cement, dat de snelheid en de omvang van de kalkafzetting bepaalt. Deze interactie tussen het instromende water en het cement bleek niet tot uiting te komen in de indexparameters die worden gebruikt om drinkwater te conditioneren.

De meest gebruikte indexparameters om drinkwater te conditioneren zijn de LSI en de CCPP, die respectievelijk de thermodynamische voordeligheid van calcietneerslag en het potentiële aantal mol calcietneerslag bij een gegeven watersamenstelling meten. De LSI en de CCPP zijn ruwweg aan elkaar gerelateerd, maar niet één op één (er zijn meerdere LSI mogelijk bij één bepaalde CCPP en vice versa). Uit de gevoeligheidsanalyse bleek dat alkaliniteit, pH en Ca logische effecten hadden op de indexparameters. Sulfaat bleek ook invloed te hebben op de LSI en de CCPP, mogelijk door de vorming van $CaSO_4$. Parameters als SiO_2 en Mg, waar de LSI en de CCPP ongevoeliger voor zijn, bleken echter grote effecten te hebben op de uitlogings- en verkalkingssnelheden. Uit de modelsimulaties blijkt dat de LSI en de CCPP slechts in beperkte mate in staat zijn de uitloging van cementbuizen te voorspellen, aangezien de invloed van SiO_2, maar ook van Mg, door de LSI en de CCPP niet in aanmerking wordt genomen. Het effect van met name SiO_2 op de uitloging van cement moet nog door experimenten worden bevestigd voordat een wijziging van de conditioneringsparameters of een bandbreedte van optimale watersamenstellingen om de uitloging te beperken, kan worden aanbevolen.

5.1 Gevolgen voor de drinkwaterbedrijven (bedrijfsparagraaf)

Oasen: Oasen heeft één locatie waar nu structureel een (te) negatieve LSI optreedt. Dit is ook de waterkwaliteit die is onderzocht. Oasen is op zoek naar een antwoord op de vraag of het noodzakelijk is de LSI te verhogen om uitloging van gecementeerde leidingen te voorkomen of dat beïnvloeding van andere parameters effectiever is.

WMD: WMD heeft meerdere locaties waarbij de LSI structureel rond de -0,2 ligt. Voor WMD is het van belang te weten of deze LSI een voorspellende waarde heeft m.b.t. de oplossnelheid van cementleidingen en om eventueel maatregelen te treffen of dat hiervoor een andere parameter meer geschikt is.

Vitens: De conclusie dat het niet mogelijk is het uitlooggedrag van (asbest)cement te voorspellen op basis van alleen de agressiviteit van het water ten opzichte van calciet is voor Vitens relevant. Ronduit vernieuwend is de mogelijke invloed van SiO2, Mg en S.

Uitloging van asbestcement kan leiden tot het vrijkomen van asbestvezels in het drinkwater. Alleen al uit het oogpunt van reputatie is het belangrijk meer inzicht te krijgen in de relatie tussen de waterkwaliteit en de uitloging van asbestcement. Voor zover bekend is Nederland uniek met een wettelijk norm voor de LSI van calciet. Aanpassing van de LSI van het drinkwater is op veel Vitens locaties alleen mogelijk door het doseren van natronloog. Vitens is terughoudend met het doseren van natronloog. Aan het doseren van natronloog zijn veiligheidsrisico's verbonden, natronloog is immers een gevaarlijke stof. Daarnaast vergt de fabricage van natronloog veel energie en draagt om die reden ook sterk bij aan de CO2-footprint van onze productiebedrijven. Het aanpassen van de pH vereist zorgvuldigheid. Als de (L)SI van calciet daarentegen te hoog wordt kan het water te kalkafzettend worden wat kan leiden tot klachten van klanten.

Het onderzoek is op dit moment nog te prematuur om nieuwe conditioneringsregels op te stellen. Bij het definiëren van nieuwe conditioneringsparameters moet altijd een afweging gemaakt worden tussen prestatie, risico's en kosten. Op het moment dat het model beschikbaar wordt gemaakt is het interessant de uitloogsnelheid voor alle productielocaties te berekenen.

PWN: In de huidige situatie conditioneert PWN het uitgaande water op haar pompstations op een LSI van +0,15 met behulp van NaOH of CO_2, met het idee dat het op deze manier de uitloging van asbestcement- en andere gecementeerde leidingen beschermd. Uit dit onderzoek komt naar voren dat de LSI en CCPP niet zo bepalend zijn voor de snelheid van uitloging en dat er altijd sprake is uitloging van het cement nabij de waterfase. Het gehalte silicaat van het uitgaande water is voor de meeste van de PWN locaties rond de 4 mg/L SiO_2, alleen op onze grondwaterwinning in 't Gooi heeft een hogere silicaat gehalte van circa 10 mg/L SiO_2. Uit dit onderzoek blijkt dat deze lage concentraties silicium juist (alhoewel het voor 10 mg/L SiO_2 dit nog nader onderzocht moet worden) uitloging bevorderen ten opzichte van watertypes die 20 mg/L SiO_2 of meer bevatten.

5.2 Aanbevelingen

Uitbouwen van het vertrouwen in het model

- De Cemdata18 database kan worden gekozen uit verschillende CSH-gel-opties. Een nieuwere versie van het CSH-gel-model, CSHQ (zie Box 1, paragraaf 2.1) moet worden getest om te zien welk verschil deze eventueel maakt voor de totale uitlogingspercentages. Dit zou met name interessant kunnen zijn omdat tijdens de gevoeligheidsstudie is vastgesteld dat de CSH-gel van belang is voor de totale uitlogingssnelheid van het cement.

- Aangezien de productieomstandigheden niet konden worden geverifieerd bij deskundigen met ervaring uit de eerste hand, moeten rechtstreekse metingen van de poreuze eigenschappen van de leidingmaterialen een meer directe benadering vormen om de vraag op te lossen wat de oorspronkelijke omstandigheden van cementbuizen zijn.

- De manier waarop diffusie en porositeit momenteel in het model worden berekend, betekent dat er een ondergrens is voor de diffusiesnelheid door cementcellen. In de praktijk betekent dit dat de diffusie nooit naar nul kan gaan, zelfs als een cel volledig met calciet is gevuld. Daarmee is het model op dit moment geschikt om het risico op uitlogen te beoordelen in de context van waterkwaliteit, maar niet geschikt voor gedetailleerde restlevensduurbepaling in de context van assetmanagement. In de toekomst moet worden gezocht naar alternatieven voor de GEM-vergelijking, waarbij de diffusie wel tot nul kan afnemen als er voldoende calciet neerslaat om de poriën volledig te blokkeren. Ook is meer inzicht nodig in de microstructuur van de calcietneerslag in de buizen zelf. Labmethoden zoals micro-CT, mercury intrusion porosimetry, dynamic vapour sorption, en kristallografie kunnen mogelijkheden bieden om de porositeit van zowel de calcietneerslag als het leidingmateriaal zelf te analyseren.

- De resultaten van de gevoeligheidsanalyse moeten worden gevalideerd door middel van experimenten, b.v. testbereik van SiO_2-concentraties en het effect op de uitloging, en andere elementen (Mg, S, Ca enz.) De experimenten moeten gericht en efficiënt worden gekozen dankzij simulaties met het model.

- Overleg is nodig met deskundigen op het gebied van cementchemie en cementmodellering om na te denken over de resultaten, met name van de gevoeligheidsanalyse, tot nu toe. Suggesties: D. Jacques (SCK-CEN), B. Lothenbach (ontwikkelaar van Cemdata18), E. Schlangen (TU Delft), L. Pel en H. Huinink (TU Eindhoven).

Toepassing van het model voor de drinkwaterbedrijven

- Het model laat zien dat de bescherming tegen uitloging niet één op één schaalt met de verschillende invloedrijke concentraties van componenten, maar afhankelijk is van complexe, specifieke combinaties van die concentraties. Met een multivariate analyse kunnen de afhankelijkheden beter inzichtelijk worden gemaakt. Daarnaast is het zaak om een groter aantal combinaties door te rekenen om een betere benadering van de volledige afhankelijkheid te verkrijgen. Op die manier kunnen we komen tot een beslisboom voor conditionering tegen uitloging.

- Het model zou gebruikt kunnen worden om het uitloogpotentieel op (alle) productielocaties te berekenen. Koppeling van de modelberekeningen aan een (kwalitatieve of kwantitatieve) beoordeling van welke productielocaties problemen met uitloging hebben, zou kunnen helpen om de gevoeligheidsanalyse te ondersteunen en een aanvaardbaar bereik van watersamenstellingen te bepalen om uitloging te voorkomen.

- De effecten van de huidige conditioeneringsmethoden die worden ingezet om aan de norm te voldoen kunnen worden gesimuleerd om hun daadwerkelijke beschermende effect tegen uitloging te beoordelen.

- Zoals uit de resultaten is gebleken, geven de huidige indexparameters slechts een beperkt beeld van het uitloog- en verkalkingsgedrag van verschillende watersamenstellingen. Het model zou hierin waardevolle inzichten kunnen verschaffen.

    - Naarmate het vertrouwen in het model wordt vergroot (bijv. via de verificaties en validaties beschreven in dit rapport, maar ook bijv. labmetingen aan de voorspelde effecten van SiO_2), zou het model kunnen worden ingebed in de bedrijfsvoering om de watersamenstelling op productielocaties te controleren en informatie te verstrekken over de conditioneringsvereisten.

    - Naarmate het vertrouwen in het model toeneemt door validatie en toepassing/toetsing in de praktijk, kan het ook gaan dienen als basis voor een discussie over gepaste normering van de conditionering van drinkwater met het oog op uitloging.

- Het model biedt perspectief om uit te groeien tot een methode voor restlevensduurbepaling van cementhoudende leidingmaterialen. Het ligt echter in de verwachting dat een dergelijke toepassing veel historische waterkwaliteitsdata nodig heeft. Dergelijke data is op het moment waarschijnlijk beperkt (digitaal) beschikbaar. In de richting van deze toepassing moet het toegepaste onderzoek zich daarom in eerste instantie richten op het boven water krijgen van de benodigde data (uit de papieren archieven die de digitalisering hebben overleefd en wellicht zelfs uit archieven van derden zoals de overheid), en pas in tweede instantie op eventuele verfijning van het model.

I References

Appelo, C. A. J., & Postma, D. (2005). *Geochemistry, groundwater and pollution* (2nd Editio). A.A. Balkema Publishers.

Bijleveld, J. G. (1974). Abestcement Buizen. *H2O*, *11*, 212–216.

Brouwers, H. J. H. (2004). The work of Powers and Brownyard revisited: Part 1. *Cement and Concrete Research*, *34*(9), 1697–1716. https://doi.org/10.1016/j.cemconres.2004.05.031

Carde, C., Escadeillas, G., & François, R. (1997). Use of ammonium nitrate solution to simulate and accelerate the leaching of cement pastes due to deionized water. *Magazine of Concrete Research*, *49*(181), 295–301. https://doi.org/10.1680/macr.1997.49.181.295

de Moel, P. J., van der Helm, A. W. C., van Rijn, M., van Dijk, J. C., & van der Meer, W. G. J. (2013). Assessment of calculation methods for calcium carbonate saturation in drinking water for DIN 38404-10 compliance. *Drinking Water Engineering and Science*, *6*(2), 115–124. https://doi.org/10.5194/dwes-6-115-2013

De Windt, L., Miron, G. D., Fabian, M., Goethals, J., & Wittebroodt, C. (2020). *EURAD Deliverable 2.8: First results on the thermodynamic databases and reactive transport models for steel-cement interfaces at high temperature*. Retrieved from https://hal-mines-paristech.archives-ouvertes.fr/hal-03107880

DIN 38404-10: German standard methods for the examination of water, waste water and sludge – Physical and physico-chemical parameters (group C) – Part 10: Calculation of the calcite saturation of water (C 10). , (2012).

Drinkwaterbesluit. (2011). Retrieved from https://wetten.overheid.nl/BWBR0030111/2015-03-21

Elzenda, C. H. J., Meyer, P. B., & Stumphuis, J. (1974). Oriënterend onderzoek naar het vóórkomen van asbest in het Nederlandse drinkwater. *H2O*, *7*(19), 406–410.

EN 197-1. (2000). *EN 197-1. Cement - Part 1: Composition, specifications and conformity criteria for common cements*. European Standard.

Eternit. (1980). *Eternit - Asbestcemen Tabellen*. Retrieved from file:///C:/Users/youhe/Downloads/kdoc_o_00042_01.pdf

Haga, K., Sutou, S., Hironaga, M., Tanaka, S., & Nagasaki, S. (2005). Effects of porosity on leaching of Ca from hardened ordinary Portland cement paste. *Cement and Concrete Research*, *35*(9), 1764–1775. https://doi.org/10.1016/j.cemconres.2004.06.034

Hiemstra, P. (1987). *Berekening agressief CO2*.

Hockin, A., Korevaar, M., & van Laarhoven, K. (2021). *De invloed van de drinkwater- samenstelling op uitloging van cementhoudende leidingmaterialen: een model. BTO 2021.052*. Nieuwegein, Netherlands.

Hofman-Caris, R. (2013). *Berekening van kalk- koolzuurevenwichten in drinkwater. Ontwikkelingen in de afgelopen twintig jaar. BTO 2013.206 (s)* (Vol. 206). Nieuwegein, Netherlands.

Jacques, D. (2009). *Benchmarking of the Cement Model and Detrimental Chemical Reactions Including Temperature Dependent Parameters : Project Near Surface Disposal of Category A Waste at Dessel NIROND-TR 2009–30 E*.

Brussels, Belgium.

Jacques, D., Perko, J., Seetharam, S., Mallants, D., & Govaerts, J. (2013). Modelling long term evolution of cementitious materials used in waste disposal. *The Behaviours of Cementittious Materials in Long Term Storage and Disposal of Radioactive Waste - Results of a Coordinated Research Project*, 1–26.

Jacques, D., Šimůnek, J., Mallants, D., Perko, J., & Seetharam, S. C. (2011). Evaluating changes of transport properties of chemically degrading concrete using a coupled reactive transport model. *1st International Symposium on Cement-Based Materials for Nuclear Wastes*, (October).

Jacques, D., Wang, L., Martens, E., & Mallants, D. (2009). *Time dependence of the geochemical boundary conditions for the cementitious engineered barriers of the Belgian surface disposal facility. Project near surface disposal of category A waste at Dessel NIROND-TR 2008–24 E*. Brussels, Belgium.

Jacques, D., Wang, L., Martens, E., & Mallants, D. (2010). Modelling chemical degradation of concrete during leaching with rain and soil water types. *Cement and Concrete Research*, *40*(8), 1306–1313. https://doi.org/10.1016/j.cemconres.2010.02.008

Kuai, D. Z. D., Leggoe, J., Ash, G., & Loh, E. (2015). Investigation of the effect of Water Quality , Lime and Calcite Dosing on Pipelines. *CEED Seminar Proceedings 2015*, 49–54.

Le, J., Leggoe, J., Ash, G., & Loh, E. (2016). Investigation of the effect of Water Quality , Lime and Calcite Dosing on Pipelines. *CEED Seminar Proceedings 2016*, (2015), 49–54.

LeRoy, P., Schock, M., Wagner, I., & Holtschulte, H. (1996). Cement-based materials. In: Internal corrosion of water distribution systems. *American Water Works Association Research Foundation and American Water Works Association.* Denver,Co.

Lothenbach, B., Kulik, D. A., Matschei, T., Balonis, M., Baquerizo, L., Dilnesa, B., … Myers, R. J. (2019). Cemdata18: A chemical thermodynamic database for hydrated Portland cements and alkali-activated materials. *Cement and Concrete Research*, *115*(October 2018), 472–506. https://doi.org/10.1016/j.cemconres.2018.04.018

Lothenbach, B., Matschei, T., Möschner, G., & Glasser, F. P. (2008). Thermodynamic modelling of the effect of temperature on the hydration and porosity of Portland cement. *Cement and Concrete Research*, *38*(1), 1–18. https://doi.org/10.1016/j.cemconres.2007.08.017

Lothenbach, B., & Winnefeld, F. (2006). Thermodynamic modelling of the hydration of Portland cement. *Cement and Concrete Research*, *36*(2), 209–226. https://doi.org/10.1016/j.cemconres.2005.03.001

Matschei, T., Lothenbach, B., & Glasser, F. P. (2007). Thermodynamic properties of Portland cement hydrates in the system CaO-Al2O3-SiO2-CaSO4-CaCO3-H2O. *Cement and Concrete Research*, *37*(10), 1379–1410. https://doi.org/10.1016/j.cemconres.2007.06.002

Mesman, G. A. M., & Wielen, J. van der. (2005). *Georadar: geschikt om conditie AC-leidingen te beoordelen? Een vergelijking met de fenolftaleïnetest KWR 05.023*. Nieuwegein, Netherlands.

Moranville, M., Kamali, S., & Guillon, E. (2004). Physicochemical equilibria of cement-based materials in aggressive environments - Experiment and modeling. *Cement and Concrete Research*, *34*(9), 1569–1578. https://doi.org/10.1016/j.cemconres.2004.04.033

NEN 3262. (1988). *Asbestcementbuizen en koppelingen voor drukleidingen Eisen en beproevingsmethoden* (pp. 1–16). pp. 1–16. Nederlandse Norm.

Oh, B. H., & Jang, S. Y. (2004). Prediction of diffusivity of concrete based on simple analytic equations. *Cement and Concrete Research*, *34*, 463–480. https://doi.org/10.1016/j.cemconres.2003.08.026

Parkhurst, D. L., & Appelo, C. a. J. (2013). Description of Input and Examples for PHREEQC Version 3 — A Computer

Program for Speciation , Batch-Reaction , One-Dimensional Transport , and Inverse Geochemical Calculations. U.S. Geological Survey Techniques and Methods, book 6, chapter A43, 497 p. *U.S. Geological Survey Techniques and Methods, Book 6, Chapter A43*, 6-43A.

Patel, R. A., Perko, J., Jacques, D., De Schutter, G., Ye, G., & Van Bruegel, K. (2018). Effective diffusivity of cement pastes from virtual microstructures: Role of gel porosity and capillary pore percolation. *Construction and Building Materials*, *165*, 833–845. https://doi.org/10.1016/j.conbuildmat.2018.01.010

Powers, T. C., & Brownyard, T. L. (1946). Studies of the physical properties of hardened Portland cement paste. Part 2. Studies of Water Fixation. *Journal of the American Concrete Institute*, *43*(9). https://doi.org/10.14359/8745

Rossum, J. R., & Merrill, D. T. (1983). An evaluation of the calcium carbonate saturation indexes. *Journal - American Water Works Association*, *75*, 95–100. https://doi.org/10.1002/j.1551-8833.1983.tb05075.x

Schock, M. R., & Buelow, R. W. (1981). Behavior of Asbestos-Cement Pipe Under Various Water Quality Conditions - 2. Theoretical Considerations. *Journal / American Water Works Association*, *73*(12), 636–651. https://doi.org/10.1002/j.1551-8833.1981.tb04827.x

Slaats, P., Meerkerk, M., & Hofman-Caris, C. (2013). *Conditionering: de optimale samenstelling van drinkwater; Kiwa-Mededeling 100 – Update 2013*. Nieuwegein, Netherlands.

Tang, C., Godskesen, B., Aktor, H., van Rijn, M., Kristensen, J. B., Rosshaug, P. S., … Rygaard, M. (2021). Procedure for calculating the calcium carbonate precipitation potential (CCPP) in drinking water supply: Importance of temperature, ionic species and open/closed system. *Water (Switzerland)*, *13*(1). https://doi.org/10.3390/w13010042

Torres, P., Bueno, K. A., Delgado, L. G., Barba, L. E., & Cruz, C. H. (2015). Corrosion control using hydroxide and bicarbonate alkalising agents in water drinking processes. *Drinking Water Engineering and Science Discussions*, *8*(1), 53–76. https://doi.org/10.5194/dwesd-8-53-2015

Verordnung über die Qualität von Wasser für den menschlichen Gebrauch (Trinkwasserverordnung - TrinkwV). , (2016).

WHO. (2011). *Guidelines for drinking water quality. 4th Ed. World Health Organization, Geneva, Switzerland.*

II Mineral Phase Descriptions

Table 12 Mineral phases in model and description

MINERAL	DESCRIPTION
ABBREVIATIONS	Cement has it own set of abbreviations: C for CaO, S for SiO_2, A for Al_2O_3, F for Fe_2O_3, M for MgO, K for K_2O, $\overline{S}$ for SO_3, N for Na_2O, H for H_2O and $\overline{C}$ for CO_2.
CALCIUM-SILICATE-HYDRATES (CSH)	CSH form the main components of hydrated OPC (Jacques, 2009). In the model, the CSH phase is described by an ideal solid solution[1] of jennite ($Ca_9Si_6O_{18}(OH)_6{\cdot}8H_2O$) and tobermorite-II ($Ca_5Si_6O_{16}(OH)_2{\cdot}4H_2O$) and a pure phase of amorpheous silciumdioxide (SiO_2).
AFT-PHASES	Alumina, ferric oxide, tri-sulfate (Aft)-phases are a group of calcium sulfoaluminate hydrates, with the general formula $Ca_3(Al,Fe)(OH)_6{\cdot}12\ H_2O]_2{\cdot}X_3{\cdot}xH_2O$ where X is a doubly charged anion. Ettringite is the most important Aft-phase. Ettringite and tricarboaluminate can form a non-ideal solid solution[1], with non-dimensional Guggenheim parameters[2] a_o= -0.823, a_1 =2.82.
AFM-PHASES	Alumina, ferric oxide, mono-sulfate (Afm)-phases are a complex group of calcium aluminate hydrates, with the general formula $[Ca_2(Al,Fe)(OH)_6)]{\cdot}X{\cdot}xH_2O$ where X is a single charged anion. Afm-phases include C_2AH_8, C_4AH_{13}, monosulfoaluminate, monocarboaluminate, hemicarboaluminate, stratlingite, amorphous $Al(OH)_3$ and CAH_{10}. A non-ideal solid solution of hydroxyl-AFm (C_4AH_{13}) and monosulfoaluminate with non-dimensional Guggenheim parameters a_o= 0.188, a_1 =2.849.
HYDROGARNET	The main hydrogarnate ($Ca_3Al_2(OH)_{12}$) phases is included (hydrogarnetOH). The siliceous and iron hydrogarnet forms are not included in the model (siliceous hydrogarnet is not present in calcite systems (Jacques et al., 2009) and iron phases were not included in the model).
HYDROTALCITE	Two forms of hydrotalcite are included; ($Mg_4Al_2(OH)_{14}{:}3H_2O$) and a carbonate form ($Mg_4Al_2(OH)_{12}CO_3{:}3H_2O$).
HYPOTHETICAL PHASES	Two hypothetical phases were added to in the CEMDATA07 database: Na_2O (log k = 24.94) and K_2O (log k = 25.71). These phases were added to control the concentration of sodium and potassium during the initial phases of cement degradation. These elements are retained in the Cemdata18 update to be consistent.
OTHER PHASES	Other cement minerals included: calcite, portlandite, gypsum, anhydrite, brucite and gibbsite. Iron was not included in the model as (Jacques et al., 2009) found it led to unnecessarily complicated calculations and its inclusion had no effect on the evolution of pH, element concentrations and solid phase composition. Therefore we assume that iron also does not affect the results of our simulations.

[1]in an ideal solid solution, the activity coefficient of the mixture is equal to 1 while in non-ideal solid solutions, the activity coefficients are great or less than 1.
[2]the excess free-energy of mixing for non-ideal solid solutions can be modelled with the guggenheim series expansion, of which the first two terms are the non-dimensional guggenheim parameters (Appelo et al., 2005).

Table 13 Name, formula type and molar mass for the main cement minerals used in this study

MINERAL	MINERAL FORMULA	MINERAL TYPE	MOLAR VOLUME cm^3/mol
Monocarbonate	Ca4Al2CO9(H2O)11	Afm	262
Tricarboaluminate	(CO3)Ca2Al0.6666667(OH)4(H2O)8.6666667	Aft	650
Calcite	CaCO3		36.9
Ettringite	((H2O)2)Ca6Al2(SO4)3(OH)12(H2O)24	Aft	707
Gypsum	CaSO4(H2O)2		74.7
Anhydrite	CaSO4		45.9
Hydrotalcite	Mg4Al2O7(H2O)10	Hydrotalcite	220
Mg2alc0.5oh	Mg2Al(OH)6(CO3)0.5(H2O)2	Hydrotalcite	111
Straetlingite	Ca2Al2SiO7(H2O)8	Afm	216
Brucite	Mg(OH)2		24.6
Jennite	(SiO2)1(CaO)1.666667(H2O)2.1	CSH	78
Tobermorite	(SiO2)1(CaO)0.833333(H2O)1.333333	CSH	59
Portlandite	Ca(OH)2		33

III Diffusion Coefficients

Table 14 Diffusion coefficients and parameters to adjust the diffusion coefficient to account for temperature effects.

SOLUTION_SPECIES	D_w^{298} (m^2/s)	DAMPING FACTOR [-]	A1	A2
H+ = H+	9.31E-09	1000	0.46	1.00E-10
CA+2 = CA+2	7.93E-10	97	3.4	24.6
MG+2 = MG+2	7.05E-10	111	2.4	13.7
NA+ = NA+	1.33E-09	122	1.52	3.7
K+ = K+	1.96E-09	395	2.5	21
SR+2 = SR+2	7.94E-10	161		
CL- = CL-	2.03E-09	194	1.6	6.9
CO3-2 = CO3-2	9.55E-10	0	1.12	2.84
SO4-2 = SO4-2	1.07E-09	34	2.08	13.4
NO3- = NO3-	1.90E-09	184	1.85	3.85
CO3-2 + H+ = HCO3-	1.18E-09	0	1.43	1.00E-10
CO3-2 + 2 H+ = CO2 + H2O	1.92E-09			
CO3-2 + 10 H+ + 8 E- = CH4 + 3 H2O	1.85E-09			
SO4-2 + H+ = HSO4-	1.33E-09			
SO4-2 + 9 H+ + 8 E- = HS- + 4 H2O	1.73E-09			
2 NO3- + 12 H+ + 10 E- = N2 + 6 H2O	1.96E-09			
NO3- + 10 H+ + 8 E- = NH4+ + 3 H2O	1.98E-09	312	0.95	4.53
CA+2 + CO3-2 = CACO3	4.46E-10			
CA+2 + CO3-2 + H+ = CAHCO3+	5.06E-10			
CA+2 + SO4-2 = CASO4	4.71E-10			
MG+2 + CO3-2 = MGCO3	4.21E-10			

MG+2 + H+ + CO3-2 = MGHCO3+	4.78E-10			
MG+2 + SO4-2 = MGSO4	4.45E-10			
NA+ + CO3-2 = NACO3-	1.20E-09	0	1.00E-10	1.00E-10
NA+ + HCO3- = NAHCO3	6.73E-10			
NA+ + SO4-2 = NASO4-	1.33E-09	0	0.57	1.00E-10
K+ + SO4-2 = KSO4-	1.50E-09	0	1.00E-10	1.00E+10

IV Drinking Water compositions

Table 15 Drinking water compositions provided by the participating drinking water companies (Oasen, Vitens, PWN and WMD).

Parameter	Unit	Oasen	Vitens	PWN	WMD
Al	mg/L	0.0059	0.0013	0.0011	0.008
Ca	mg/L	43.1	29.9	34.1	44.0
Cl	mg/L	52.5	13.7	161.0	29.0
K	mg/L	2.3	1.2	0	1.8
Mg	mg/L	0.00014	2.86	12.85	8.10
NO_3	mg/L N	0.0026	1.89	1.00	0.36
Na	mg/L	32.9	11.0	126.0	19.0
S	mg/L S	8.8	8.2	27.0	0.0
Si	mg/L	3.7	7.1	1.5	12.0
O_2	mg/L	10.2	7.8	8.0	10.7
pH	pH	7.8	7.9	8.2	8.2
Temp	°C	12.9	10.1	11.3	11.5
Alkalinity	mg/L HCO3	132.0	74.1	137.5	173.0
SI	-	-0.08	-0.41	0.11	0.58
From PHREEQC					
EC	µS/cm	326.2	162.3	650.8	257.9
SI	-	-0.03	-0.41	0.12	0.45
Langelier SI	-	-0.03	-0.37	0.11	0.40
CCPP	mmol/L	-0.005	-0.036	0.017	0.089
Agressieve CO_2	mg/L	0.22	1.57	-0.73	-3.91

V Exit test – Validation from practice

Figure 30 Photograph of AC Test 2 performed in Texel on the Willem van Beierenstraat

VI Index Parameters

Saturation Index and Langelier Saturation Index

The index parameters used for monitoring drinking water vary per country. Currently in the Netherlands the Langelier saturation index (LSI) is used and the requirement is that the LSI > -0.2 (*Drinkwaterbesluit*, 2011).

Often, the LSI is reported simply as the saturation index (SI), though the SI and LSI are not exactly the same parameter. The SI is calculated by comparing the chemical activities of the dissolved ions of the mineral (ion activity product, IAP) with their solubility product (K), Eq. 3 Appelo et al. (2005):

$$SI = \log\left(\frac{IAP}{K}\right) \quad \text{Eq. 3}$$

The Langelier SI (LSI), on the other hand, is the difference between the measured pH and the pH when the mineral of interest, in this case calcite, is saturated (pH_s, Eq. 4).

$$LSI = pH - pH_s \quad \text{Eq. 4}$$

In many cases the LSI is similar enough to the SI to be a good estimate. For both the SI and the LSI, a value of zero indicates the water is in thermodynamic equilibrium, a negative value indicates the water is undersaturated (possible dissolution of calcite) and a positive value indicates the water is oversaturated (possible precipitation). Both the SI and the LSI can be calculated using PHREEQC.

Calcium Carbonate Precipitation Potential

The Calcium Carbonate Precipitation Potential (CCPP, NL: Theoretisch Afzetbaar Calcium Carbonaat (TACC)) gives the amount of $CaCO_3$ which can theoretically precipitate or dissolve at a given water composition. A CCPP of zero indicates the water is in thermodynamic equilibrium with $CaCO_3$, while a negative CCPP indicate the water may dissolve $CaCO_3$ and a positive CCPP indicates the water may precipitate $CaCO_3$ (Tang et al., 2021). In PHREEQC the CCPP is calculated for a given water composition and the result is given as the moles/L (or mg/L) of calcite which can precipitate or dissolve.

In Germany the *Calcitlösekapazität* ("Calcite dissolution capacity"), which has the opposite sign to the CCPP, is used to monitor drinking water. The *Trinkwasserverordnung* (2016))states that waters may have a *Calcitlösekapazität* value of <5 mg/L $CaCO_3$ for waters with a pH < 7.7. If two waters are mixed, then the *Calcitlösekapazität* can be up to 10 mg/L. If the pH > 7.7 there is no requirement . In the Netherlands there is no legal requirement for the CCPP. The $CCPP_{90}$ ($TACC_{90}$ in Dutch) is the calculation of the CCPP at 90 °C, this parameter is used in norms to prevent extensive precipitation of $CaCO_3$ in water heaters.

Aggressive CO_2

Aggressive CO_2 is another way to express the CCPP and can be calculated in a similar manner. Aggressive CO_2 is the carbon dioxide in excess of the concentration in equilibrium with $CaCO_3$ (LeRoy et al., 1996). Aggressive CO_2 can be calculated from the calcium carbonate-carbon dioxide equilibrium, given as:

$$CaCO_3 + CO_2 + H_2O \rightleftarrows Ca^{2+} + 2H_2O \quad \text{Eq. 5}$$

Given the reaction equation above, the amount of aggressive CO_2 can be calculated the same way as the CCPP by allowing calcite to dissolve or precipitate in PHREEQC. In the reaction there is a 1:1 molar ratio of calcite to CO_2, therefore the amount of aggressive CO_2 in mg/L can be calculated from the amount of calcite which has dissolved aggressive CO_2 has the opposite sign of CCPP (Hofman-Caris, 2013).

In addition, aggressive CO_2 can also be calculated by iteratively without the help of a geochemical speciation software. For this, the concentrations of Ca, HCO_3^-, temperature (°C), electrical conductivity at 20 °C and either the pH or concentration of CO_2 are necessary. The procedure for how to calculate the amount of aggressive CO_2 iteratively is given in (Hiemstra, 1987). The calculations are in fact a simplification as they do not consider the influence of components other than Ca and HCO_3^- in the water. It is therefore more accurate to calculate the aggressive CO_2 therefore using a geochemical software such as PHREEQC.

VII Stimela vs. Cemdata18: Index Parameters

The Stimela and Cemdata18 databases were compared to determine if they produced similar results when calculating the four index parameters: SI, LSI, CCPP/ aggressive CO_2. As can be seen in Figure 31 below, for the 177 147 simulations performed, the Stimela and Cemdata18 databases produced similar results for all four index parameters. The straight black line in the graphs indicate a 1:1 relationship between the Stimela and Cemdata18 data.

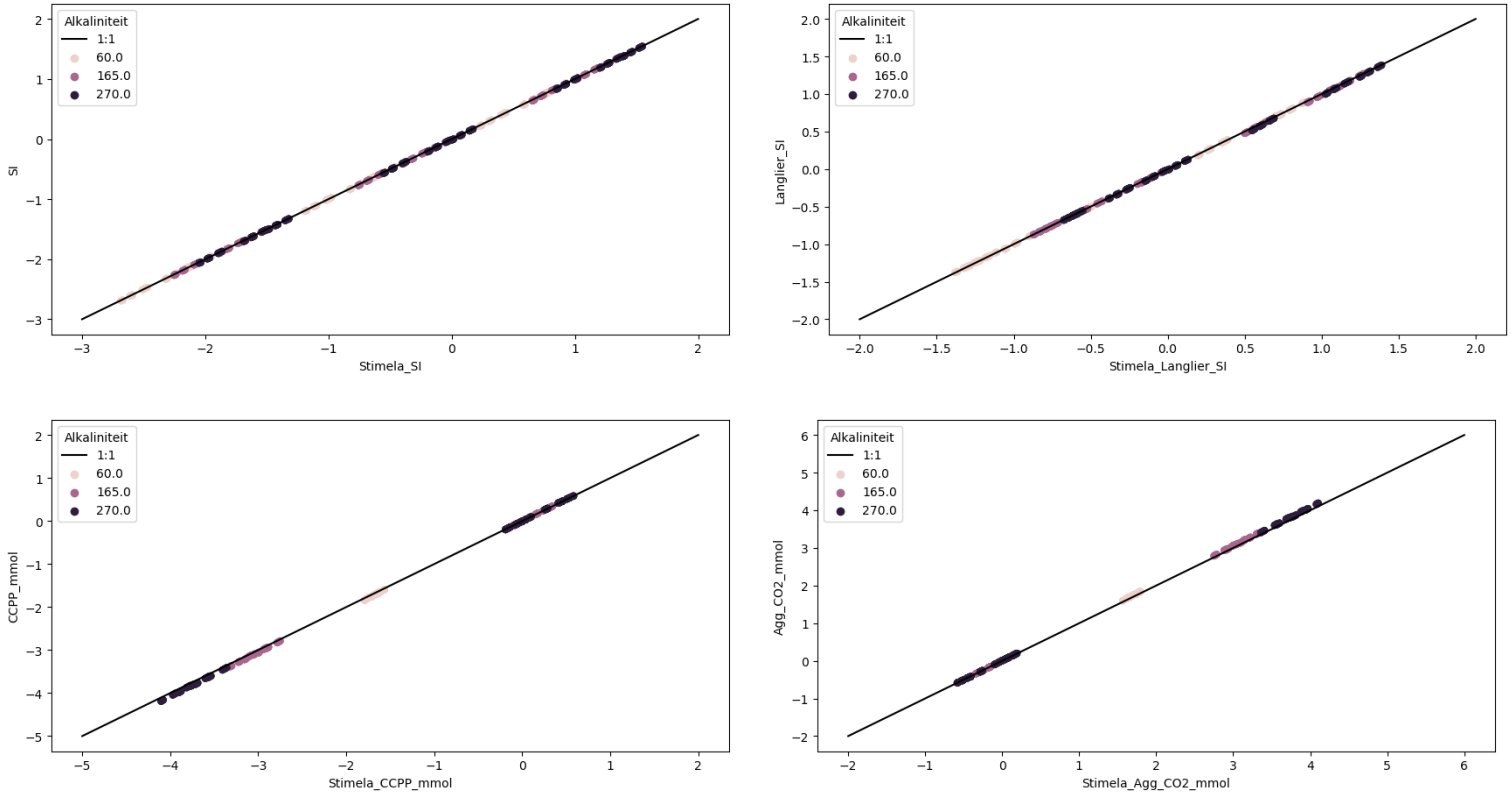

Figure 31 Calculation of four index parameters of interest, clockwise from top-left: SI, LSI, aggressive CO_2 (Agg. CO_2) and CCPP. The results show that the data fall on the 1:1 relationship between the index parameters calculated by the Stimela database and the Cemdata18 database.

VIII Extended Sensitivity Analysis Water Compositions

Table 16 Water composition of the 64 simulations from the extended sensitivity analysis of the effect of water composition on leaching and scaling.

Num.	Alkalinity mg/l $HCO3^-$	Ca mg/l	pH -	Mg mg/l	S mg S/l	SiO_2 mg Si /l	SI -	LSI -	CCPP mmol/l	Calcite precipitation moles
0	60	20	7	0	10	4	-1.49	-1.18	-0.23	0.41
1	60	20	7	0	10	20	-1.49	-1.17	-0.24	0.91
2	60	20	7	0	150	4	-1.69	-1.37	-0.24	1.57
3	60	20	7	0	150	20	-1.69	-1.36	-0.26	1.03
4	60	20	7	20	10	4	-1.50	-1.19	-0.23	7.68
5	60	20	7	20	10	20	-1.50	-1.18	-0.24	1.07
6	60	20	7	20	150	4	-1.69	-1.37	-0.24	6.85
7	60	20	7	20	150	20	-1.69	-1.36	-0.26	1.34
8	60	20	8	0	10	4	-0.50	-0.46	-0.03	6.64
9	60	20	8	0	10	20	-0.50	-0.45	-0.04	0.73
10	60	20	8	0	150	4	-0.70	-0.64	-0.05	7.09
11	60	20	8	0	150	20	-0.70	-0.62	-0.07	0.89
12	60	20	8	20	10	4	-0.51	-0.47	-0.04	5.67
13	60	20	8	20	10	20	-0.51	-0.46	-0.05	0.88
14	60	20	8	20	150	4	-0.70	-0.64	-0.05	7.23
15	60	20	8	20	150	20	-0.70	-0.62	-0.07	1.17
16	60	72	7	0	10	4	-0.95	-0.78	-0.19	0.25
17	60	72	7	0	10	20	-0.95	-0.78	-0.19	0.90
18	60	72	7	0	150	4	-1.14	-0.95	-0.20	3.41
19	60	72	7	0	150	20	-1.14	-0.95	-0.21	1.01
20	60	72	7	20	10	4	-0.96	-0.79	-0.19	8.06
21	60	72	7	20	10	20	-0.96	-0.79	-0.19	1.04
22	60	72	7	20	150	4	-1.13	-0.95	-0.20	8.41
23	60	72	7	20	150	20	-1.13	-0.95	-0.21	1.31
24	60	72	8	0	10	4	0.04	0.04	0.00	6.66
25	60	72	8	0	10	20	0.04	0.03	0.00	0.72
26	60	72	8	0	150	4	-0.15	-0.14	-0.01	6.88
27	60	72	8	0	150	20	-0.15	-0.14	-0.01	0.87
28	60	72	8	20	10	4	0.03	0.03	0.00	5.83
29	60	72	8	20	10	20	0.02	0.02	0.00	0.85
30	60	72	8	20	150	4	-0.15	-0.14	-0.01	6.43
31	60	72	8	20	150	20	-0.15	-0.14	-0.01	1.13
32	270	20	7	0	10	4	-0.89	-0.46	-0.60	2.72
33	270	20	7	0	10	20	-0.89	-0.46	-0.60	3.61
34	270	20	7	0	150	4	-1.06	-0.58	-0.68	-1.31
35	270	20	7	0	150	20	-1.06	-0.58	-0.68	2.71
36	270	20	7	20	10	4	-0.89	-0.47	-0.60	7.23
37	270	20	7	20	10	20	-0.89	-0.47	-0.60	3.67
38	270	20	7	20	150	4	-1.06	-0.58	-0.68	-1.31
39	270	20	7	20	150	20	-1.06	-0.58	-0.68	3.07
40	270	20	8	0	10	4	0.10	0.08	0.03	9.88
41	270	20	8	0	10	20	0.10	0.08	0.03	2.64
42	270	20	8	0	150	4	-0.07	-0.06	-0.02	10.18
43	270	20	8	0	150	20	-0.07	-0.06	-0.02	2.23
44	270	20	8	20	10	4	0.10	0.07	0.02	8.93
45	270	20	8	20	10	20	0.09	0.07	0.02	2.76

46	270	20	8	20	150	4	-0.07	-0.05	-0.02	14.61
47	270	20	8	20	150	20	-0.07	-0.05	-0.02	2.57
48	270	72	7	0	10	4	-0.34	-0.22	-0.33	5.79
49	270	72	7	0	10	20	-0.34	-0.22	-0.33	3.32
50	270	72	7	0	150	4	-0.50	-0.33	-0.45	3.59
51	270	72	7	0	150	20	-0.50	-0.33	-0.45	2.67
52	270	72	7	20	10	4	-0.35	-0.23	-0.33	6.12
53	270	72	7	20	10	20	-0.35	-0.23	-0.33	3.42
54	270	72	7	20	150	4	-0.50	-0.33	-0.45	-1.31
55	270	72	7	20	150	20	-0.50	-0.33	-0.45	3.01
56	270	72	8	0	10	4	0.65	0.55	0.25	8.74
57	270	72	8	0	10	20	0.64	0.54	0.26	2.54
58	270	72	8	0	150	4	0.48	0.42	0.17	3.23
59	270	72	8	0	150	20	0.48	0.41	0.17	2.19
60	270	72	8	20	10	4	0.64	0.54	0.25	7.76
61	270	72	8	20	10	20	0.64	0.54	0.25	2.66
62	270	72	8	20	150	4	0.48	0.42	0.17	8.91
63	270	72	8	20	150	20	0.48	0.41	0.17	2.51

IX Extended sensitivity analysis: CCPP and calcite precipitation

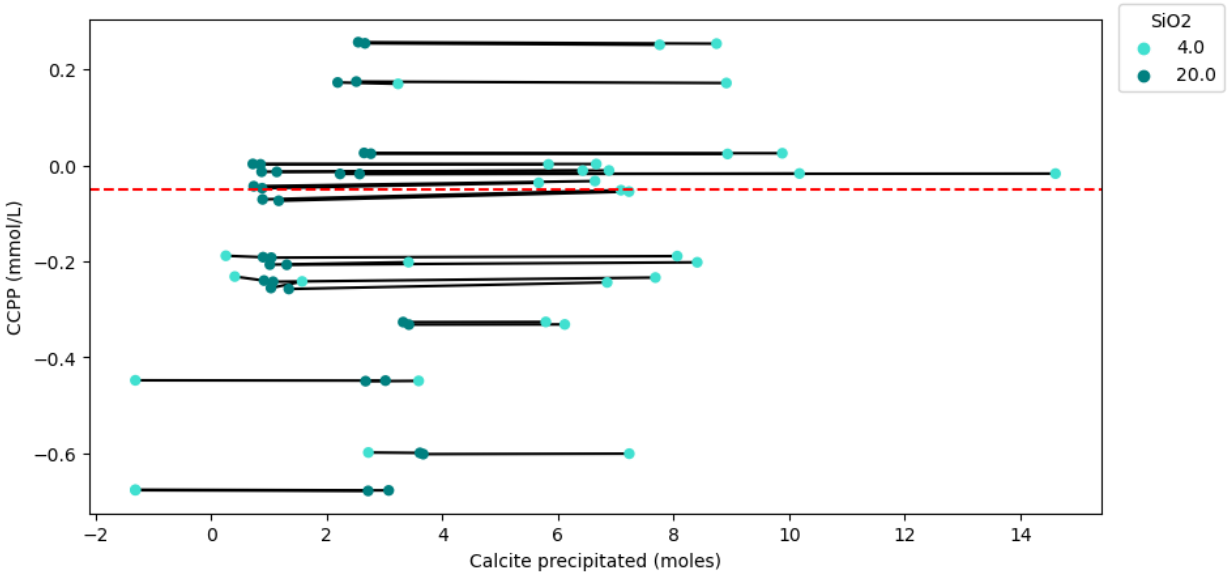

Figure 32 Total moles of calcite precipitated after 10 years versus the CCPP for different SiO_2 concentrations. The red dotted line gives the CCPP norm of -0.05 mmol/L. The black lines join matching pairs of water compositions where the only difference is the concentration of SiO_2, indicated by the color of the symbol.

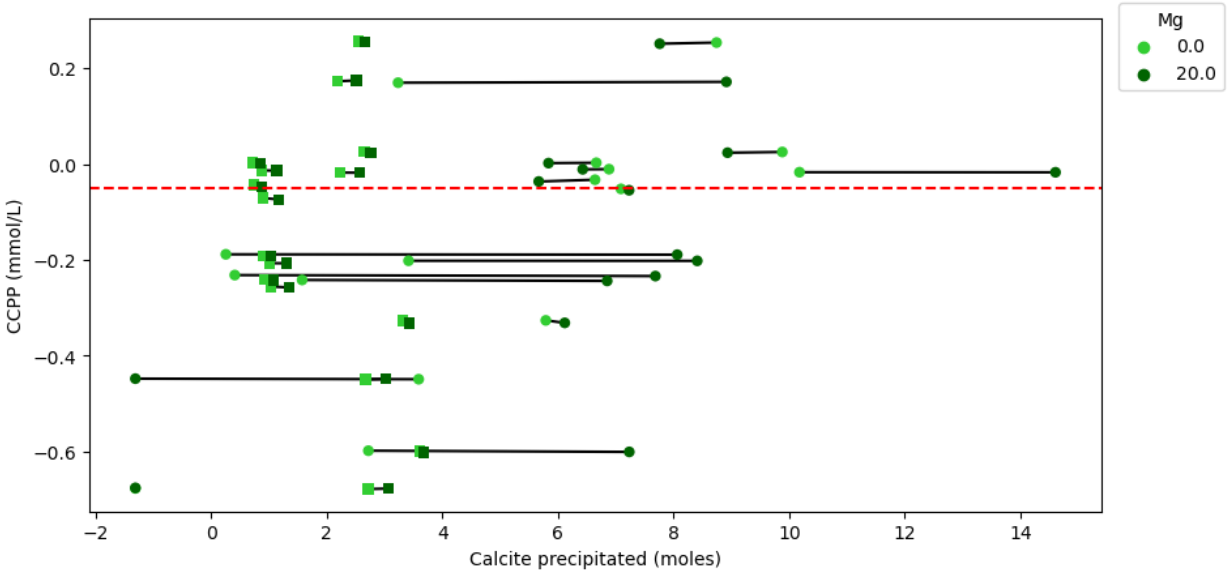

Figure 33 Total moles of calcite precipitated after 10 years versus the CCPP for different Mg concentrations. The red dotted line gives the CCPP norm of -0.05 mmol/L. The black lines join matching pairs of water compositions where the only difference is the concentration of Mg, indicated by the color of the symbol. The square symbols indicate water compositions with high SiO_2 concentrations (20 mg/L) while the round symbols indicate low SiO_2 concentration (4 mg/L).

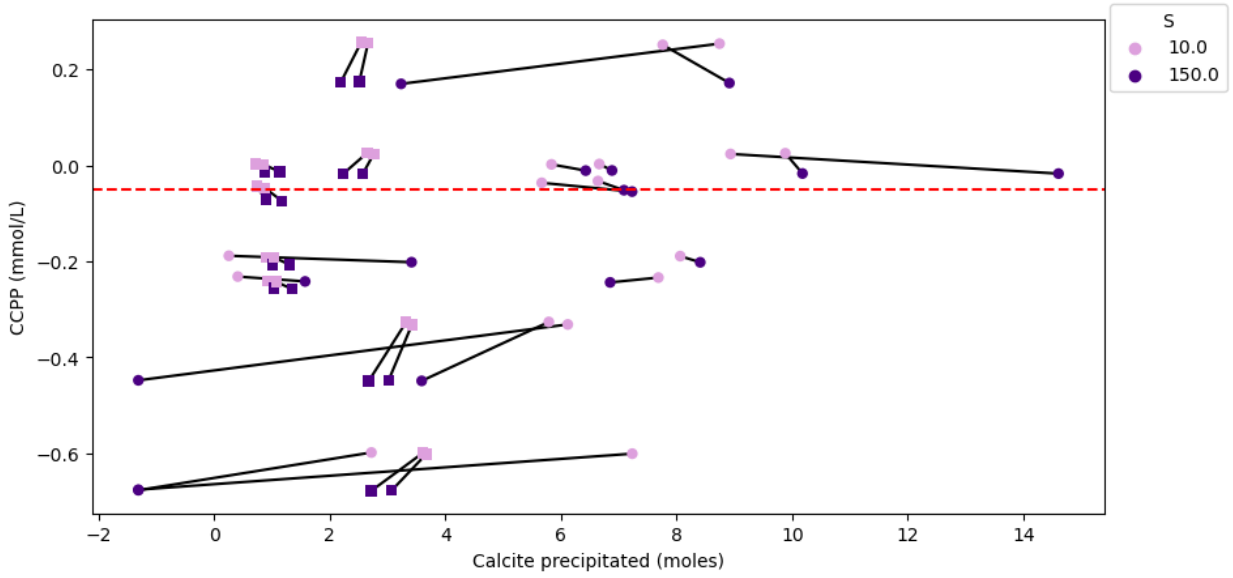

Figure 34 Total moles of calcite precipitated after 10 years versus the CCPP for different S concentrations. The red dotted line gives the CCPP norm of -0.05 mmol/L. The black lines join matching pairs of water compositions where the only difference is the concentration of S, indicated by the color of the symbol. The square symbols indicate water compositions with high SiO_2 concentrations (20 mg/L) while the round symbols indicate low SiO_2 concentration (4 mg/L).

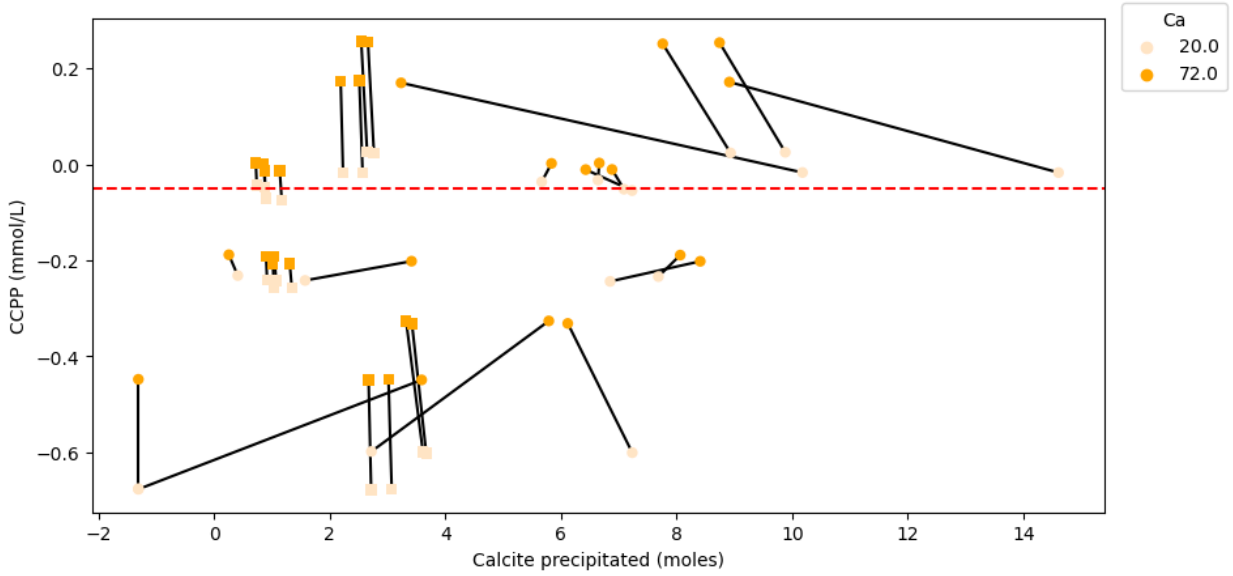

Figure 35 Total moles of calcite precipitated after 10 years versus the CCPP for different Ca concentrations. The red dotted line gives the CCPP norm of -0.05 mmol/L. The black lines join matching pairs of water compositions where the only difference is the concentration of Ca, indicated by the color of the symbol. The results show no little or no difference in the moles of calcite precipitated for most compositions when the Ca concentration in the influent water is increased. The square symbols indicate water compositions with high SiO_2 concentrations (20 mg/L) while the round symbols indicate low SiO_2 concentration (4 mg/L).

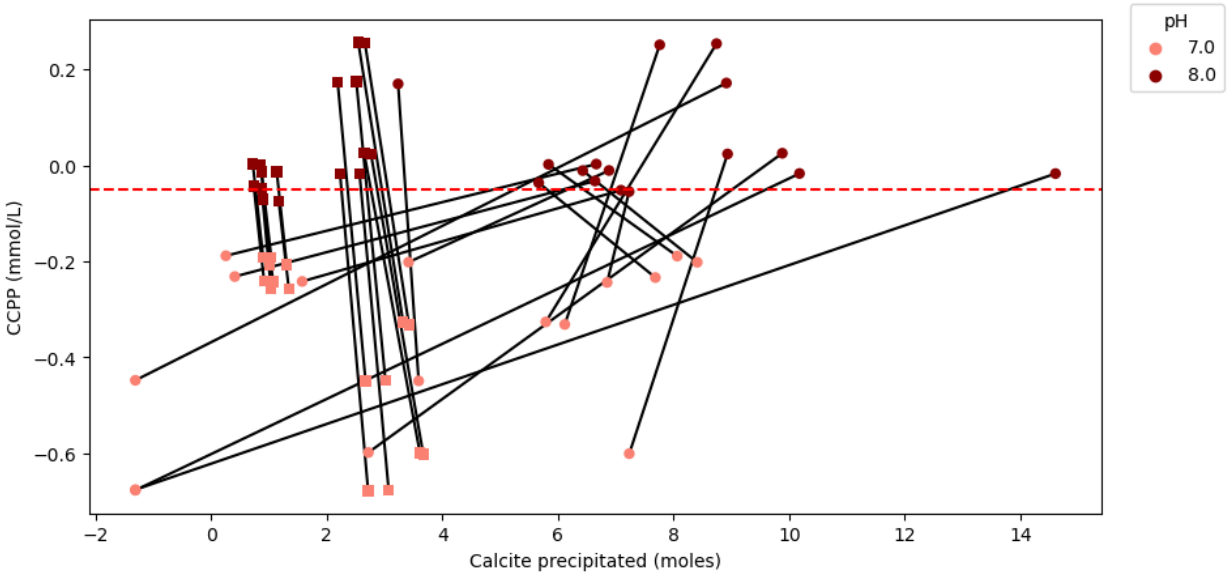

Figure 36 Total moles of calcite precipitated after 10 years versus the CCPP for different pH. The red dotted line gives the CCPP norm of -0.05 mmol/L. The black lines join matching pairs of water compositions where the only difference is the pH, indicated by the color of the symbol. The square symbols indicate water compositions with high SiO_2 concentrations (20 mg/L) while the round symbols indicate low SiO_2 concentration (4 mg/L).

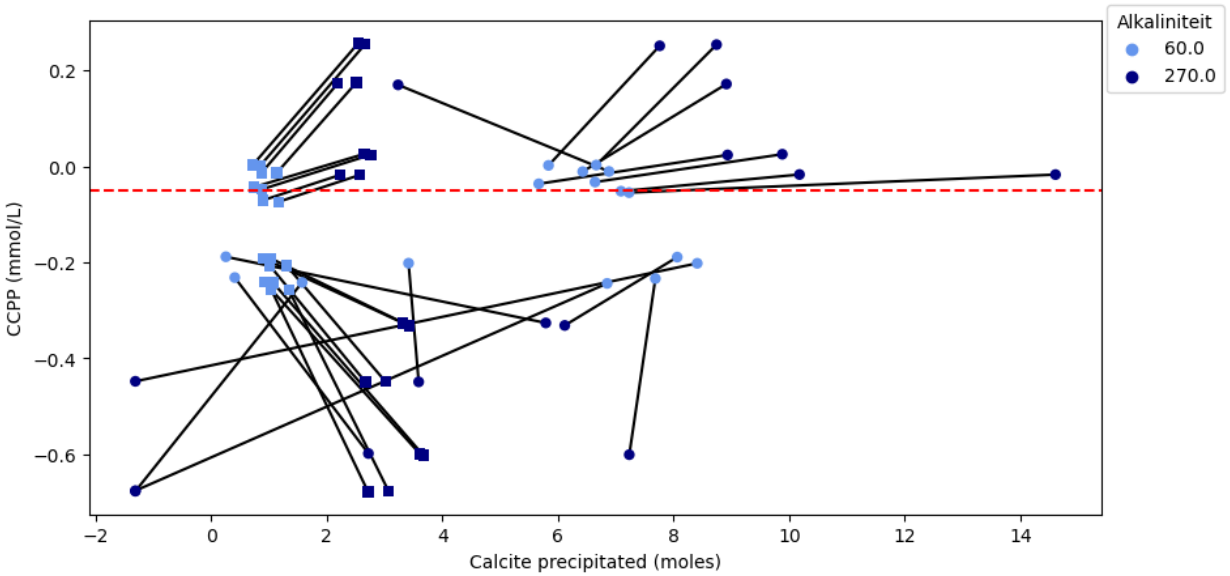

Figure 37 Total moles of calcite precipitated after 10 years versus the CCPP for different alkalinity concentrations (in mg HCO_3^- per L). The red dotted line gives the CCPP norm of -0.05 mmol/L. The black lines join matching pairs of water compositions where the only difference is the alkalinity concentration, indicated by the color of the symbol. The square symbols indicate water compositions with high SiO_2 concentrations (20 mg/L) while the round symbols indicate low SiO_2 concentration (4 mg/L).

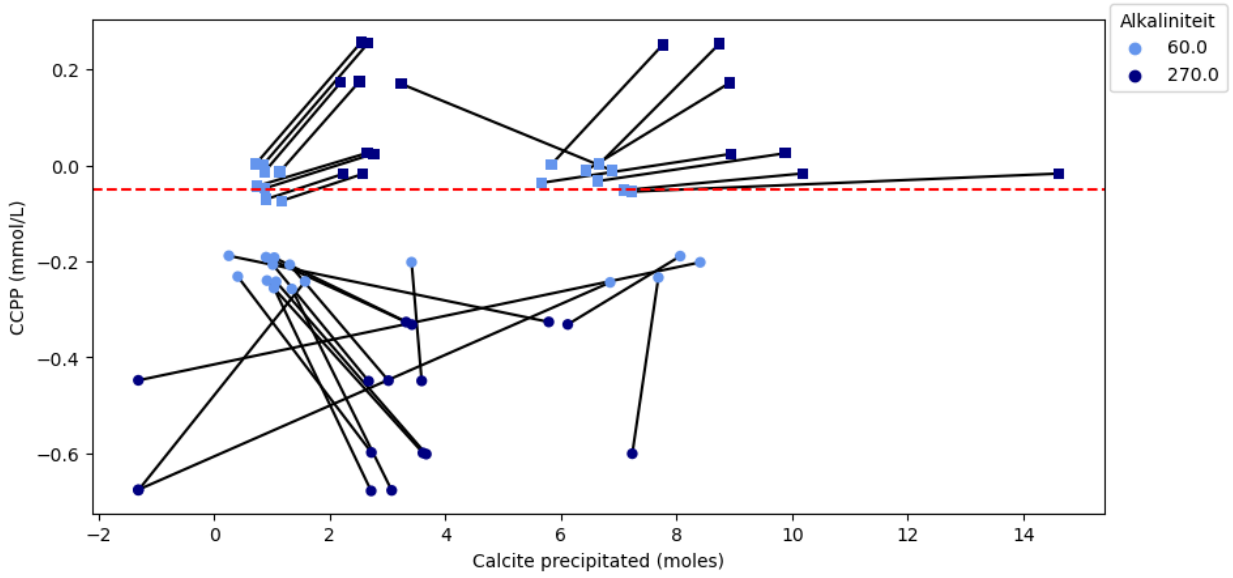

*Figure 38 Total moles of calcite precipitated after 10 years versus the CCPP for different alkalinity concentrations (in mg HCO_3^- per L). The red dotted line gives the CCPP norm of -0.05 mmol/L. The black lines join matching pairs of water compositions where the only difference is the alkalinity concentration, indicated by the color of the symbol. The square symbols indicate water compositions with **high pH** (pH =8) while the round symbols indicate **low pH** (pH = 7).*